DESIGN AND ANALYSIS OF A NOVEL ELECTROHYDRAULIC DRAFT CONTROL SYSTEM IN AGRICULTURAL MACHINERY

A THESIS SUBMITTED TO
THE GRADUATE SCHOOL OF NATURAL AND APPLIED SCIENCES
OF
MIDDLE EAST TECHNICAL UNIVERSITY

BY

EMIR MURAT KARAKOÇ

IN PARTIAL FULFILLMENT OF THE REQUIREMENTS
FOR
THE DEGREE OF MASTER OF SCIENCE
IN
MECHANICAL ENGINEERING

AUGUST 2019

Approval of the thesis:

DESIGN AND ANALYSIS OF A NOVEL ELECTROHYDRAULIC DRAFT CONTROL SYSTEM IN AGRICULTURAL MACHINERY

submitted by **EMIR MURAT KARAKOÇ** in partial fulfillment of the requirements for the degree of **Master of Science in Mechanical Engineering Department, Middle East Technical University** by,

Prof. Dr. Halil Kalıpçılar
Dean, Graduate School of **Natural and Applied Sciences** _____

Prof. Dr. Mehmet Ali Sahir Arıkan
Head of Department, **Mechanical Engineering** _____

Prof. Dr. Raif Tuna Balkan
Supervisor, **Mechanical Engineering, METU** _____

Prof. Dr. Yavuz Samim Ünlüsoy
Co-Supervisor, **Mechanical Engineering, METU** _____

Examining Committee Members:

Assoc. Prof. Dr. Yiğit Yazıcıoğlu
Mechanical Engineering, METU _____

Prof. Dr. Raif Tuna Balkan
Mechanical Engineering, METU _____

Prof. Dr. Yavuz Samim Ünlüsoy
Mechanical Engineering, METU _____

Assist. Prof. Dr. Kıvanç Azgın
Mechanical Engineering, METU _____

Assist. Prof. Dr. Kutluk Bilge Arıkan
Mechanical Engineering, TED University _____

Date: 07.08.2019

I hereby declare that all information in this document has been obtained and presented in accordance with academic rules and ethical conduct. I also declare that, as required by these rules and conduct, I have fully cited and referenced all material and results that are not original to this work.

Name, Surname: Emir Murat Karakoç

Signature:

ABSTRACT

DESIGN AND ANALYSIS OF A NOVEL ELECTROHYDRAULIC DRAFT CONTROL SYSTEM IN AGRICULTURAL MACHINERY

Karakoç, Emir Murat
Master of Science, Mechanical Engineering
Supervisor: Prof. Dr. Raif Tuna Balkan
Co-Supervisor: Prof. Dr. Yavuz Samim Ünlüsoy

August 2019, 117 pages

A three-point hitch system is a mechanism that controls the movement of various agricultural equipment. Connection dimensions between the equipment and working range of mechanisms are defined by standards. The mechanism is actuated by hydraulic cylinders and the required hydraulic power for movement is provided by a hydraulic pump.

Constitutively, there are two types of methods to control the three-point hitch mechanism. Draft control is a type of control mechanism that ensures the tractor not to slip and minimizes the inefficiencies. The force applied from equipment to the tractor depends on the equipment depth, soil characteristics, and vehicle velocity. An excessive amount of load may cause slippage on tires, even stopping the tractor during tillage operations. In order to prevent this situation, draft control adjusts the depth of the three-point hitch mechanism under the soil according to the force value from the ground during the tillage process. As for the position control, the control mechanism arranges the height of the mechanism according to the given angle input.

In this study, a three-point hitch draft control system is examined. Solid model of the three-point system is constructed by using computer-aided design software, PTC Creo

3.0® (CAD) and transferred to MATLAB®. With the transferred model, the tractor's hydraulic system consisting mainly of pumps, valves and cylinders, position and draft sensors and the controller are modeled, and the resulting system is created by using MATLAB Simulink module. Established kinematic equations of the three-point hitch mechanism are validated with ADAMs® simulation software.

The aim of the thesis is to control the pulling force by the measured pressure transmitted to the main external lift cylinders, instead of using a force sensor, as opposed to the application in existing tractors. Simulations of the current model with force sensors and the simulations of the proposed model with pressure sensors are performed and the feasibility of the proposed scheme is discussed in detail.

Keywords: Tractor, Three-Point Hitch System, Electro-hydraulic Draft Control, Position Control

ÖZ

TARIM MAKİNALARINDA ÖZGÜN ELEKTRO-HİDROLİK ÇEKİ KONTROLÜ TASARIMI VE ANALİZİ

Karakoç, Emir Murat
Yüksek Lisans, Makina Mühendisliği
Tez Danışmanı: Prof. Dr. Raif Tuna Balkan
Ortak Tez Danışmanı: Prof. Dr. Yavuz Samim Ünlüsoy

Ağustos 2019, 117 sayfa

Üç nokta askı sistemi, tarım traktörlerinde çeşitli tarım ekipmanlarının hareketlerinin kontrol edildiği mekanizmalardır. Ekipmanla çalışma mekanizması arasındaki bağlantıyı sağlayan parçaların boyutları standartlara göre belirlenmektedir. Mekanizma hidrolik silindir tarafından tetiklenmektedir ve hareket için gerekli olan hidrolik güç, bir hidrolik pompa ile sağlanmaktadır.

Traktörlerde üç nokta askı mekanizması iki ayrı yöntemle kontrol edilebilmektedir. Çeki kontrolü, traktörün patinaja kalmasını önleyen ve verimsizlikleri minimuma indirgeyen bir kontrol sistemidir. Ekipmandan traktöre uygulanan kuvvet, ekipman derinliğine, toprak özelliklerine ve araç hızına bağlıdır. Aşırı miktarda uygulanan yük, toprak işleme sırasında lastiklerde patinaja, hatta traktörün durmasına neden olabilmektedir. Bu durumu önlemek için, çeki kontrolü, üç nokta askı mekanizmasının toprak altındaki derinliğini, toprak işleme sırasında zeminden gelen kuvvet değerine göre ayarlar. Konum kontrolü ise, mekanizmanın yüksekliğini, verilen açı girdisine göre ayarlayan kontrol sistemidir.

Bu tezde, üç nokta askı mekanizmasının çeki kontrol sistemi ele alınmaktadır. Bilgisayar destekli tasarım yazılımı, PTC Creo 3.0® (CAD) ile modellenen üç nokta

askı sistemi, Matlab® Simulink modeline aktarılmıştır. Aktarılan model ile beraber, traktörün temel olarak pompa, valfler ve silindirlerden oluşan hidrolik sistemi, konum ve çeki sensörleri ve kontrolcü MATLAB® Simulink ortamında modellenerek mevcut traktör sistemi oluşturulmuştur. Üç nokta askı sisteminin oluşturulan kinematik denklemlerinin doğrulaması ADAMS® simülasyon yazılımı ile yapılmıştır.

Bu çalışmanın amacı, mevcut traktörlerden farklı olarak çeki kuvvetinin, kuvvet sensörü yerine, ana silindirlerde oluşan basıncın ölçülmesi ile kontrol edilmesini sağlamaktır. Mevcut traktör MATLAB Simulink® modeline ek olarak yeni özgün tasarımın da modeli oluşturulmuş ve simülasyonları yapılmıştır. Sadece basınç sensörleri kullanılarak çeki kuvvetinin kontrol edilebilme performansı tez içerisinde ayrıntılı bir şekilde tartışılmıştır.

Anahtar Kelimeler: Traktör, Üç Nokta Askı Sistemi, Elektro-hidrolik Çeki Kontrolü, Konum Kontrolü

To my dear family

ACKNOWLEDGEMENTS

First of all, I would like to express my sincere gratitude to my supervisor Prof. Dr. Raif Tuna Balkan for his contributions, suggestions and guidance. I would like to say thank you for taking the time out of his busy schedule. It is a privilege to be his student.

Secondly, I am grateful to Samet Adem Cömert for his sharing experiences, contributions and encouragement. In all stages of the thesis, being influenced by his engineering perspective is a great chance for me.

Thirdly, I would like to express my gratitude to my old company, TürkTraktör, which has supported me from beginning to end of the thesis materially and spiritually.

I also express my sincere appreciation to Prof. Dr. Yavuz Samim Ünlüsoy for his precious contributions and advice.

Then, I would also like to express my sincere gratitude to my family for their encouragement, supports and consciousness.

Finally, I would like to endless thank to my wife for her support and patience. She supports me in every step of my life.

TABLE OF CONTENTS

LIST OF TABLES

TABLES

LIST OF FIGURES

FIGURES

LIST OF ABBREVIATIONS

ABBREVIATIONS

3PL : Three-point linkage

3PH : Three-point hitch

CCW : Counter clock wise

CVT : Continuous Variable Transmission

CW : Clock wise

EDC : Electro-hydraulic draft control

ECU : Electric control unit

HPL : Hydraulic Power Lift

LOM : Lift-o-matic

PTO : Power Take Off

LIST OF SYMBOLS

P : Hydraulic Pump

F : Filter

C : Control Valve

R : Relief Valve

L : Maximum distance in between PTO and lower hitch points

CP_m : Horizontal virtual hitch point where the lower links are coincident virtually when the lower links are horizontal and laterally symmetrical

CP_v : Vertical convergence distance where the upper link and lower links are coincident virtually when the lower links are horizontal and laterally symmetrical

l_1 : The distance between the lower links

l_2 : The rocker (left-right motion) distance of the links

W_D : Draft load or draught force (N)

W_{Dx} : x component of draft load (N)

W_{Dy} : y component of draft load (N)

W_{Dz} : z component of draft load (N)

θ : Angle of draft load (between x and y axis)

F_i : Dimensionless soil texture adjustment parameter

i : Category of the soil

T_s : Tractor speed (km/h)

W_{ew} : Equipment width, (m) or number of tools

T_D : Tillage depth, (cm) for major tools

|GE| : External lift cylinder (mm)

|DEF| : HPL arm

θ_2 : The angle of the external lift cylinder (degree)

θ_1 : The angle of HPL arm (degree)

θ_7 : The angle of body |DG| (degree)

α_1 : |GDE| angle (degree)

α_2 : |FDE| angle (degree)

θ_3 : The angle of adjustable arm (degree)

θ_4 : The angle of lower link (degree)

|ABC| : Lower link

|FB| : Adjustable arm (mm)

θ_{11} : The angle of body |DA (degree)|

α_7 : The angle between the bodies |DG| and |DA| (degree)

θ_{10} : The angle of the body |AH| (degree)

θ_5 : The angle of the top link (degree)

θ_6 : The angle of the implement (degree)

|HI| : Top link (mm)

|IC| : Implement connection link (mm)

P_1 : External lift cylinder pressure (bar)

P_2 : Hydraulic top link bore side pressure (bar)

m_e : Weight of the implement (kg)

W_c : Equipment to implement connection point force (N)

W_I : Top link force (N)

γ : The angle of the equipment (degree)

W_B : Adjustable arm force (N)

W_A : Load cell force (N)

S_e : External lift cylinder stroke (mm)

$|EG_i|$: Initial length of the external lift cylinder (mm)

D_p : Pump displacement (cm^3/rev)

P_{max} : Maximum system pressure (bar)

S_{max} : Maximum engine speed (rpm)

N_{pm} : Pump to motor ratio

I_1 : Lifting current signal (ampere)

I_2 : Lowering current signal (ampere)

θ_p : User input for 3PH mechanism position (degree)

θ_{delta} : Angle difference btw. user input and 3PH system actual position (degree)

W_p : User input force (N)

W_{delta} : Load difference in between the applied force and user input force (N)

$W_{sensing}$: Setting sensitivity value (N)

k_1 : 3PH lifting velocity constant

k_2 : 3PH lowering velocity constant

γ : Covariance matrix gain

a_1, a_2, a_3, a_4, a_5 : Parameters of the controller characteristic equations

γA_r : Arduino transformation constant

V_{ard} : Arduino voltage (V)

MV_{LC} : Measured value from control panel for load cell force

F_{max} : Maximum force that the sensor can be read (N)

V_{LC} : Maximum load cell voltage (V)

α_{HPL} : HPL unit angle wrt. longitudinal axis (deg.)

V_{AS} : Maximum angle sensor voltage (V)

α_{max} : Maximum allowable measured angle (deg.)

MV_{AS} : Measured value from control panel for HPL angle

P_{Ex} : External lift pressure (bar)

V_{PT} : Pressure transducer maximum voltage (V)

P_{max} : Maximum allowable pressure (bar)

MV_{PT} : Measured value for pressure transducer

$\theta_{1_{TEST}}$: HPL arm angle for test (deg)

$W_{A_{TEST}}$: Load cell force for test (N)

$W_{E_{TEST}}$: Hydraulic top link force for test (N)

W_E : External lift cylinder force (N)

P_{cyl} : External lift cylinder pressure (bar)

A_{cyl} : Bore side area of the external lift cylinder (mm^2)

V_{cyl} : Velocity of the external lift cylinder (mm/s)

CHAPTER 1

INTRODUCTION

1.1. Motivation

The human being lives in dependence on the soil from the very beginning of existence. In all generations, people feel the need to work on the land and produce their nutrition to keep themselves alive.

The cultivation process firstly started with a hand that used as basic equipment for soil cultivation. In progress of time, with auxiliary equipment like grubber or rake, the process got easy.

With industrialization, mechanization has begun and became an essential role in agriculture. The aim is reducing the dependency of the manpower and taking maximum efficiency in minimum time. Agriculture has to be done depending on the climate. Sometimes, even a few hour delays can cause significant losses financially. Therefore, mechanization has great importance to the concept of time as well as the increase of the workforce.

The tractor is a great invention that can be regarded as a revolution in industrialization. In the beginning, the tractor was originally only used for towing and fieldwork. Nowadays, it can be easily used in all kinds of work that a farmer may need such as plowing, fielding, leveling and picking. It also has the capability to do heavy work that the backhoe loader can do.

In developed countries, agriculture is made with less human power, more agricultural tools principle. Nowadays since the tractor has the ability to do all the necessary work, in some countries, thousands of acres of field can be processed with a single person and in this way provide a significant contribution to production.

As an agricultural country, keep pace with agricultural technology is very important for Turkey. For that reason, primitive agricultural tools are rapidly abandoned and the use of advanced agricultural machinery is rapidly increasing. As a result of this development and with developing technology, the tractor has become an indispensable part of the farmers.

The tractor has lots of components. Engine, cabin or platform, transmission, power take of system and lift system could be count as essential components of the tractor.

The predecessors of modern tractors used steam engines for power. Modern farm tractor generally employs with the diesel engine. The range in power output starts from 18 to reach 575 horsepower (15 to 480 kW). The tractor size and power output are dependent on applications. Smaller tractors are used for lawn mowing, landscaping, orchard work, and truck farming. Larger tractors are used in vast fields for heavy-duty issues[1]. In the future, instead of diesel engines, the electric tractor could be produced and take an important role in the field [2].

Cabin or platform is the living space and the command center of the tractor for the driver. Cabin is a closed version of the platform.

Next, in the modern tractor, there are several transmission types. One of the oldest methods is a manual transmission. Power-shift [3], semi power-shift and continuously variable transmission, CVT [4], are the other types of modern transmission.

PTO is the acronym of the power take of system. Most tractors transfer power to another machine such as mower. Early tractors used belts or cables wrapped around the flywheel or a separate belt pulley to power stationary equipment, such as a threshing machine. Modern tractors use the PTO shaft to provide rotary power to machinery that may be stationary or pulled. The PTO is usually at the rear side of the tractor and can be connected to an implement that is either towed by a drawbar or a three-point hitch [5].

Lastly, the lift system connects the tractor to equipment such as plows or chisel plough. Hydraulic power lift, drawbar and three-point hitch mechanism are the main parts of the lift system.

The main purpose of the tractor is transmitting the power to equipment. Engine power is transmitted by using power take-off, three-point hitch or drawbar mechanism. PTO transmits the rotational motion, whereas other mechanisms transmit the linear motion. Engine power is converted to the draft force with the help of the wheel and drive train.

1.2. Details

In thesis, the main subject is the hydraulic lift system. The tractor lift system is composed of two main components, which are hydraulic lift system and three-point linkage or three-point hitch mechanism.

1.2.1. Hydraulic Lift System

The hydraulic system is found mainly in the back of the tractor, but, in some cases, a separate hydraulic system takes place on the front. This system is the heart of the tractor. It makes easier the mounting, handling, actuating and adjusting of the equipment.

Hydraulic pump (P) converts the mechanical energy that comes from motor, into the hydraulic energy. Generally, fixed displacement gear pumps are used in the tractor. The pump has one inlet, suction line (1) and one output, pressure line (2). Filter (F) is used in the suction line, just before the pump. It removes the contamination in the system. Pressurized fluid comes to the control valve (C). The control valve is the directional control valve of the hydraulic lift. Specifications of the valve change tractor to tractor. Relief valve (R) sets the system maximum working pressure. In all hydraulic power lift systems, R must be occurred to protect the system from high pressure. The oil that passes from the relief valve returns the tank from the return line (3). HPL arm (4) is the connection link between the 3-point linkage and the HPL unit.

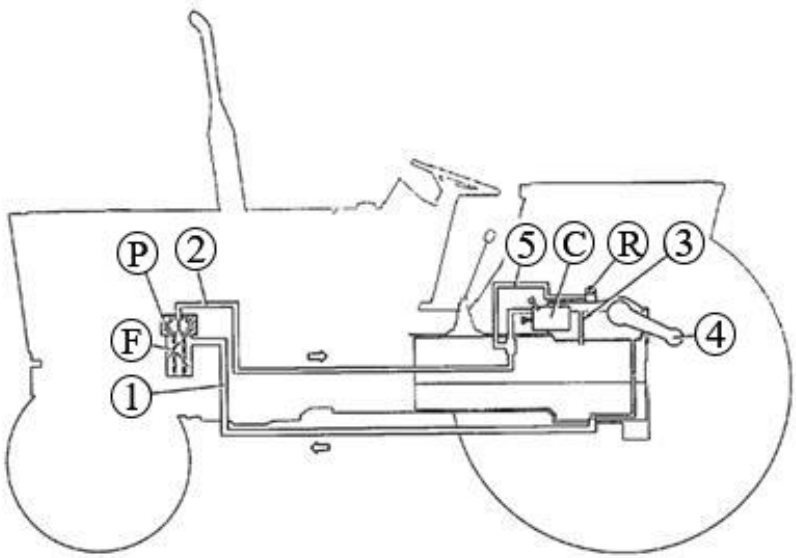

Figure 1.1. Hydraulic Lift System

In the hydraulic lift system, hydraulic power lift, HPL, is the casing of some certain parts which are located behind the tractor. The hydraulic power lift is composed of several main components. Hydraulic power lift unit or rockshaft, HPL arms, main shaft, crank handle, piston rod, cylinder, piston and distributor valve are the main components of the HPL. This system is called an HPL with internal lift cylinders.

In certain types of HPL, crank handle, and the piston rod does not occur. In this type of mechanism, hydraulic lift cylinders are directly connected to the HPL arms. This system is called an HPL with external lift cylinders.

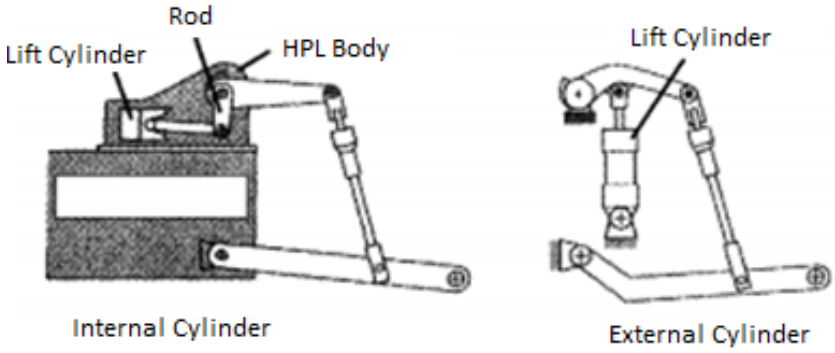

Figure 1.2. Types of Lifting Mechanism [6]

1.2.2. Hydraulic Lift System Control

According to the variant, the external or internal lift cylinder is the triggering device of the mechanism. The movement of the equipment can be controlled by controlling the oil movements in the cylinder. Formerly, mechanical controllers are used, but at present electrical controllers come into prominence. Position control and draft control are the main control mechanisms of the tractor. Lift-o-matic and slip control are auxiliary control mechanisms.

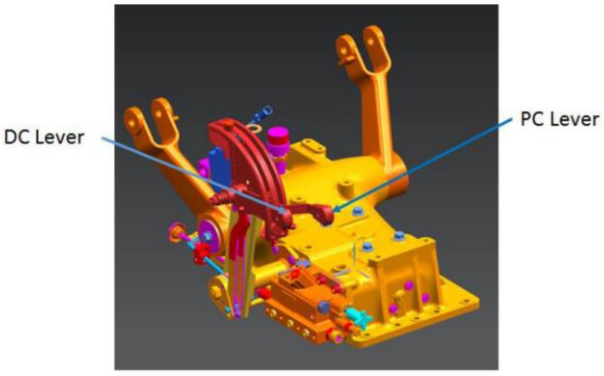

Figure 1.3. Position and Draft mechanical control levers [7]

1.2.2.1. Position Control

Position control provides accurate control of implements such as sprayers that operate above the ground. The system shall have a position control mode to sense changes in the position of the linkage in the movement range. When the system is in position control mode, the draft and slip control commands shall be ignored. In position control, the angle at the HPL arm is the only variable [8].

There are two types of position control which are mechanical and electrical position control. In most of the case, there is a cam mechanism in the mechanical position control. Lever and HPL arm is connected with the cam mechanism. The angle of the HPL arm is directly proportional to the amount of movement of the lever, which is controlled by the user.

In an electrical control system, there is a position sensing potentiometer to set the working position of the hitch. Electrical control is more precise with respect to the mechanical one.

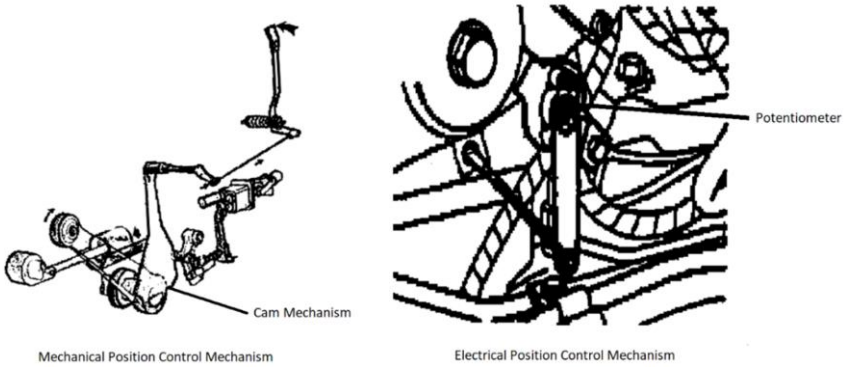

Figure 1.4. Types of Position Control Mechanism [9]

1.2.2.2. Draft Control

Draft control mode is designed for mounted or semi-mounted implements operating in the ground. The system has a draft control mode to stand sense changes in the draft load of the linkage. In draft control, apart from the angle of the HPL arm, draught force or draft load is also the variable [8].

Like position control, there are two types of draft control, which are mechanical and electrical.

In mechanical draft control, there are two main methods. In the first method, the draft load signal is taken from the flex bar. This method is called as a lower link sensing mechanical draft control. Flex bar is located between two lower links. During the cultivating process, draft load or draught force is appeared and transmitted to the lower links. This force creates bending in the flex bar. With bending, certain displacement occurs in the mechanism. There is a critical displacement point to activate the HPL arm. After passing the critical extension, then lift cylinders are activated and go towards upwards in order to decrease the magnitude of the force acting upon the system. The lever is connected with the flex bar, and the farmer can be arranged the

threshold value of the draft load with the help of the lever by giving pre-displacement of the flex bar.

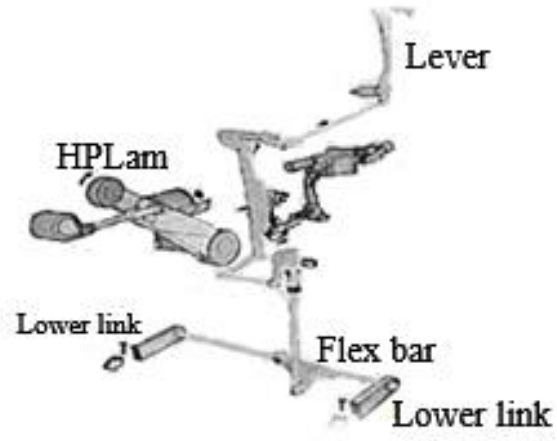

Figure 1.5. Lower Link Sensing Mechanical Draft Control [9]

In the second method, instead of using a flex bar, spring is used. It is located to the upper link point. This method is called as a top link sensing mechanical draft control. Applied draught force is transmitted to the upper link. This force creates tension or compression in the spring. This movement causes certain displacement in the mechanism. The remaining steps are the same as the previous case. The lever is connected with the spring, and the farmer could be arranged the threshold value of the draft load with the help of the lever by giving pre-tension of the spring.

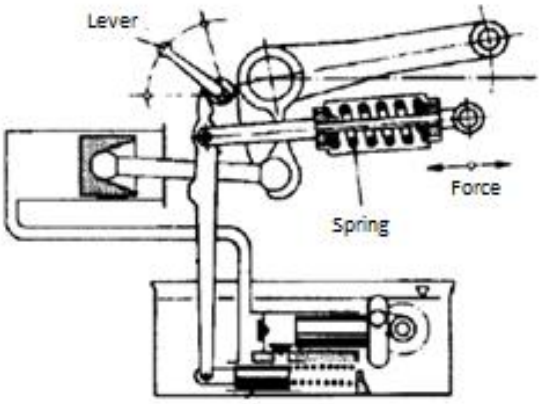

Figure 1.6. Top Link Sensing Mechanical Draft Control [9]

In the electrical draft control system, generally, the load sensing pins sense draft variations applied by an implement on the lower links. The pins react to draft shear forces only in the horizontal plane.

In electrical draft control, the driver arranges the controller at a certain level. This level corresponds to a particular draft load. During the cultivating process, the controller cannot keep the force in an exact force value. At that point, the sensitivity controller plays a part. The sensitivity controller keeps the value in a sensitivity band.

Draft control is controlled by the draft loading (red band) and draft sensitivity (blue band) applied to the load sensing pins.

If draft loading fluctuates within the sensitivity band, the lift control valve will remain in the neutral condition and implement depth will remain constant. When low draft sensitivity is selected, a large variation area is allowed in the draft control. This situation provides a more constant implement working depth.

If the draft loading applied to the implement exceeds the sensitivity setting the control valve raising solenoid is energized, and the implement is raised sufficiently until draft loading is restored to the nominal value set by the draft loading control.

When draft loading decreases due to lighter soil being encountered the lowering solenoid would be energized to lower the implement further into the ground and restore the draft force. The working depth of the implement, however, never be lower than that set by the lift arm position control lever.

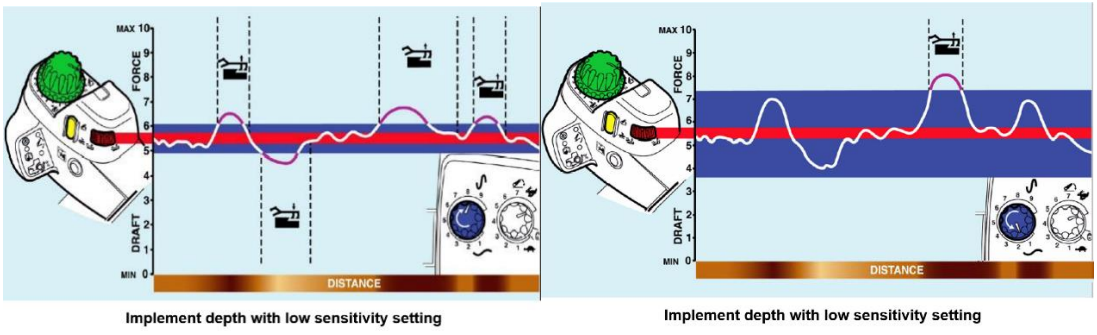

Figure 1.7. The Working Principle of the Electrical Draft Control [8]

When high sensitivity is selected, the draft forces will often reach the minimum and maximum draft control settings. In this situation, the hydraulic control valve will make more corrections to implement depth to achieve the required draft loading [8].

1.2.2.3. Auxiliary Control Mechanisms

Lift-o-matic (LOM): In the field, the driver sets the equipment depth with the help of the position control and draft control. Lift-o-matic enables to lift the equipment up and down back to the same position without canceled the hydraulic lift settings. This feature generally used at the corner of the field. During the cultivating process, when the farmer reaches the end of the territory, s/he activates the lift-o-matic, turns the tractor and deactivates the lift-o-matic.

Slip Control: Slip limit control only occurs in the tractor with the electrical control mechanism. It is directly related to the draft control system. The system reduces the draft set to reduce wheel slip whenever the calculated slip exceeds the slip limit setting. Slip is calculated by using the slip limit potentiometer.

1.2.3. Three-Point Linkage System

Formerly, the tractor just used as a pulling device. Therefore, drawbars are used to transmit the linear force to the equipment, including the plow. The equipment is mounted to the drawbar only in one point.

Figure 1.8. Drawbar

Thanks to the drawbar, the implement could be readily attached and removed and so the tractor to be used for other purposes daily. Moreover, the drawbar still uses for pulling the equipment such as a trailer.

With developing technology, equipment capabilities are increased, so the necessity of the control of the equipment is also increased. Therefore, a three-point hitch mechanism is invented for satisfying this need. As a basic definition, a three-point hitch system is a mechanism, which connects the equipment from three points and gives up and down motion to the implement.

1.2.3.1. History

Three-point hitch firstly had designed by Harry Ferguson in the 1920s and 1930s. Most early tractor plows were mounted to the drawbar only in one point and pulled behind the tractor. The biggest problem was gaining enough traction to put the power to use. Therefore, early tractors were very heavy and employed steel lugs to try and achieve enough traction.

Ferguson began experimenting with mounted plows. Ferguson's mounting system evolved from two link arms (one top, one bottom). Ferguson-Brown model A is produced with Ferguson's three-point system with the help of David Brown in 1933. However, production stopped in 1937 due to the poor sales and disagreements between Ferguson and Brown.

In 1938, Ferguson revealed his hitch system to Henry Ford. Ferguson impressed Ford enough to enter into a production agreement. The N-series tractors became a great success for Ford. In 1947, Henry Ford II was in control of Ford and decided to continue production without Ferguson's involvement. Ferguson began production with another company, which is Massey-Harris in 1959.

The success of the three-point hitch on Ford N-series tractors led other manufacturers to begin building their versions of the hitch. Most major manufacturers developed a

similar hitch, each with variations to avoid violating Ferguson's patents. By 1960, Ferguson's patents had expired and a judge refused to extend them, noting their value to agriculture. The three-point hitch specifications became standardized in the industry by the American Society of Agricultural Engineers (ASAE S217) and the International Organization for Standardization (ISO 730-1) [10].

1.2.3.2. Components

Three-point linkage mechanism is the other name of the three-point hitch system. Linkage means a combination of one upper link and two lower links. In order to connect the implement to the tractor, each of them is mounted to the tractor on one side and mounted to equipment on the opposite side. Next, the hitch point is the articulated connections between link and the attachment and link point is the articulated connection between link and the tractor.

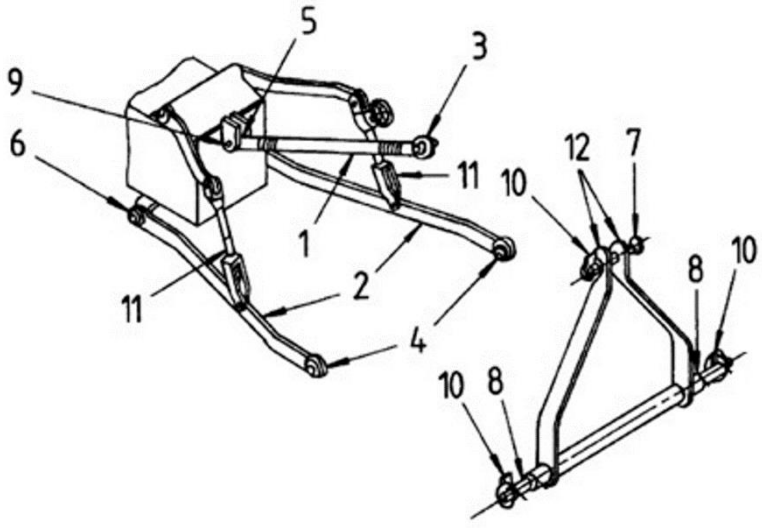

1	Upper link	7	Upper hitch attachment
2	Lower link	8	Lower hitch attachment
3	Upper hitch point	9	Upper link attachment
4	Lower hitch point	10	Linch pin
5	Upper link point	11	Lift rods
6	Lower link point	12	Mast

Figure 1.9. Components of the 3PH [11]

Upper link (1) is an upper linkage element of 3PH. It connects the tractor in the upper link point (5) and connects implement in the upper hitch point (3). In high series tractors, 3PH depth and sensitivity can be arranged by hydraulic top link cylinder. In other cases, the length of the upper link is fixed. Lower links (2) are lower linkage elements, which connect tractor in the lower link, point (6) and connect the implement in lower hitch point (4). They are the other two elements of the three-point hitch. The name of the three-point linkage comes from these three elements. Upper hitch attachment (7) is the pin, which usually detachable and forming part of the upper link assembly. Lower hitch attachments (8) are pin or clevis and pin, usually attached to the implement. Upper link attachment (9) is also pin by which the upper link is connected to the tractor. Linch pin (10) generally fitted with a spring retaining device where an articulated connection is retained in a position [12]. Then, lift rods (11) are the connection elements between the HPL arm and the lower links. They transmit the motion to the lower links during raising and lowering. Due to arranging the mechanism depth, they are adjustable. Next, mast (12) is the component that provides the location of the upper hitch point (4) on the equipment [11].

The 3PL mechanism allows motion in the lateral direction to the tractor due to the use of the knuckle in every connection point. A stabilizer is an adjustable sub-component of the three-point hitch mechanism. It is mounted to lower links and prevent a certain amount of lateral motion from preventing the interference in between wheels and three-point hitch mechanism.

1.2.3.3. Standards

Since a large variety of implements occur, the three-point linkage should be designed by regarding some standards to connect each implement smoothly. ASAE S217.12 and ISO 730-1 are the major authority standards.

First of all, tractors divided into four main categories,

Table 1.1. *Tractor Categories*

Category	Engine Power (kw)
1	up to 48
2	up to 92
3	80 to 185
4	150 to 350

There are some constraints to follow during the design of the 3PL mechanism. The measurements are changed with respect to the category of the tractor. The design constraints are shown in Appendix A.1.

Firstly, mast height (13) is a vertical distance between the upper hitch point and the common axis of the lower hitch points. 3PH mechanism moves with the help of the lift arms. When lift arms move downwards, then mechanism also moves downward and reaches its lowermost position. Lower hitch point height (14) is the height of the center of the lower hitch points with respect to the ground level at the lowermost position of the lift arm and the three-point linkage mechanism.

Next, movement range (15) is the vertical movement of the lower hitch points when the lift arm moves upward from the lowermost position to the uppermost position, and transportation height (16) is the uppermost position of the lower hitch points above the ground. Lower hitch point clearance (17) is the nearest longitudinal distance from the lower hitch point axis to the outside diameter of the tire.

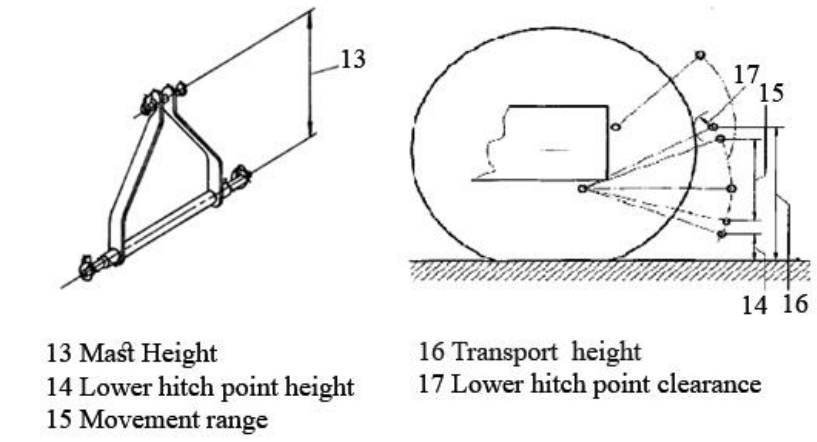

Figure 1.10. Dimensions of the 3PL [11]

When the lower links are in the horizontal with respect to the ground, L measurement corresponds to the maximum distance in between PTO and lower hitch points. Horizontal converge distance (18) is a horizontal distance between the CP_m and lower hitch points. CP_m is the horizontal virtual hitch point where the lower links are coincident virtually when the lower links are horizontal and laterally symmetrical. Vertical convergence distance (19) is a horizontal distance between the CP_v and lower hitch points. CP_v is the vertical convergence distance where the upper link and lower links are coincident virtually when the lower links are horizontal and laterally symmetrical.

3PL is not a rigid structure. There must be gaps and knuckles in the elements connection points to absorb the applied high load. In lower links parallel position, l_1 shows the distance between the lower links and l_2 shows the rocker (left-right motion) distance of the links. Besides, at the time of the motion, the implement angle must not be exceeded the ±5° in the vertical axis to the ground.

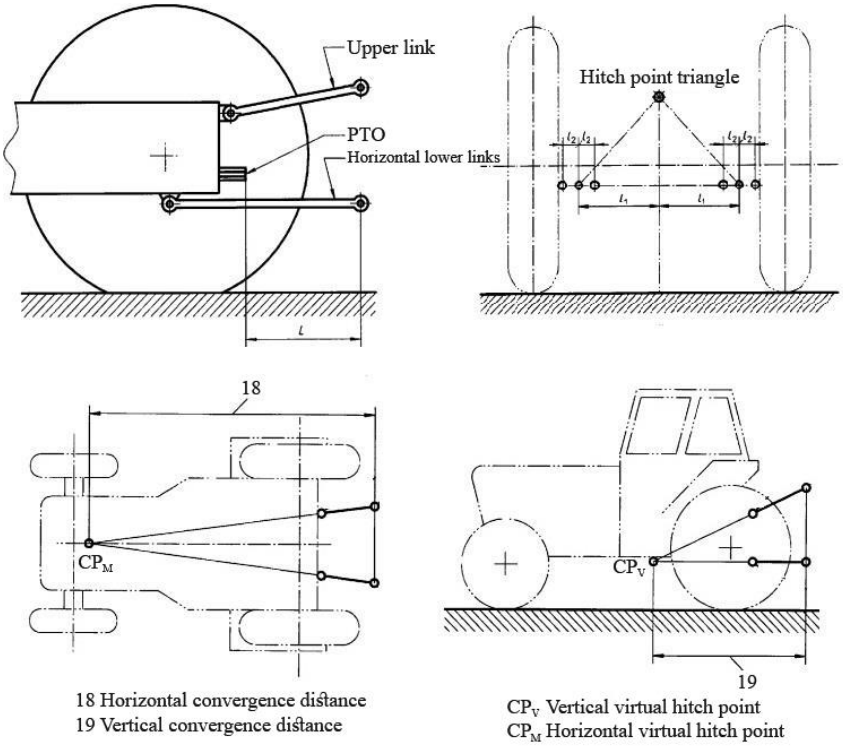

Figure 1.11. Limiting conditions [11]

1.3. Objective of the Thesis

In most of the applications, such as plowing or pulling, hydraulic lift mechanism plays a crucial role in agricultural machine. In order to use hydraulic power efficiently, there should be a control unit in the system. In the past, almost all control mechanisms are mechanical. However, day by day, electrical equipment and controllers supersede the mechanical ones.

In the 3PL mechanism, draft control is presented. Draft control is an important specification that controls draught force or draft load in the tractor that transmits from the implement. In early steps, draft control performed mechanically with the help of the spring or flex bar like in part 1.2.2.2.

With developing technology, sensors take the place of the mechanical controllers. In modern tractors, generally, load cell pins measure the load cell forces and control the 3PL mechanism. In most of the case, load cells are located at the lower links and measured the forces that are acting on the lower link point. By proper transformation equations, this force could be transformed into draught force.

The main purpose of the thesis is that instead of reading and controlling the forces at the load cell that are acting on the lower link point, reading and controlling the pressures from the main cylinders by using pressure sensors. With obtained data, the draft load could be found by using proper conversions, kinematic equations, and mathematical models. Note that, 3PL mechanism force control is not performed with pressure measurement so far.

In the current design, force measurement is done at only one direction, a longitudinal direction. Whereas in new design, the data collected by the pressure sensor cover both axes. For that reason, the new design is more precise than the current design. Secondly, for the electrical system, one of the most expensive sensors is the force sensor. Besides, the support of the load cell also brings cost. The pressure sensor is cheaper than the force sensor, and it does not need support. For that reason, since load sensing force sensors and pins are canceled, the new design is cheaper than the current one.

1.4. Scope of the Thesis

This study has been divided into seven main categories. Chapter 1 gives general information about the tractor and gives detailed information about the hydraulic lift mechanism and controller mechanism. Additionally, the main purpose of the thesis is given in this part. In chapter 2, theoretical information of the mechanism is given, and a literature survey about the 3PL mechanism and any other related subjects are presented. In the third chapter, the methodology of the design is explained. The detailed presentation of each study can be found in this chapter. Mainly, it focusses on the modeling and analysis of the 3PL mechanism, modeling of the hydraulic system and controller design. Test materials and their specifications are handled in chapter 4. All test process explains in that chapter, and some certain scenarios in the field test are discussed. The results of selected scenarios are also shown in this section. Simulations for the current system and proposed new systems are performed by regarding the test data in Chapter 5. Note that, determination of control gains are also discussed in this chapter. Outline of the study, general conclusions, and discussions about the study are presented in Chapter 6. Additionally, recommendations and future works are also handled in this chapter. A list of reference and appendix section can be found in Chapter 7.

CHAPTER 2

LITERATURE SURVEY

2.1. Literature Overview

In the literature, there are numerous resources about the tractor HPL mechanism and measurement of the draft force. HPL and three-point linkage mechanisms have been studied for many years, as can be understood from the literature. On the other hand, for the draft control mechanism, especially about the thesis topic, there are restricted resources that occurred in the literature. For this reason, it is planned to write a patent about pressure operated draft control mechanism.

The tractor has a large variety of sub-components. As the quantity of the part, the tractor has two even three times greater components than an automobile. Therefore, books [13], [14], [15] and catalogs [8], [16], [17] are the best choice to understand the tractor and components better. Additionally, patents [18], [19], [20] are a good choice to investigate the development of the mechanisms.

HPL mechanism and 3PL mechanism are the main issues of the thesis. Therefore, details about these mechanisms [6], [7], [21], [22] must be well known in order to design a new mechanism.

There are many types of equipment such as plow, chisel plough, or tiller. In order to connect all equipment to the same tractor at a certain category, ISO 730-1 [12] and ASABE S217.12 [11] standards occur. During the design process of the 3PL mechanism, these standards must be considered.

The main issue of the study is controlling the draft force with the measurement data coming from the pressure sensors instead of controlling with the measurement values of the force sensor. Note that, 3PL mechanism force control is not performed with

pressure measurement so far. For that reason, measuring the draft load during the cultivation process is an important issue in order to evaluate the new design.

Researchers have generally focused on three types of measuring methods based on the location of the force transducers. In reality, there is no method to measure the forces acting upon directly to the equipment. Therefore, the force transducers are located at any particular position, and the draft load is estimated by transforming the measured forces.

In the first method, [23], [24] the measurement sensors such as force sensor, are directly mounted to the contacting surface of the equipment to the soil like plough moldboard surface. Three orthogonal forces could be measured with the help of the mounted sensors. Since the draft load is directly measured, this system gives a precise idea about the strain distribution of the implement. However, it is expensive because each tested tool has to be equipped with sensors. Moreover, the transducer's installation is required for some changes to implement global geometry that could modify the soil–tool interaction and the tool weight. On the other side, in reality, under cultivating conditions, there is no possibility of applying this method.
In the second method, [25] transducers are mounted to the separate frame for measuring the forces between the tractor and implements. Frames are interchangeable between different tractors and tools and are easy to manufacture. On the other side, this system does not reflect real working conditions due to the two reasons. Firstly, in order to fix the transducers, the system requires a heavy frame that causes a change of the total weight. Secondly, fixing the transducers and the frame to the tractor necessitates many extra elements at the articulations that are a source of error in the measurements.

In the last and most preferred method, [26] transducers are mounted to 3PL mechanism certain locations like upper link, lower links, lift rods, or HPL arms. In the majority of the published work, researchers are considered the 3PH mechanism as a planar system. System was modeled in two-dimensions to represent the forces in the

original geometrical configuration between the tractor and the implement [27]. This two-dimensional approximation, which causes the loss of the lateral force, can be accepted for the studies of symmetric implements such as chisel plough.

The majority of the studies take the tractor longitudinal axis as an “x” axis, and lateral component as a “z” axis and the remaining vertical axis takes as a “y” axis. In the thesis, all calculations are performed according to that Cartesian plane.

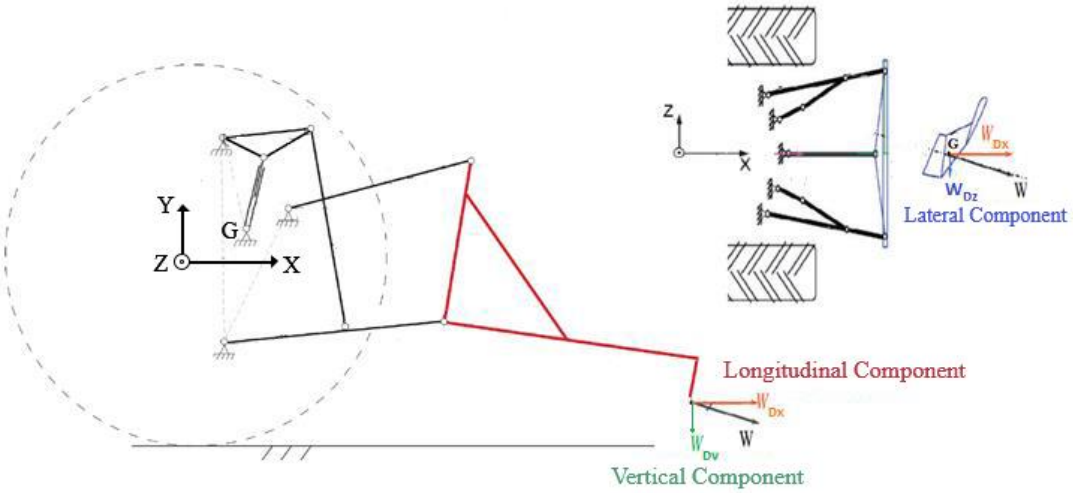

Figure 2.1. Cartesian Plane of the Tractor

Depth of the operation, tractor-implement characteristic, speed of the tractor, type of soil are the major variables affecting the draft load. There are lots of studies [28], [29], [23] about predicting the draft load for different tillage implements in different soil and working conditions. There is also [30] ASAE-D497.4 standard available about the draft requirements.

Studies show that draft load is increased when the depth of operation and speed of the tractor are increased. A large variety of implement is available, and tractor-implement characteristic is changed implement to implement. Machine specific parameters determine the implement characteristic. The most heavy-duty implement is a moldboard plow. Next, implement width must be considered. When the width of the implement is increased, the draft load is also increased.

There are many kinds of soil on earth. Therefore, they are categorized by the standard. Draft parameters and an expected range in drafts estimated by the model parameters for tillage and seeding implements table is shown in Appendix B.

According to the ASAE-D497.4, theoretical draft requirements can be calculated as,

$$W_D = F_i * [A + B * (T_s) + C * (T_s)^2] * W_e * T_D \quad (2.1)$$

In the formula, W_D is implement draft load (N), F_i is a dimensionless soil texture adjustment parameter where i is the category of the soil. 1 for fine, 2 for medium and 3 for coarse-textured soils. A, B, and C are machine-specific parameters. T_s is tractor field speed (km/h). W_e is equipment width, (m). T_D is tillage depth, (cm) for major tools. For minor tillage tools and seeding implements, T_D should be taken as a unity, 1. The details about the variables occur in Appendix B.

The main idea of the study is instead of prediction and optimization of the draft load, control the draft load effectively. Therefore, the magnitude of the force acting from implement is not important. Although there are lots of additional research about the prediction and optimization of the implement draft load, there is no need to spend extra effort to investigate the draft load.

The resistance of the soil creates a draft load force from the implement. Then, it is transmitted to the tractor with the help of the 3PL element. 3PH mechanism elevation control is provided by the interpretation of the measured values from the sensors. In order to control the implement properly, theoretical force transmission analysis should be made consummately. For this reason, kinematic analysis and mathematical model of the 3PH mechanism have a key role in transmitting the draft load force to the sensor locations.

[26], [31] [32] and [33] are the studies about the kinematic and force analysis of the 3PL mechanism. In [26], the coordinates of each joint are calculated in the Cartesian coordinate system (X_0, Y_0, Z_0) with I_0, the center of the rear wheel, as the point of the origin. The calculus equations of all the pin-joint positions are developed. The position

of the tillage application point ‘‘G’’ is a reference to this coordinate system. Then, the force equilibrium of the system and other related equations are calculated by using force and moment equilibriums.

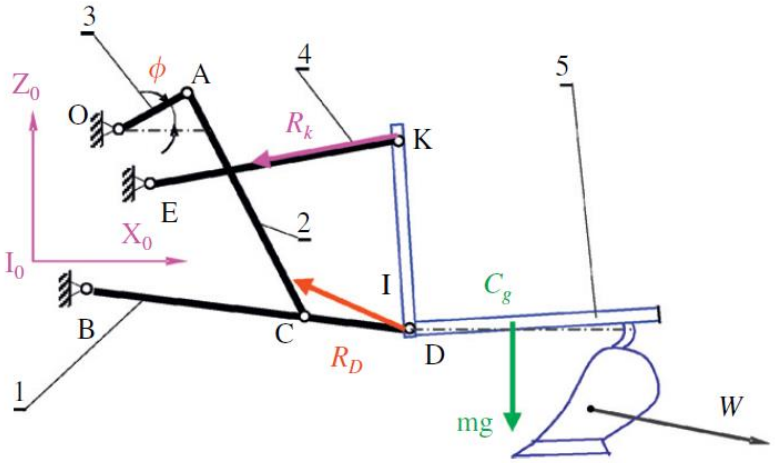

Figure 2.2. Free body diagram of implement and 3PH mechanism in Bentaher model [26]

In the Laceklis-Bertmanis study [33], the 3PH mechanism was considered as a planar system like previous ones. In order to evaluate the draught force of tillage tools, a two-dimensional study of the 3PL mechanism is needed. The mechanisms consist of seven articulated beams. For simplicity, the mechanism is described by ties and pin joints. The coordinates of each joint are calculated in a global coordinate system.

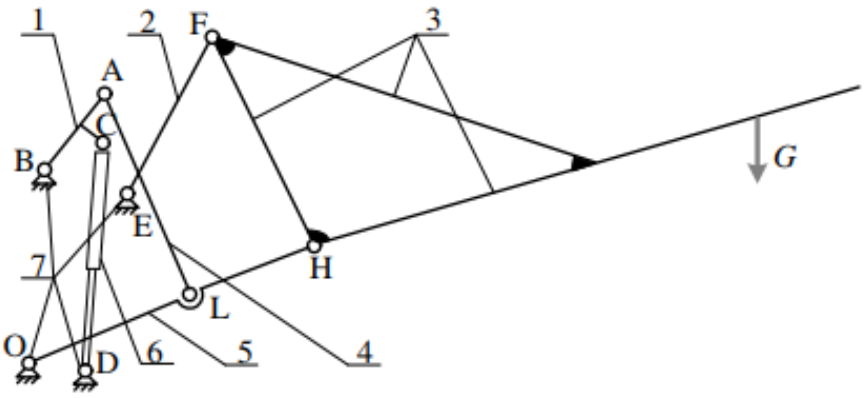

Figure 2.3. Side view of the 3PL mechanism in Laceklis-Bertmanis model [33]

In Figure 2.3, 1 corresponds to the HPL arm, and 2 corresponds to upper link. These links are adjustable like in a test tractor. Next, 3 is the simplified version of the implement, 4 is lift rod, 5 is lower link, 6 is an external lift rod, and 7 is support.

Physically, 3PH mechanism has two lower links, two lift rods, two HPL arms, and two external lift rods. However, theoretically, since the mechanism is modeled in two-dimensions, lower links, lift rods, HPL arms and external lift rods are taken as one. In the formulation part, this situation is considered, and these component forces multiply with two.

Firstly, the draft load is distributed to lower links and upper link. Then, the force that exerted to the lower link hitch point is calculated with the help of the lower link. The free-body diagram of the distributed mechanism and lower link are shown in Figure 2.4.

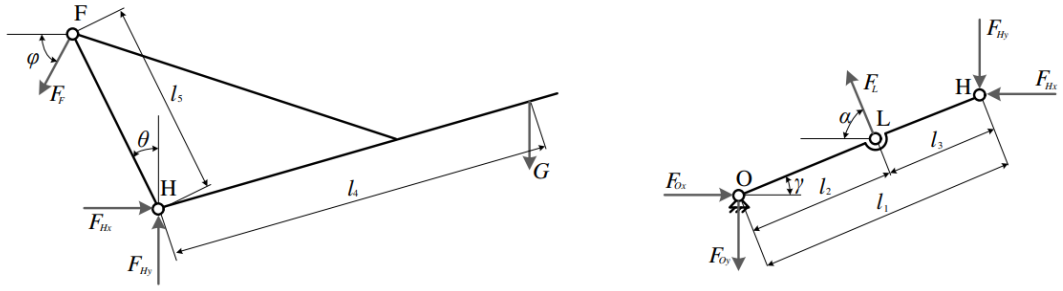

Figure 2.4. Unit of upper link and implement (left) and hitch system lower link unit (right) [33]

The projections of forces and moment of the unit of the upper link and implement give the following system of equations,

$$\mathrm{Ey_i} = 0$$

$$\mathrm{F_f} * \sin(\varphi) + \mathrm{F_{Hy}} - \mathrm{G} = 0 \tag{2.2}$$

$$\mathrm{Ex_i} = 0$$

$$\mathrm{F_f} * \cos(\varphi) + \mathrm{F_{Hx}} = 0 \tag{2.3}$$

$$\mathrm{EM_H} = 0$$

$$\mathrm{F_f} * \cos(\varphi) * \mathrm{l_4} * \cos(\theta) + \mathrm{F_f} * \sin(\varphi) * \mathrm{l_5} * \sin(\theta) - \mathrm{G} * \mathrm{l_4} * \sin(\theta) = 0 \tag{2.4}$$

The F_f, F_{Hx} and F_{Hy} are the lift rod reaction forces at point F, and H. G is the weight of the implement. During the cultivating process, draft load W_D must be added to the system. The lower link one side is connected to the tractor frame, and the other side is connected with the implement lower support.

The projections of forces and moment of the lower link give the following system of equations,

$$Ey_i = 0$$

$$-F_{Oy} + F_L * \sin(\alpha) - F_{Hy} = 0 \quad (2.5)$$

$$Ex_i = 0$$

$$-F_{Ox} - F_L * \cos(\alpha) - F_{Hx} = 0 \quad (2.6)$$

$$EM_o = 0$$

$$F_L * \sin(\alpha) * l_2 * \cos(\gamma) + F_L * \cos(\alpha) * l_2 * \sin(\gamma) - F_{Hy} * l_1 * \cos(\gamma) + F_{Hx} * l_1 * \sin(\gamma) = 0 \quad (2.7)$$

where F_{Ox} and F_{Oy} are the reaction force at point O, but F_L is the reaction force at point L. These values depend on the tractor hitch-system cylinder position.

The kinematic equations in the thesis have been established based upon the reference [33]. Equations in the range 2.2 to 2.6 are directly related to the reference. The symbols in methodology part kinematic equations are different from literature survey part equation symbols.

CHAPTER 3

DESIGN METHODOLOGY

In order to establish a new feature of the vehicle, it is necessary to model the existing physical system. In this direction, the current tractor system will be patterned and verified with test data. Then, the new system would be integrated into the verified model. In design methodology part, every sub-component of the system will be discussed in detail.

The tractor with the EDC system has a classical closed-loop control system block diagram. The hydraulic valve system and hydraulic cylinder are the actuators of the mechanism. 3PH mechanism is the plant of the system. The controller is the ECU of the tractor. As a MATLAB® Simulink tool, Stateflow is used in the control algorithm. Position sensor potentiometer, load cells, and pressure sensors are count as feedback elements of the mechanism.

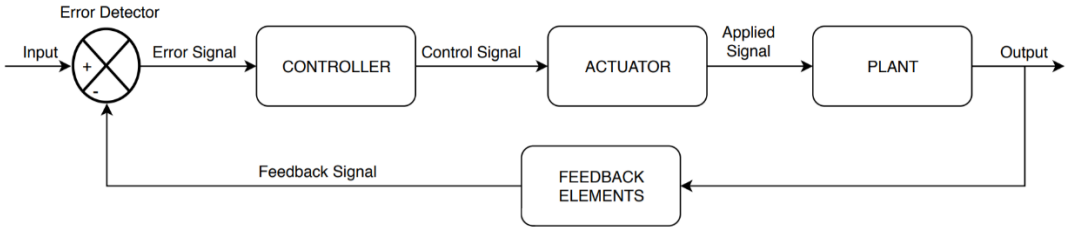

Figure 3.1. Control system block diagram

3.1. Plant Design

A plant in control theory is a process, so the 3PL mechanism is the process of the system. In order to use transformation equations, 3PL mechanism kinematic analysis and force analysis is performed. Moreover, the mechanism is also modeled in a solid

model and integrated into the system. Both models will be explained further section in depth.

3.1.1. 3PL Kinematic and Force Analysis and ADAMS Model

The main element of the system is the 3PL mechanism. For that reason, it is better to comprehend the mechanism by dividing it and handling every part in depth. Transformation equations that are used in many parts of the thesis are formed with the kinematic analysis and force analysis. In the light of this information, the theory of the 3PL system design has a key role in analyzing the whole system.

For simplicity, kinematic analysis begins with the free body diagram.

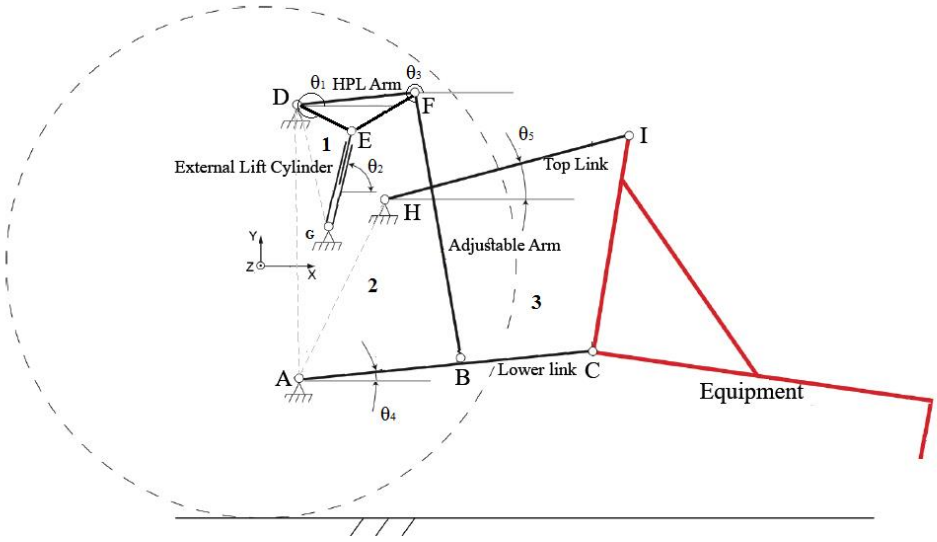

Figure 3.2. Free body diagram of the 3PL mechanism

As a type of lifting mechanism, the tractor has external lift cylinders. They are the actuator of the 3PL mechanism. In the system, “x” axis is the longitudinal component and “y” axis is the vertical component. It is assumed that the lateral component forces are neglected and so the system is analyzed as two-dimensional. Additionally, the center of the rear tire is count as an origin or word frame of the tractor.

External lift cylinder, HPL arm, adjustable arm, lower link, top link, and equipment are the main components of the mechanism. The motion given to external lift cylinders is firstly transferred to the HPL arm. Then the motion is transmitted to the equipment with the help of the adjustable arm and lower link. Actually, in the physical system, there are two pieces of external lift cylinders, HPL arms, adjustable arms and lower links exist. Yet, in the free body diagram, since it is assumed that the system is two-dimensional, these parts seem like a single. During the calculations, this situation will be considered.

Mainly, there are three connection joints in the equipment. Lower arms are connected to the 3PL mechanism lower hitch points. The remaining joint is connected to the top link upper hitch point to get balance the system. All components are shown as a link in the free-body diagram. In the meantime, the red links represent the implement.

There are two four bars and one three bar in the 3PH mechanism. The first loop, DGE, is a three-bar mechanism which corresponds to the transformation from external lift cylinders to the HPL arm.

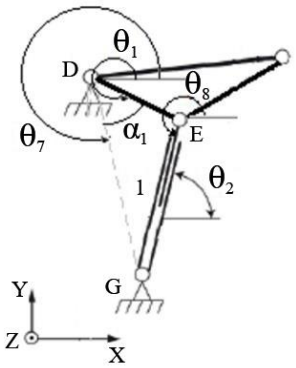

Figure 3.3. FBD of first loop, DGE

The loop closure equation of the three -ar mechanism is;

$$|DG| * e^{j\theta_7} = |DE| * e^{j\theta_1} + |EG| * e^{j\theta_8}$$

$$|DG| * cos(\theta_7) = |DE| * cos(\theta_1) + |EG| * cos(\theta_8) \quad (3.1)$$

$$|DG| * sin(\theta_7) = |DE| * sin(\theta_1) + |EG| * sin(\theta_8) \quad (3.2)$$

The length of the external lift cylinder, link |EG|, is changeable. Point D and G are the fix points, and the coordinates are;

D(130,410), G(250.1,-30)

In the model, the external lift cylinder length is the input, the angle of body |DG|, θ_7, is a constant value. Then, the angle of the HPL arm, θ_1, and the angle of the external lift cylinder, θ_2, are the unknowns.

Then;

$$\alpha_1 = acos\left(\frac{|DG|^2+|DE|^2-{s_1}^2}{2*|DG|*|DE|}\right) \tag{3.3}$$

$$\theta_1 = \theta_7 + \alpha_1 \tag{3.4}$$

$$\theta_2 = \theta_8 - \pi \tag{3.5}$$

From equations (3.1) and (3.4);

$$\theta_8 = 2 * \pi - acos\left(\frac{|DG|*cos(\theta_7)-|DE|*cos(\theta_1)}{s1}\right) \tag{3.6}$$

The second loop ABFD is a four-bar mechanism which corresponds to the transformation from HPL arm to the equipment lower arms with the help of the adjustable arm and lower link.

For that system, the angle of body |DA|, θ_{11}, and |FDE| angle, α_2, are the constant values, and the HPL arm angle is the input. The angle of the adjustable arm, θ_3, and the angle of lower link, θ_4, are the unknowns that are found from the loop closure equation and cosine theorem.

Typically, the length of the adjustable arm, BF, is alterable. However, a farmer does not tamper the adjustable arm setting during the cultivating process. They arrange it only at the beginning of the cultivating. During the test, before starting the process, the length of the adjustable arm is recorded and this value is used in all calculations. For that reason, the length of the adjustable arm is taken as a constant in all calculations.

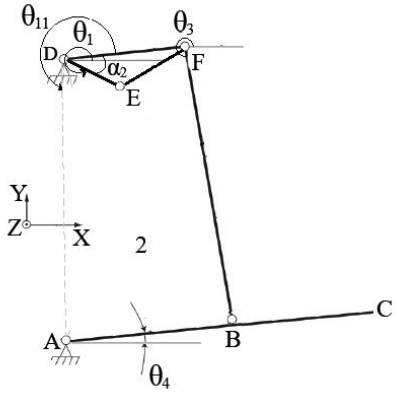

Figure 3.4. FBD of second loop, ABFD

Next, lower link, AC, is mounted to the equipment at point C, which connects with the adjustable arm at point B and is fixed to the body at point A. Point A is the location where the force sensors or load cells are mounted. In the mechanism, there are two fix points. The coordinates are written according to the center of the rear tire.

A (160.1, -212), D(130,410)

The loop closure equation for ABFD is;

$$|DA| * e^{j\theta_{11}} = |DF| * e^{j(\theta_1+\alpha_2)} + |FB| * e^{j\theta_3} + |BA| * e^{j(\theta_4+\pi)}$$

$$|DA| * cos(\theta_{11}) = |DF| * cos(\theta_1 + \alpha_2) + |FB| * cos(\theta_3) + |BA| * cos(\theta_4 + \pi) \quad (3.7)$$

$$|DA| * sin(\theta_{11}) = |DF| * sin(\theta_1 + \alpha_2) + |FB| * sin(\theta_3) + |BA| * sin(\theta_4 + \pi) \quad (3.8)$$

Then, from cosine theorem;

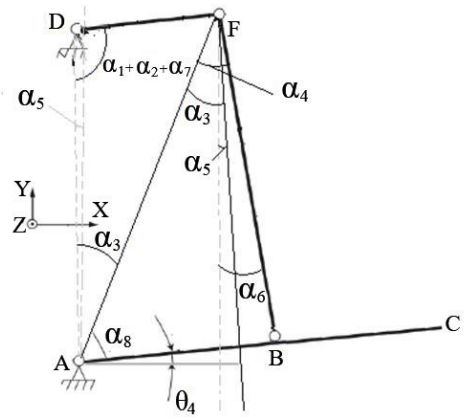

Figure 3.5. Cosine theorem of loop ABFD

α_7 is the angle in between the bodies |DG| and |DA|;

$$\alpha_7 = acos\left(\frac{|DG|^2 + |DA|^2 - |AG|^2}{2 * |DG| * |DA|}\right) \tag{3.9}$$

Remaining equations are;

$$\alpha_5 = \theta_{11} - \pi \tag{3.10}$$

$$|AF| = \sqrt{|DF|^2 + |AD|^2 - 2 * |AD| * |AD| * cos(\alpha_1 + \alpha_2 + \alpha_7)} \tag{3.11}$$

$$\alpha_3 = acos\left(\frac{|AF|^2 + |DA|^2 - |DF|^2}{2 * |DF| * |DA|}\right) \tag{3.12}$$

$$\alpha_4 = acos\left(\frac{|AF|^2 + |FB|^2 - |AB|^2}{2 * |AF| * |FB|}\right) \tag{3.13}$$

$$\alpha_6 = \alpha_4 - \alpha_3 + \alpha_5 \tag{3.14}$$

$$\theta_3 = \frac{3\pi}{2} + \alpha_6 \tag{*3.15*}$$

θ_4 angle could be found in two ways. Firstly, from cosine theorem;

$$\alpha_8 = \text{acos}\left(\frac{|\text{AF}|^2 + |\text{AB}|^2 - |\text{FB}|^2}{2 * |\text{AF}| * |\text{AB}|}\right) \tag{3.16}$$

$$\theta_4 = \frac{\pi}{2} - \alpha_8 - \alpha_3 + \alpha_5 \tag{3.17}$$

Or it can be found from equation (3.7) and (3.15);

$$\theta_4 = \text{acos}(|DA| * \cos(\theta_{11}) - |DF| * \cos(\theta_1 + \alpha_2) - |FB| * \cos(\theta_3)) - \pi \tag{3.18}$$

Now, the angle of the adjustable arm and the angle of lower link are the known variables.

The third loop ACIH is again a four-bar mechanism which corresponds to the transformation from top link to equipment upper arm and lower link to equipment lower arms.

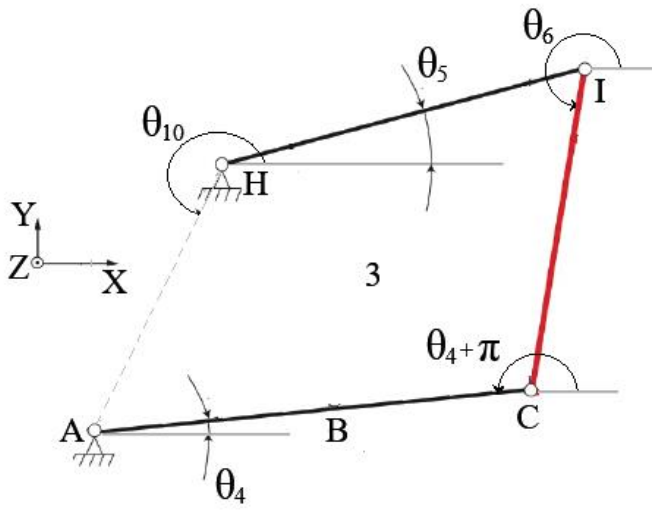

Figure 3.6. FBD of third loop, ACIH

Nearly the same procedure is applied with loop 2. In the system, the angle of body |AH|, θ_{10}, is constant. Moreover, the angle of the lower link, θ_4, is known from loop 2. The angle of the top link, θ_5, and the angle of the implement, θ_6, are the unknowns. Normally, the length of the top link, |HI| is changeable. Like adjustable arm, the farmer arranges the length of the top link only at the beginning of the cultivating. Therefore, it is assumed that the top link length is constant and it is measured and recorded just before the test.

Next, in the mechanism, there are two fix points. The coordinates are written according to the center of the rear tire.

A (160.1, -212), H(430.1,285)

The loop closure equation for ACIH is;

$$|HA| * e^{j\theta_{10}} = |HI| * e^{j(\theta_5)} + |IC| * e^{j\theta_6} + |CA| * e^{j(\theta_4+\pi)}$$

$$|HA| * cos(\theta_{10}) = |HI| * cos(\theta_5) + |IC| * cos(\theta_6) + |CA| * cos(\theta_4 + \pi) \quad (3.19)$$

$$|HA| * sin(\theta_{10}) = |HI| * sin(\theta_5) + |IC| * sin(\theta_6) + |CA| * sin(\theta_4 + \pi) \quad (3.20)$$

Next, from cosine theorem,

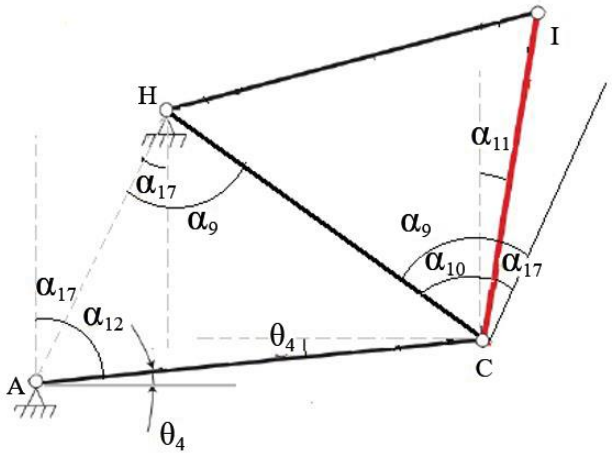

Figure 3.7. Cosine theorem of loop ACIH

In cosine theorem, following equations are written;

$$\alpha_{17} = \frac{3\pi}{2} - \theta_{10} \tag{3.21}$$

$$\alpha_9 = acos\left(\frac{|HA|^2 + |HC|^2 - |AC|^2}{2 * |HA| * |HC|}\right) \tag{3.22}$$

$$\alpha_{12} = \frac{\pi}{2} - \alpha_{17} - \theta_4 \tag{3.23}$$

$$|HC| = \sqrt{|HA|^2 + |AC|^2 - 2 * |HA| * |AC| * cos(\alpha_{12})} \tag{3.24}$$

$$\alpha_{10} = acos\left(\frac{|IC|^2 + |HC|^2 - |HI|^2}{2 * |IC| * |HC|}\right) \tag{3.25}$$

$$\alpha_{11} = \alpha_9 - \alpha_{17} - \alpha_{10} \tag{3.26}$$

$$\theta_6 = \frac{3\pi}{2} + \alpha_{11} \tag{3.27}$$

Then from equation (3.27) and (3.19);

$$\theta_5 = \text{acos}\left(\frac{|HA| * \cos(\theta_{10}) - |IC| * \cos(\theta_6) - |CA| * \cos(\theta_4 + \pi)}{|HI|}\right) \tag{3.28}$$

The kinematic model MATLAB code is shown in Appendix C. The whole stroke of the external cylinder is simulated in the code. One of the steps of the simulation is shown in Figure 3.8.

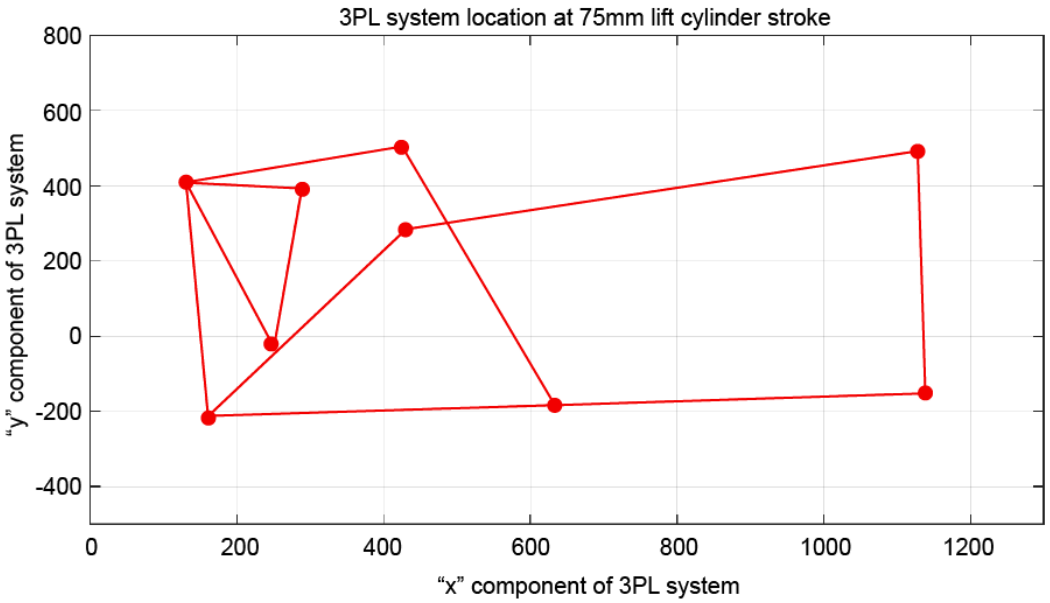

Figure 3.8. 3PL mechanism MATLAB simulation

Some assumptions are made during the calculations. There is a load cell in the lower link at point A. Load cells only read the longitudinal force during the cultivating process. Therefore, only the longitudinal axis take into account in the course of the calculation of the forces at point A. Note that, according to the reference [26], the effect of the vertical load is very small with respect to the longitudinal load. Therefore, this assumption is not to influence the system too much. The pressure sensors are integrated into the system and measure the external lift pressure, P_1, and top link pressure, P_2. Besides, since the model is two-dimensional and neglected the z-axis, it is assumed that the lateral component forces are negligible. Additionally, since the movement of the system is slow, the masses and the effect of moment of inertia of the components are neglected during the analysis.

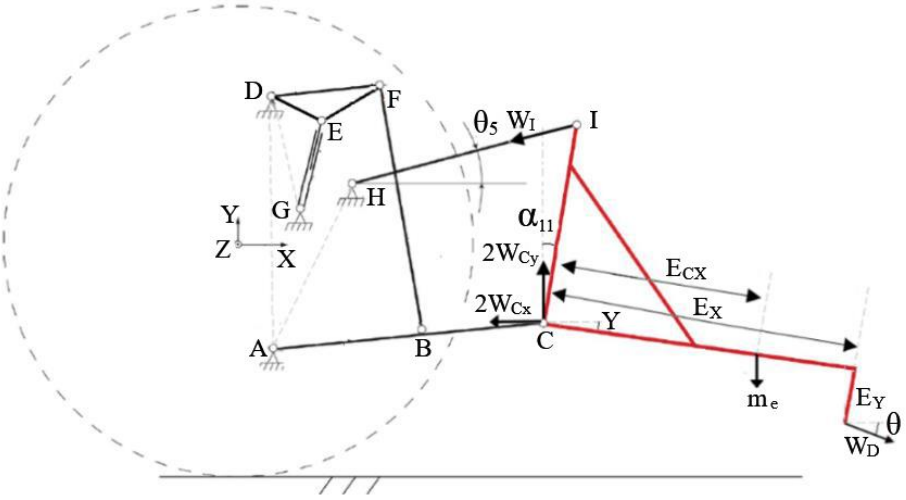

Figure 3.9. Force diagram of the 3PH mechanism

Force analysis is the second part of the theory. The moment equilibrium with respect to the point C could be written by regarding the reference [33]. Draught force, W_D, is the disturbance of the system. It is the applied force to the implement from the soil. In force analysis, it might be taken as an input. By the way, normally, in the 3PL system, there are two lower links, HPL arms, and external lifts. However, since the model is two-dimensional, they are seen as a single link. Therefore, equipment to implement connection point force, $W_{c,}$ must be multiplied with two during the force analysis. The weight of the implement, $m_{e,}$ and top link force, W_I are the other variables in the force body diagram.

In the system, implement vertical and longitudinal distances are varied at every changing position of the mechanism. In order to calculate them, the following calculations must be taken into account.

$$E_{xx} = E_x * cos(\gamma)$$

$$E_{xy} = E_x * sin(\gamma)$$

$$E_{yy} = E_y * cos(\gamma)$$

$$E_{yx} = E_y * sin(\gamma) \quad (3.29)$$

$$E_{xt} = E_{xx} + E_{yx}$$

$$E_{yt} = E_{yy} - E_{xy}$$

$$E_{cxx} = E_{cx} * cos(\gamma)$$

$$E_{xxy} = E_{cy} * sin(\gamma)$$

The angle of the equipment γ plays an important role in the change of the values. Next, the forces are calculated as;

$$\sum F_x = 0;$$

$$W_D * cos(\theta) - W_I * cos(-\theta_5) - 2 * W_{Cx} = 0 \tag{3.30}$$

$$\sum F_y = 0;$$

$$-W_D * sin(\theta) - m * g + W_I * sin(-\theta_5) + 2 * W_{Cy} = 0 \tag{3.31}$$

$$\sum M_c = 0;$$

$$W_D * cos(\theta) * E_{yt} - W_D * sin(\theta) * E_{xt} - m * g * E_{cxx} + W_I * cos(-\theta_5) * |IC| * cos(\alpha_{11}) \tag{3.32}$$

$$-W_I * sin(-\theta_5) * |IC| * sin(\alpha_{11}) = 0$$

Then from equations (3.30), (3.31) and (3.32).

$$W_I = \frac{W_D * sin(\theta) * E_{xt} + m * g * E_{cxx} - W_D * cos(\theta) * E_{yt}}{cos(-\theta_5) * |IC| * cos(\alpha_{11}) - sin(-\theta_5) * |IC| * sin(\alpha_{11})} \tag{3.33}$$

$$W_{Cx} = \frac{W_D * cos(\theta) - W_I * cos(-\theta_5)}{2} \tag{3.34}$$

$$W_{Cy} = \frac{W_D * sin(\theta) + m * g - W_I * sin(-\theta_5)}{2} \tag{3.35}$$

Now, top link force and equipment to implement connection point force are the known values. Next, to determine the load cell force, W_A, and adjustable arm force, W_B, force, and momentum equilibrium equations should be calculated in lower link.

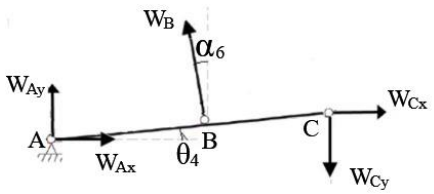

Figure 3.10. Force body diagram of the lower link

$$\sum F_x = 0;$$

$$W_{Ax} - W_B * sin(\alpha_6) + W_{Cx} = 0 \tag{3.36}$$

$$\sum F_y = 0;$$

$$W_{Ay} + W_B * cos(\alpha_6) - W_{Cy} = 0 \tag{3.37}$$

$$\sum M_A = 0;$$

$$W_B * cos(\alpha_6) * |AB| * cos(\theta_4) + W_B * sin(\alpha_6) * |AB| * sin(\theta_4) - W_{Cx} * |AC| * sin(\theta_4) \tag{3.38}$$

$$- W_{Cy} * |AC| * cos(\theta_4) = 0$$

Then, from equation (3.36), (3.37) and (3.38) W_B, and W_A values are;

$$W_B = \frac{W_{Cy}*|AC|*\cos(\theta_4)+W_{Cx}*|AC|*\sin(\theta_4)}{|AB|*\cos(\alpha_6)*\cos(\theta_4)+|AB|*sin(\alpha_6)*s\,in(\theta_4)} \tag{3.39}$$

$$W_{Ax} = W_B * sin(\alpha_6) - W_{Cx} \tag{3.40}$$

$$W_{Ay} = -W_B * cos(\alpha_6) + W_{Cy} \tag{3.41}$$

In the system, since load cells are measured just the longitudinal forces that are acting on the lower links from point A, the load cell forces are W_{Ax} values.

Since the adjustable arm is a two-force member, the adjustable arm force is directly acting to the HPL arm. Besides, W_E is the external lift cylinder force.

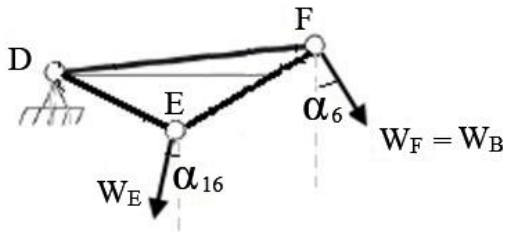

Figure 3.11. Force body diagram of the HPL arm

From equation (3.5), angle α_{16} is;

$$\alpha_{16} = \frac{3\pi}{2} - \theta_8 \tag{3.42}$$

$$\sum M_D = 0;$$

$$W_B * cos(\alpha_6) * |DF| * cos(\theta_1 + \alpha_2) + W_B * sin(\alpha_6) * |DF| * sin(\theta_1 + \alpha_2) \quad (3.43)$$

$$-W_E * |DE| * cos(\alpha_{16}) * cos(\theta_1) - W_E * |DE| * sin(\alpha_{16}) * sin(\theta_1) = 0$$

Then, the external lift cylinder piston forces, W_E are;

$$W_E = \frac{W_B * \cos(\alpha_6) * |DF| * \cos(\theta_1 + \alpha_2) + W_B * \sin(\alpha_6) * |DF| * \sin(\theta_1 + \alpha_2)}{|DE| * \cos(\alpha_{16}) * \cos(\theta_1) + |DE| * \sin(\alpha_{16}) * \sin(\theta_1)} \quad (3.44)$$

Finally, the pressures from external lift cylinder, P_1 and top link P_2 are found as;

$$P_1 = \frac{W_E}{A_1} \quad where\ A_1 = 5026.5\ mm^2 \quad (3.45)$$

$$P_2 = \frac{W_I}{A_2} \quad where\ A_2 = 3117.2\ mm^2 \quad (3.46)$$

Now, all angles and forces are known in the model. Draught force and the length of the external lift cylinder are the input of the establishing MATLAB® model. The stroke of the cylinder, Se, actually change the length of the cylinder. For that reason;

$$|EG| = |EG_i| + S_e \quad (3.47)$$

If the user gives particular value to the draught force, then the forces acting on the top link W_I, load sensor W_{Ax} and external lift cylinder, W_E could be tabulated in the code with respect to the stroke interval of the lift cylinder easily. The MATLAB® code of the force analysis occurs in Appendix C.

While performing the force analysis for each angle in MATLAB®, a similar procedure is applied in the ADAMS® software at the same time. The results are compared with ADAMS® data and MATLAB® data to check the accuracy of the kinematic model and force model.

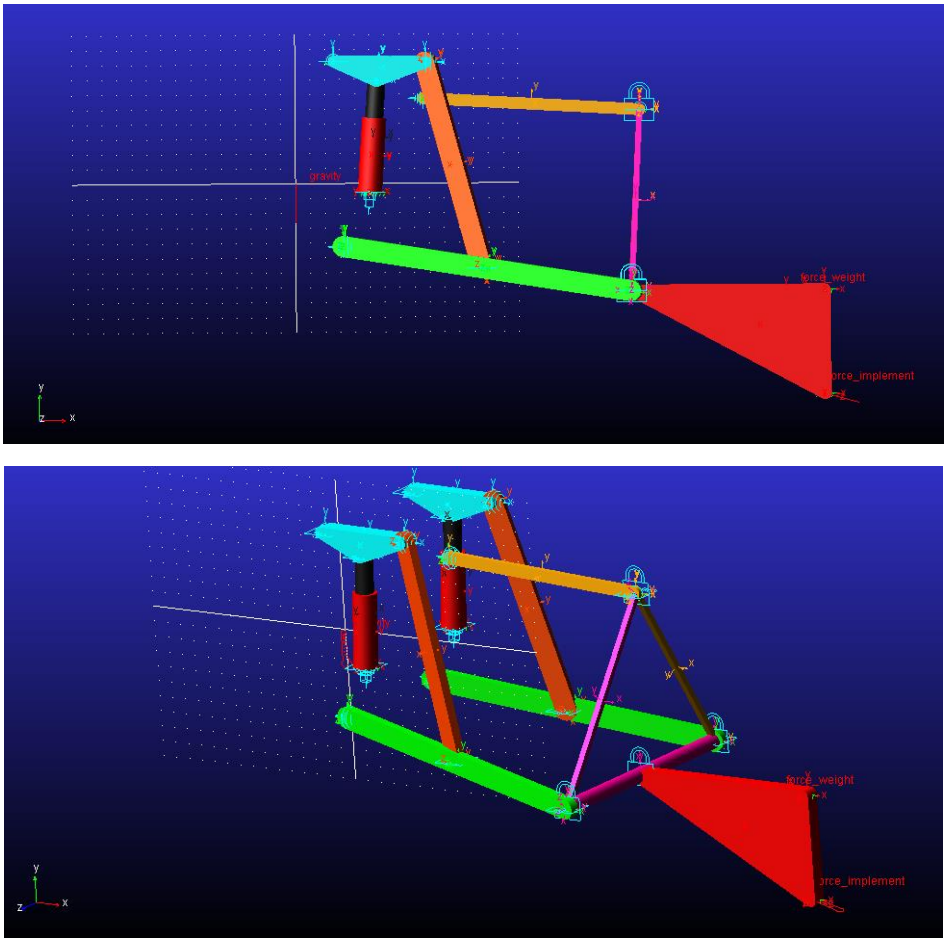

Figure 3.12. 2D and 3D view of the ADAMS model

In ADAMS®, since the system movement is not fast, the effect of moment of inertia is neglected like the kinematic analysis. Therefore, masses of the components are not taken into account, and the mechanism is modeled just by using simple links like the previous model. The mass of the implement, m_e is added to the system as an external force from the center of gravity of the implement. The coordinate system of the ADAMS® model is the same as with the MATLAB® model.

To verify the MATLAB® results, an 18 kN draught force is given to both systems. Under normal working conditions, the angle of draught force varies according to different equipment and according to the implement working depth. However, in the model, it is assumed that the angle of the draught force is constant, which is 15°. Draught force and its angle value are determined by the test values. The stroke of the

cylinder, S_e, is 175 mm and the initial length of the external lift cylinder $|EG_i|$ is 375 mm. Under the defined load, some certain points applied forces along the whole movement of the cylinder are tabulated both for MATLAB® model and ADAMS® model.

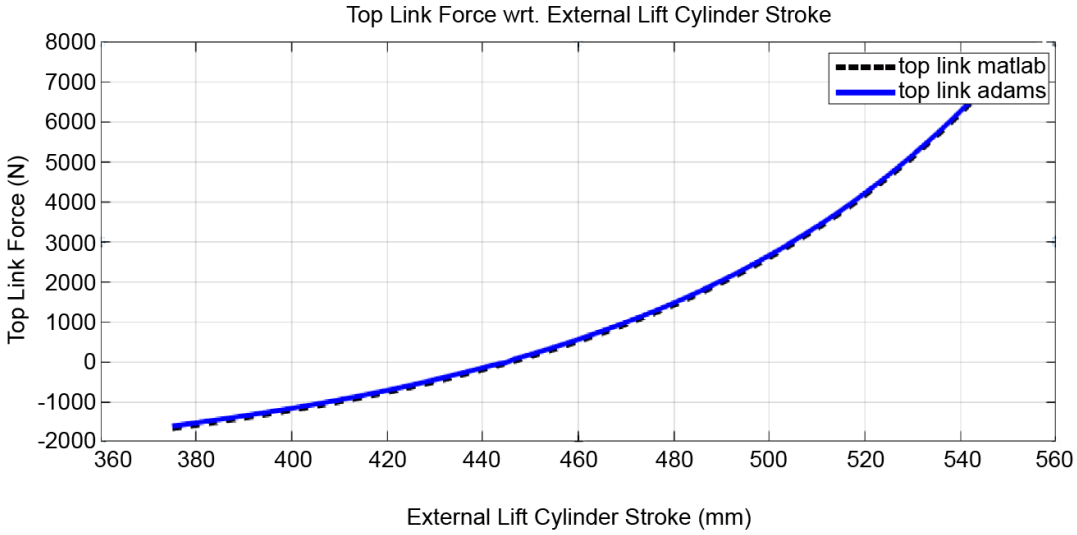

Figure 3.13. Top link force vs. lift cylinder stroke comparison for MATLAB and ADAMS models

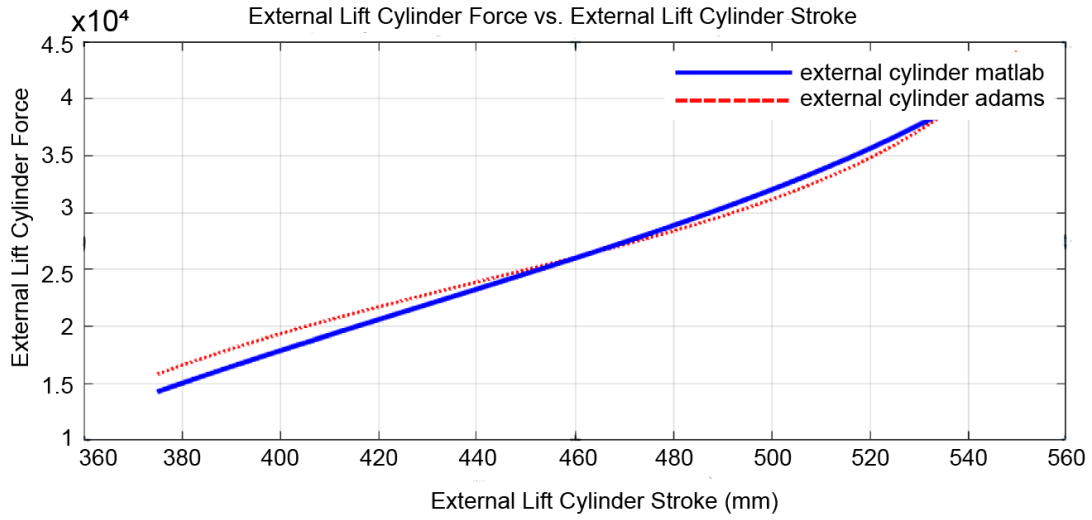

Figure 3.14. External lift cylinder force vs. lift cylinder stroke comparison for MATLAB and ADAMS models

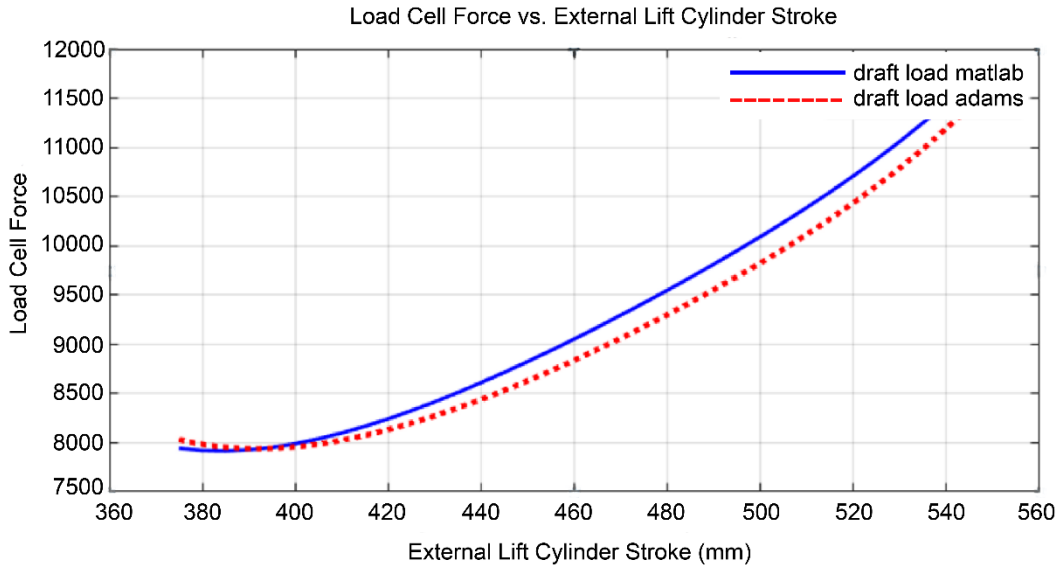

Figure 3.15. Load cell force vs. lift cylinder stroke comparison for MATLAB and ADAMS models

The results are nearly the same. The maximum difference between the two systems is 2.6%. The model in the ADAMS® tool is three-dimensional. On the other hand, the mathematical model in the MATLAB® tool is two-dimensional. The small chancing between these two data is originated from that situation.

As a conclude, in this section, kinematic analysis and force analysis of the 3PL mechanism are performed in MATLAB® software. The simulation could be shown for every stroke of the external lift cylinder. All results are verifying with the help of the ADAMS®. With analysis, the external lift cylinder pressure, P_1, top link pressure, P_2, external lift cylinder force, W_E and load cell forces, W_A, are easily determined at any applied draught force and at any stroke, S_e of the external lift cylinder.

3.1.2. Solid Modelling

Formerly, two-point linkage system was used as a hitch system in the tractor. However, since the controllability and durability of this design are complicated, the three-point linkage system was invented in late 1920s. Then, to be able to standardize, the system is classified in a certain category such as cat1 or cat2. The main advantage

of the classification is the compatibility between the equipment and the tractor. The details about that issue are written in section 1.2.3.

In test, the medium premium series tractor is used which has semi-automatic transmission, and the control system of the tractor is electro-hydraulic. The tractor`s maximum lifting capacity is 5500 kg. The power of the tractor is 88 hp.

By looking at table 1.1, the only category with 88 horsepower corresponds to category 2. Therefore, the design of the tractor and also 3PH mechanism is performed by regarding the category 2 regulations. For example, the mast height is 610 mm just as regulation. The length of the adjustable arms and hydraulic top link are changeable. However, both of them are adjusted at only one state and unchanged throughout the test. In that case, they are taken as constant. The design of the 3PH system belongs to CNH industries and TürkTraktör.

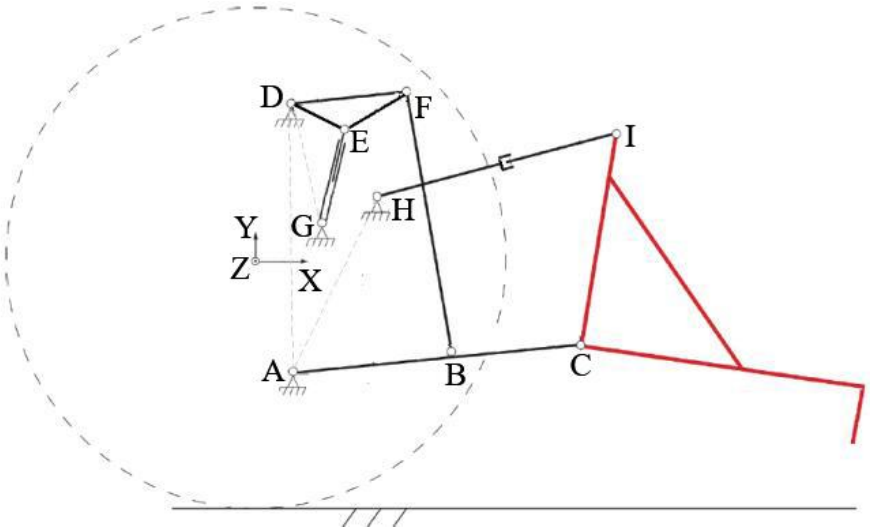

Figure 3.16. FBD of the 3PL mechanism

In the system, top link, |HI| is hydraulic. The length of this link tunes with hydraulic oil. Besides, the adjustable arm could be arranged mechanically. The length of the top link and adjustable arm are measured just before the cultivating process, and all of the calculations are performed according to these measurements. Mechanism lengths are written in table 3.1.

Table 3.1. 3PL mechanism dimensions

PART NAME	SYMBOL	MEASUREMENT
External lift cylinder length	|EG|	375-550 mm
Stoke of the cylinder	S_e	177 mm
HPL arm length	|DF|	310 mm
Lower link length	|AC|	980 mm
Lower links pivot point to adjustable arm length	|AB|	473.6 mm
HPL arm pivot point to external lift cylinder rod side length	|DE|	158.5 mm
HPL arm pivot point to external lift cylinder pivot point bore side length	|DG|	456.1 mm
HPL arm pivot point to lower links pivot point length	|AD|	622.7 mm
Adjustable arm length	|FB|	717.9 mm
Top link length	|HI|	730 mm
Mast Height	|IC|	610 mm
Top link pivot point to lower links pivot point length	|HA|	565.5 mm

The tractor 3PH system was modeled in PTC Creo 3.0® and necessary connections like cylindrical, revolute, and spherical joints are defined in the program. Then, the solid model is exported to the MATLAB R2018a Simscape® Multibody® version: 5.0. This is a model data file derived from a Simscape Multibody® Import XML file using the smimport function. The data in this file sets the block parameter values in an imported Simscape Multibody® model [34].

More than half of the connection ports are defined in the MATLAB® Simscape tool automatically, which are previously defined in PTC Creo 3.0® model. Inappropriate connections are fixed manually.

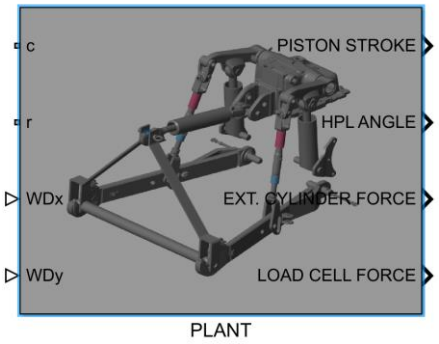

Figure 3.17. 3PH mechanism plant model Simulink representation

3PH Simulink model has four inputs. Ports R and C are mechanical translational conserving ports associated with the cylinder and the body of the mechanism respectively. The fluid flow is converted to velocity in the valve, and this velocity is transmitted to the valve with these connection ports. Since all of the mechanisms exported from PTC Creo 3.0, all moment of inertias and weights are taken into considerations.

Remaining two inputs are the components of the draught force, coming from the implement. Since the lateral forces are neglected, z axis is not taken into consideration. Besides, the draught force is applied to the 3PL mechanism from implement by regarding the test equipment measurements. (1000,300).

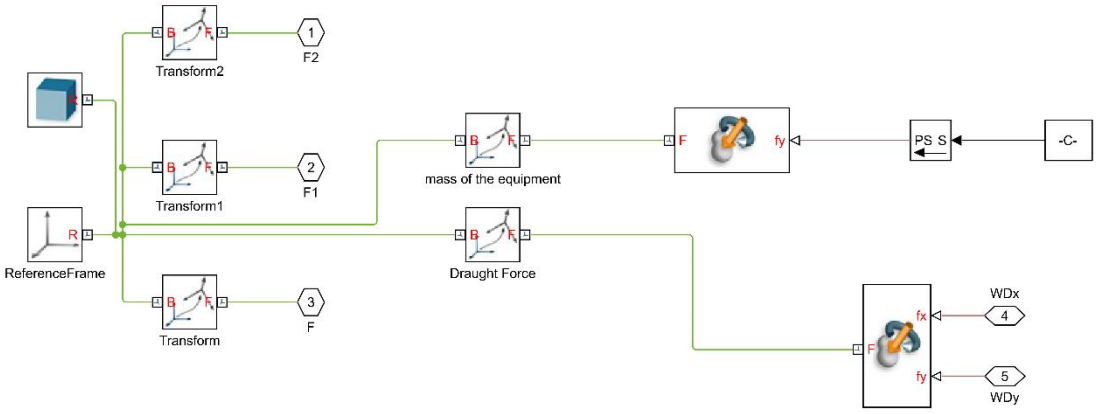

Figure 3.18. Applied forces to the 3PH system

Implement weight is also added to the system by considering the test implement center of gravity. In general view of the Simulink 3PH solid model, there are four outputs. Red block represents the piston stroke output signal. Green block represents the external lift cylinder piston force signal, orange block represents the load cell force signal, and finally, blue block represents the HPL arm signal.

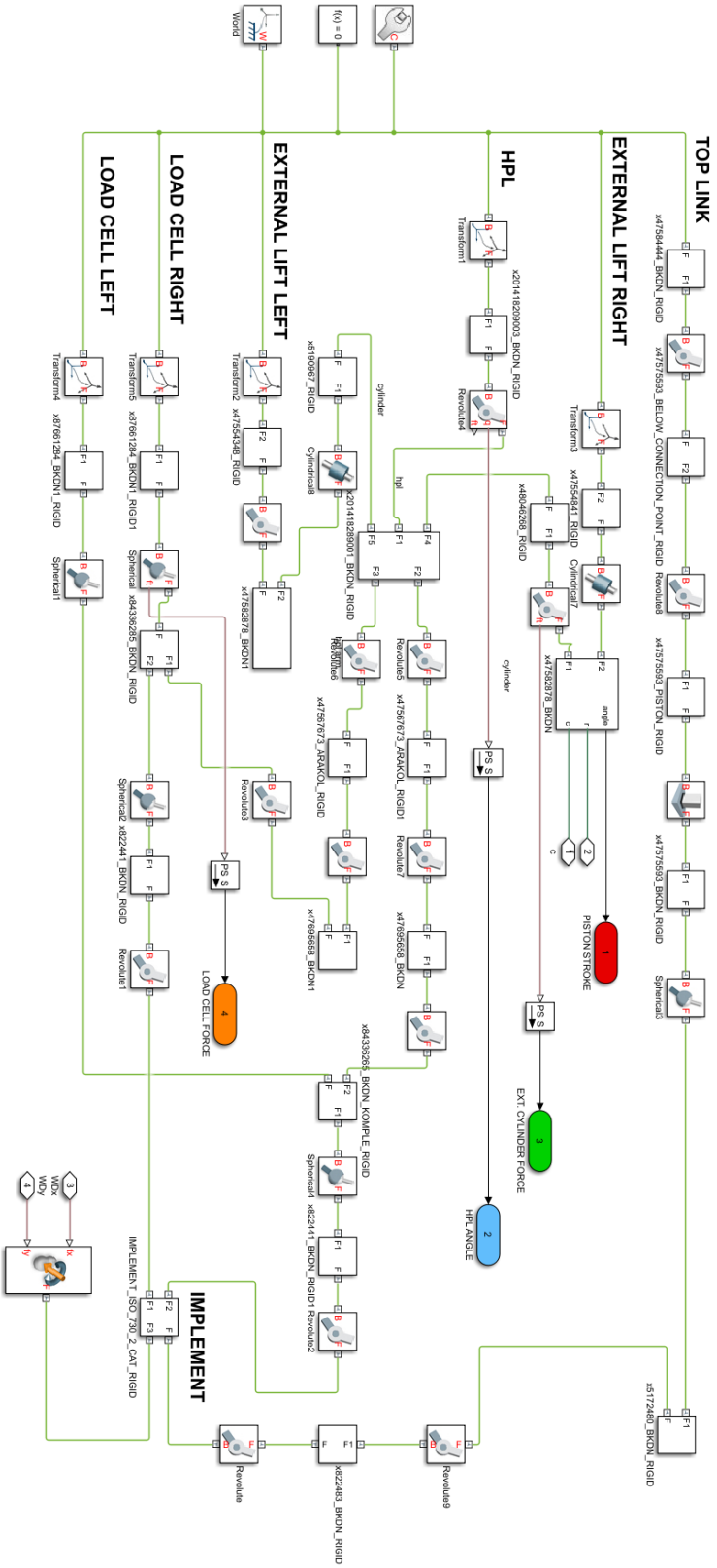

Figure 3.19. General view of the 3PH system Simulink solid model

3.2. Actuator Design

The hydraulic system gives motion to the 3PL mechanism. For that reason, it is count as an actuator in the system. There are four main parts in the hydraulic system, which are hydraulic pump, control valve, hydraulic oil, and lift cylinders.

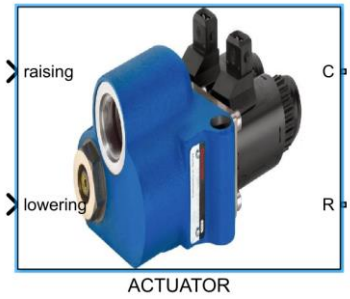

Figure 3.20. Actuator Simulink representation

The actuator model has two inputs. Raising and lowering are the signals that are acting to the solenoids of the valve. Moreover, the system has two outputs. Ports R and C are mechanical translational conserving ports. The details about these parts are summarized in section 3.1.1.

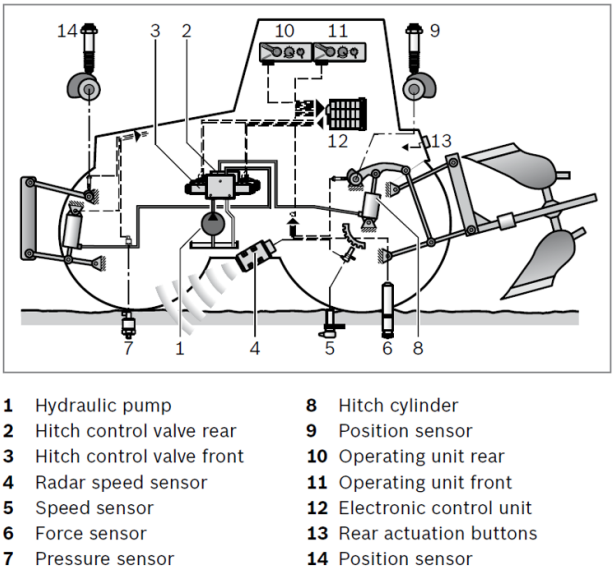

Figure 3.21. Hydraulic System [35]

The hydraulic pump (1) conveys an oil flow to the hitch control valve (2) which controls the hitch cylinders (8). External lift cylinders transmit the motion to the top

links with the help of the HPL arm, and they have an effect on the lower links so that attachments can be lifted, held or lowered. Position sensor (9), force sensor (7), operating unit (10), and electrical control unit (12) are the other system components. In order to trigger the hydraulic mechanism, a fixed displacement hydraulic pump unit (P) is used in the test tractor. 88 Hp diesel engine feeds the pump and pump supply variable amount of hydraulic oil according to the chancing engine rpm.

Table 3.2. Pump parameters

Definition	Symbol	Measurement	Unit
Pump displacement	D_p	25,40	cm^3/rev
System maximum pressure	P_{max}	190	bar
Maximum engine speed	S_{max}	2300	rpm
Pump to motor ratio	N_{pm}	1,08	-

The rest tractor has 25.4 cm^3/rev as a maximum pump displacement. In calculations, instead of rpm, lpm is used. The unit conversion is;

$$D_p(lpm) = D_p(rpm) * S * n_{pm} \tag{3.48}$$

With equation 3.48, the maximum displacement of the pump is 60 lpm. Nevertheless, it is almost impossible to work with maximum engine speed under normal operating conditions. In the field, generally, tractor runs at 1500 rpm which corresponds to 40 lpm as a pump displacement under normal working conditions. In the model, by considering this situation, it is assumed that the tractor runs 1500 rpm in the field.

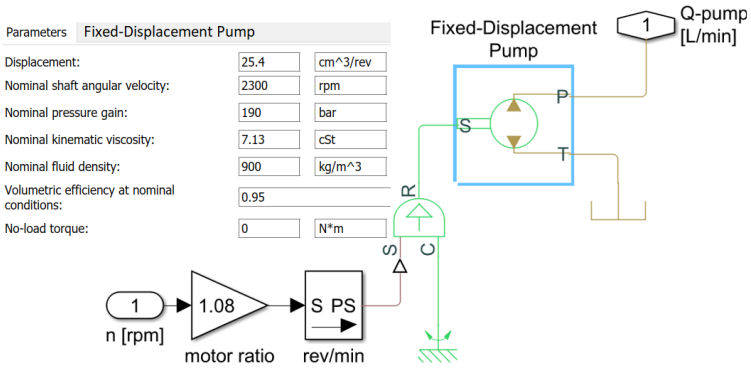

Figure 3.22. Pump MATLAB Simulink model

One of the most critical variables of the hydraulic system is oil. According to the hydraulic oil specifications, the characteristic of the system could be changed drastically. In New Holland tractors, Opet Fulltrac Fluid X 10W-30 hydraulic oil is used. The specifications of the oil are written in Appendix D.

Since SAE30 hydraulic oil specifications are very similar to Opet Fulltrac Fluid X 10W-30 oil, SAE30 hydraulic oil is chosen as a fluid of the system.

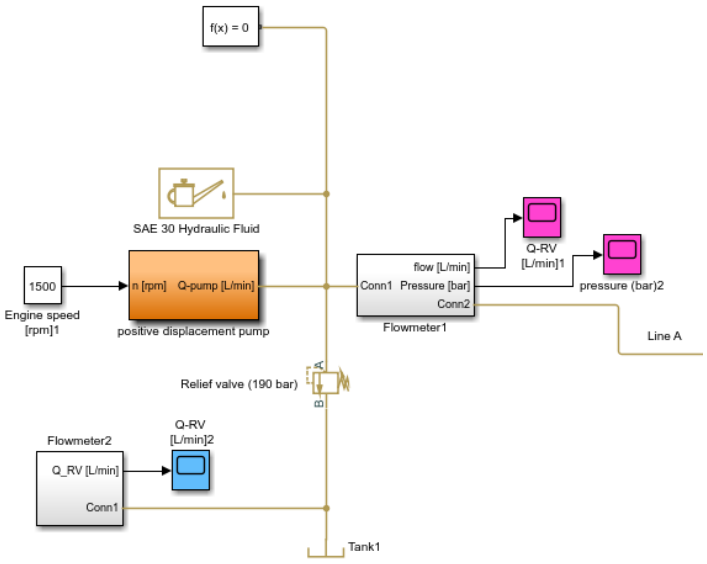

Figure 3.23. Pressurization system MATLAB Simulink model

In the pressurization system, engine, pump, and relief valve models occur. Relief valve set to 190 bar, which is the maximum system pressure. Next, the pressurized oil goes to the valve throughout line A.

After the hydraulic flow is pressurized with the help of the pump and passing from line A, it needs guidance. In order to control the fluid, valves are used in the system. In the test tractor, all of the control units are electrical. BOSCH EHR5 electro-hydraulic proportional valve is used in the system. The technical specifications of the BOSCH EHR5 valve occurred in Appendix E.

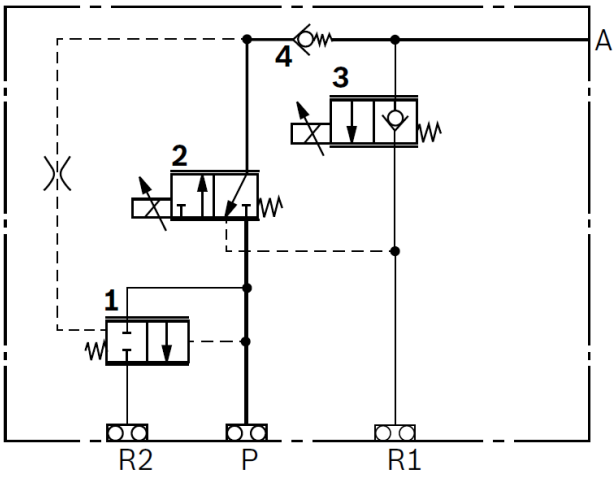

Figure 3.24. Hydraulic schema of the BOSCH EHR 5 valve [35]

Pressure compensator (1), lifting module (2), lowering module (3) and check valve (4) are the components of the valve. In the valve, lifting and lowering parts are separate. The compensator (1) compensates for the pressure just for lifting side. Whereas, for lowering side, there is no compensator. 3PH system goes towards downward with the help of the weight of the implement and with the help of the external forces like draught force without compensating the loads. This system is modeled in MATLAB Simulink tool.

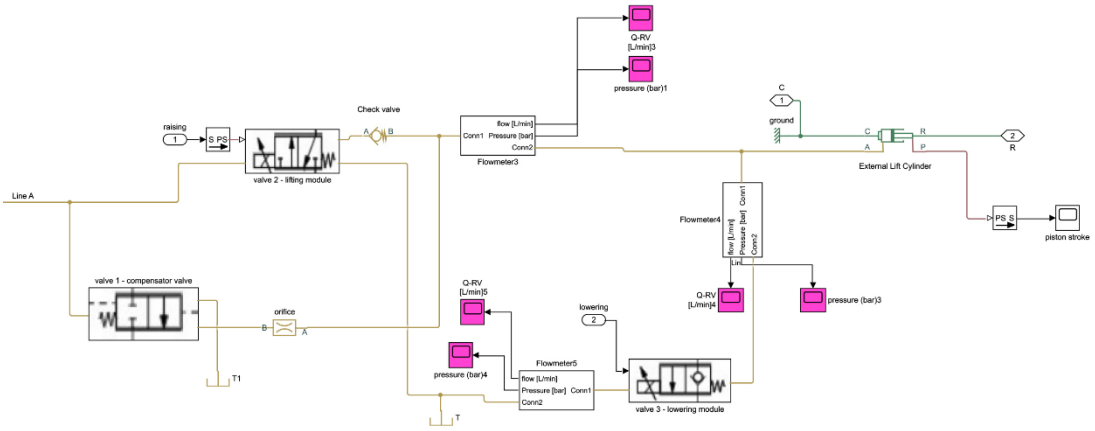

Figure 3.25. MATLAB Simulink model of the valve

The pressurized oil coming from line A. Since the valve has slices; three main components are examined separately. The first one is the compensator. The compensator (1) is a 2-position 2-way hydraulic operation actuator spring-actuated directional control valve. It is usually closed with the help of the spring. When the pressurized oil passing line A and reaches the compensator (1), without any signal, the compensator valve (1) is closed with the help of the spring. Then, pressurized fluid cannot pass the valve and cannot reach the tank.

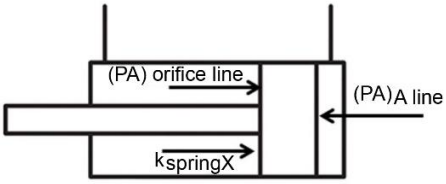

Figure 3.26. Hydraulic operation signal logic for compensator valve

In the Simulink model, the hydraulic operation signal of the compensator valve is modeled like a hydraulic cylinder. The diagram of forces acting on both surfaces of the valve is shown in Figure 3.27. When the right-hand side forces greater than the left-hand side forces, then the compensator starts to open, and fluid starts to go tank. Since the compensator is proportional, the spool opens gradually. The maximum stroke of the valve is 10 mm.

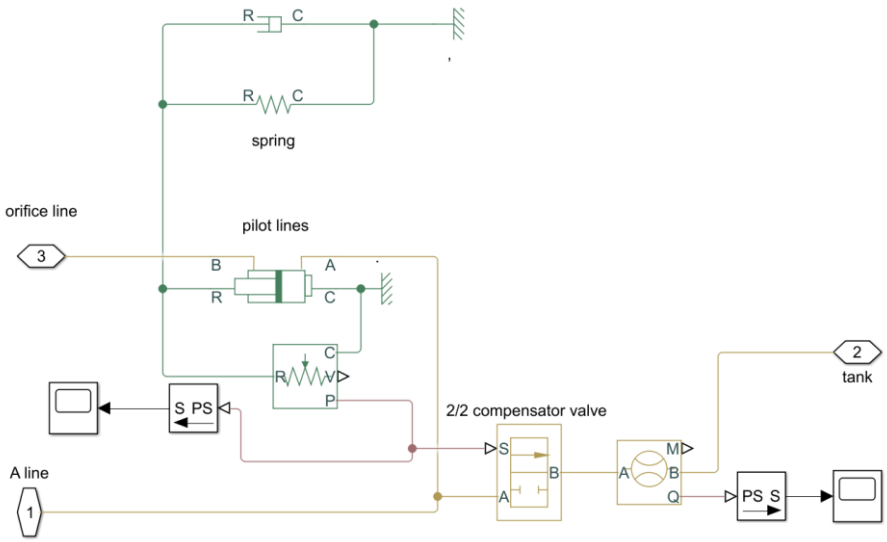

Figure 3.27. Simulink model of compensator valve

Lifting module (2) is a 2-position 3-way solenoid actuator spring-actuated directional control valve. Typically, if an electrical signal is not given to the solenoid of the valve, pressurized fluid does not pass through the lifting module. If the electrical input is given to the solenoid, then the solenoid opens gradually according to the intensity of the given electrical signal current. Meanwhile, lifting module solenoid takes the electrical signal only from lifting the current signal, $I_{1,}$ which comes through controller.

The characteristic curve of the lifting and lowering module is shown in figure 3.28. In lifting module, the valve maximum spool stroke arranges to 3.5 mm. Spool opens at 1 mm and fully opened at 3.5 mm stroke. Open-loop PWM control is used in the solenoids of the valve and run in between 125 MHz and 1000 MHz. Moreover, solenoids have a 100 milliseconds delay in the rising and lowering valves [8].

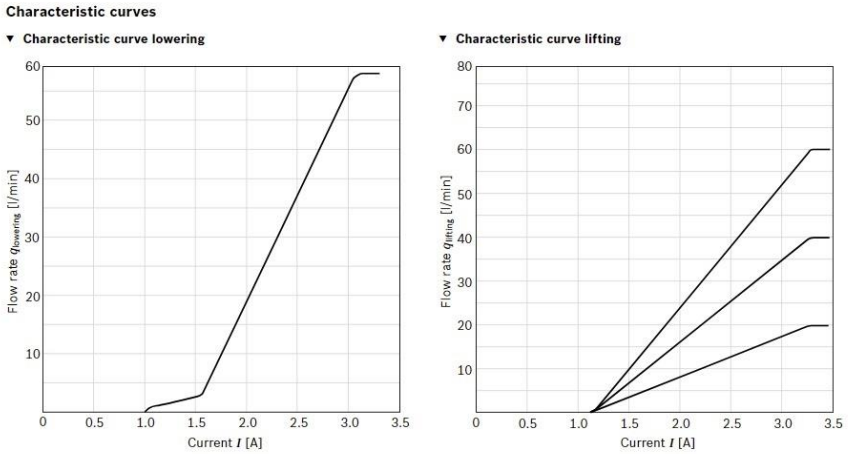

Figure 3.28. Characteristic curve of lowering and lifting module [35]

There are two ways in lifting module (2). Therefore, in the Simulink model, two variable orifices are modeled. Pump to cylinder variable orifice represents the left-hand sideway, and the main line-main piston variable orifice represents the right-hand sideway of the valve. Pump to cylinder orifice opens in a positive direction. It is initially closed with a 1 mm stroke, and the maximum orifice opening is 3.5 mm by regarding the characteristic of the valve. Next, the main line-main piston orifice opens

in a negative direction. The orientation is reversed with respect to the other orifice. It is initially open with 1 mm stroke, and maximum orifice stroke is 1 mm. With that logic, in the first 1 mm stroke, the main line-main piston variable orifice is opened, and for remaining stroke, pump to cylinder variable orifice is opened and the quantity of flow rate is changed by changing the stroke. Besides both variable orifice has 1.7671 mm^2 as a maximum orifice area.

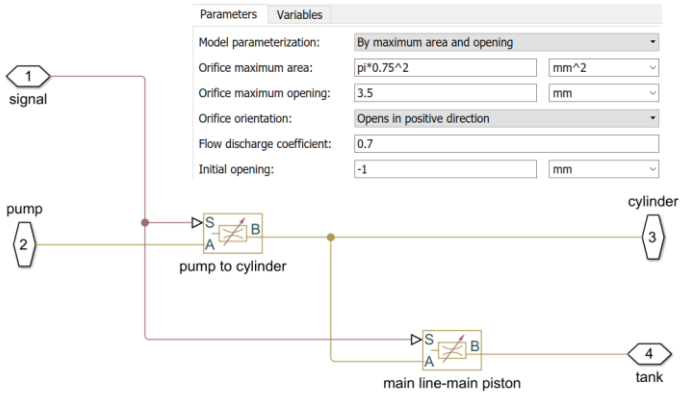

Figure 3.29. Simulink model of lifting module

Lowering module (3) is a 2-position 2-way solenoid actuator spring-actuated directional control valve. It is also normally closed like a lifting valve. Lowering module solenoid takes the electrical signal only from lowering the current signal, I_2, which comes through controller.

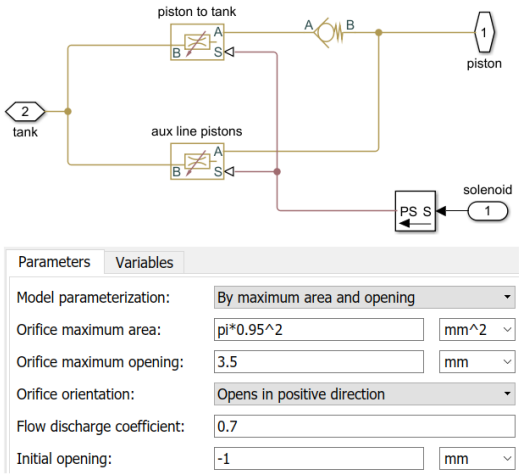

Figure 3.30. Simulink model of lowering module

The logic of the lowering module (3) is nearly similar to lifting module (2). Piston to tank and aux. line pistons are the two ways of the variable directional control valve. Aux. line pistons variable orifice represent the left-hand side and piston to tank variable orifice represent the right-hand side of the valve. Aux. line pistons orifice opens in a positive direction. It is initially closed with a 1 mm stroke, and the maximum orifice opening is 3.5 mm by regarding the characteristic of the valve. Next, piston to tank orifice opens in a negative direction. The orientation is reversed with respect to the other orifice. It is initially open with a 1 mm stroke, and maximum orifice stroke is 1 mm. With that logic, in the first 1 mm stroke, piston to tank variable orifice is opened and for remaining stroke, aux. line pistons variable orifice is opened and the quantity of flow rate is changed by changing the stroke. Both variable orifices have 2.8353 mm^2 as a maximum orifice area. Moreover, there is a check valve in piston to tank side, and it also puts to the Simulink model.

In order to obtain the maximum orifice areas, two different tests are performed for lifting and lowering conditions. For lifting condition, while the test tractor runs at a constant 1500 rpm, the 3PL mechanism is moved from the lowermost position to the uppermost position. The traveling time is recorded. Next, in the mathematical model, the system rpm sets to 1500 and lifting solenoid current adjust to the maximum value. Then, the traveling time in the mathematical model is overlapped with the test data while the orifice area is 1.7671 mm^2.

For lowering condition, the test equipment which is chisel plough is mounted to the tractor. Then the mechanism goes towards upwards. While the test tractor runs at a constant 1500 rpm, the 3PL mechanism is moved from the uppermost position to the lowermost position. The traveling time is re-recorded. Next, in the mathematical model, the system rpm sets to 1500, the equipment weight sets to chisel plough mass and lifting solenoid current adjusts to the maximum value. Then, the traveling time in the mathematical model is overlapped with the test data while the orifice area is 2.8353 mm^2.

3.3. Controller Design

The 3PH mechanism controller system consists of position control and draft control. Since the auxiliary control mechanisms do not directly affect the control system, they are not taken into account in that section.

Main controllers are modeled in Simulink with the Stateflow module. There are two inputs and two outputs in the controller.

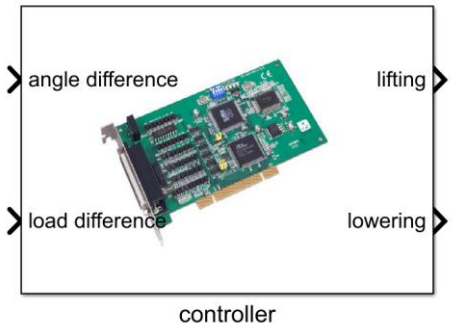

Figure 3.31. Controller Simulink representation

In order to select the controller type, a mathematical model and test results are analyzed. The speed of the tractor and the speed of the 3PH mechanism is too slow, especially when compared to the robotic systems. Moreover, as a construction machine, the tractor does not need a low response time like robotic systems. On the contrary, with low response time, the controller might have an impact on the system frequently. This situation can cause a non-smooth surface on the soil during the cultivating process, which is undesirable. Normally, derivative control tries to reduce the overshoot and rise time error. In our system, no matter how much you give a proportional constant, the system cannot reach the overshoot. Since the study system is slow, there is no need to use derivative control.

As a requirement, there is an offset error in the system. The mechanism works in a manner that does not react within a specified range. This specified range is called sensitivity. In control theory, integral control tries to minimize the offset error. Yet, in the study, offset error and corresponding certain band is occurred. In the meantime,

integral control might be creating wind up problem. For those reasons, I-control is not used in the mechanism. In the light of this information, only the P-control is used in the controller.

Position control communicates between 3PH mechanism actual position (θ_1) and user input angle (θ_p) and tries to correlate them. Meanwhile, since the angle sensor is located behind the HPL arm and measure the angle of this component, HPL arm angle count as the complete 3PH mechanism angle.

When the driver wants to lift the system, then, s/he turns the knob to the desired level, and the difference is occurred between user input and the actual mechanism position. Then, the controller closes the difference by giving lifting current signal, I_1, to the solenoid of the lifting valve. The angle difference (θ_{delta}) is the first input of the controller. Vice versa is acceptable during the lowering condition.

$$\theta_{delta} = \theta_p - \theta_1 \tag{3.49}$$

Draft control makes contact between user input force (W_p) and applied force to the system from the implement. In current design, the applied force is measured from load cells, which are located in lower links at point A. In this direction, the controller draft force algorithm is established by considering the point A location load cell force, W_A. When the new proposed system is installed, it will be difficult to change the controller. Therefore, the force given to the system at any certain location is transformed to defined location point A and so the controller might be done the comparison by providing the same environment.

If the load difference (Wdelta) between the applied force, (load cell force) WA and user input force (Wp) is occurred, the controller triggers the system. The load difference (Wdelta) is the second input of the controller.

$$W_{delta} = W_A - W_p \tag{3.50}$$

If the load difference (W_{delta}) is greater than the setting sensing value ($W_{sensing}$) than the mechanism starts to go upwards. Otherwise, if the load difference is lower than

setting sensing value than the mechanism goes towards downwards. If the load difference is in the range of the setting sensing value, the mechanism remains hold stage.

Incidentally, the amount of load difference or the amount of angle difference determines the amount of electrical signal current. Since lifting and lowering valves are proportional, the amount of electrical signal that passes to the solenoid of the valves adjusts the amount of fluid that passes through the valves.

The inner side of the controller is shown in Figure 3.32. Gray blocks are the inputs of the controller, whereas red blocks are some constraints of the system.

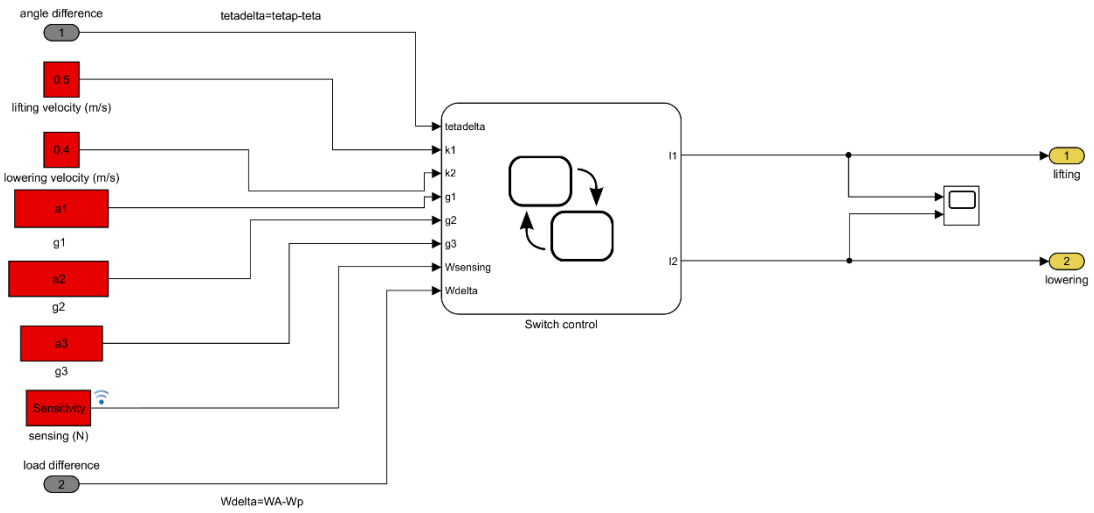

Figure 3.32. Detail view of the controller

In proportional directional control valves, the flow rate might be interchangeable. With the help of drop rate control potentiometer knob (2), the driver should be select the velocity of the system. In the Simulink model, lifting velocity constant k_1, and lowering velocity constant k_2, determines the velocity of the 3PH mechanism. During test, the drop rate control potentiometer is adjusted as 5, and it remains stable throughout the test.

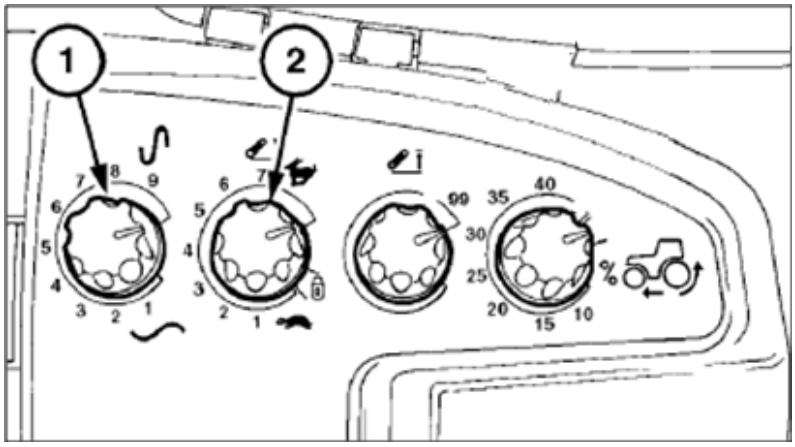

Figure 3.33. Electro-hydraulic control panel [8]

One of the most critical issues in draft control mechanism is sensitivity. According to the sensitivity value, the running-up time and response time of the controller are alterable. If the system is highly sensitive, the control mechanism comes into play frequently, which creates rough work. If the driver selects a non-sensitive option, draft control mechanism does not get involved easily, and this situation provides smooth and precise cultivating (equal depth on each side) but causes increasing of the fuel consumption and create slipping. In a tractor, sensitivity is arranged with draft sensitivity control knob (1). Sensitivity ($W_{sensing}$) is added as a constraint in the Simulink model. It could be changed as in reality. In the test tractor, sensitivity select as 5, which is equal to 500 N.

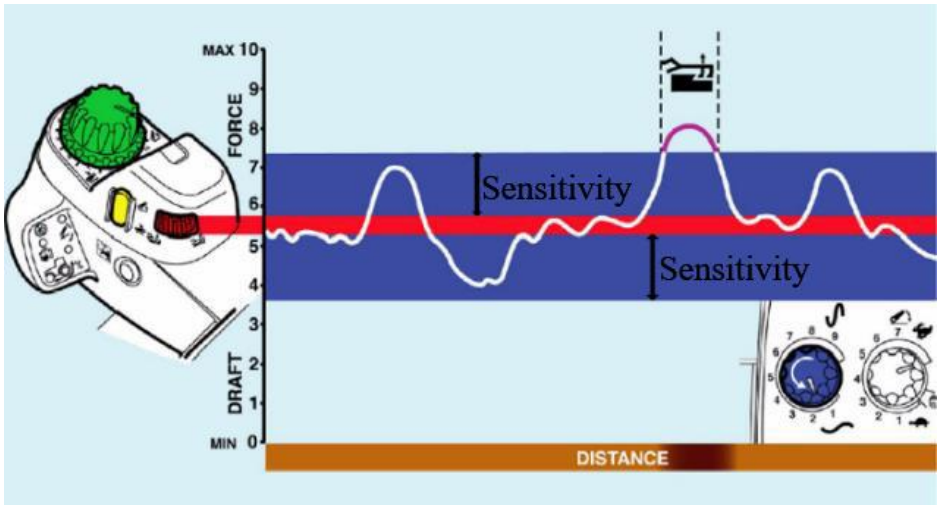

Figure 3.34. Draft control and draft sensitivity [8]

Imagine that the driver arranges the draft control potentiometer as 5.5, which corresponds to the red band. Then, s/he adjusts the draft sensitivity control knob (1) at a certain point which corresponds to blue bands. In all blue and red regions, the controller does not trigger the 3PH mechanism. The width of the blue region is changed by changing the draft sensitivity control knob (1) setting.

Unfortunately, there is no information about the controller system characteristic. During the test, it is observed that the character of the lifting or lowering valve module current is changed non-linearly during chancing the magnitude of the load difference. Since the system is non-linear, it is not enough to use a single constant proportional gain. For that reason, gain scheduled P control is used to determine the characteristic of the draft control [37]. Normally, the characteristic of the controller is non-linear. However, for simplicity, instead of taking a non-linear equation, three different linear equations are taken

Test data is the only acceptable choice to determine the adaptive gain P control variables. The parameter estimation method is used to determine the variables and a specified section of the test is the experiment of the parameter estimation method. Detail information about the parameter estimation method will be given in the next chapter.

The maximum allowable current to the controller is 4 Amperes. This value corresponds to the 3PH mechanism maximum speed. The magnitude of the current is changed by changing the load difference value.

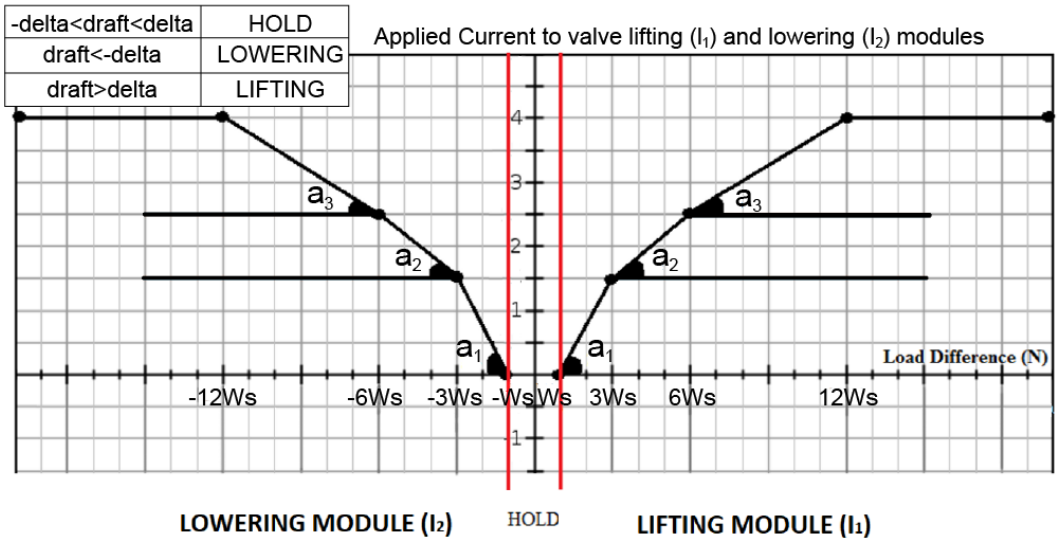

Figure 3.35. Applied current to valve lifting and lowering module vs. load difference diagram

The controller characteristic equations for lifting case;

$$I_1 = a_1 * W_{\ lifting} \qquad for \quad W_s < W_{lifting} \leq 3W_s \tag{3.51}$$

$$I_1 = a_2 * W_{\ lifting} + a_4 \qquad for \quad 3W_s < W_{lifting} \leq 6W_s \tag{3.52}$$

$$I_1 = a_3 * W_{\ lifting} + a_5 \qquad for \quad 6W_s < W_{lifting} \leq 12W_s \tag{3.53}$$

For lowering case;

$$I_2 = -a_1 * W_{lowering} \qquad for \quad -3W_s < W_{lowering} \leq W_s \tag{3.54}$$

$$I_2 = -a_2 * W_{lowering} + a_4 \qquad for \quad -6W_s < W_{lowering} \leq -3W_s \tag{3.55}$$

$$I_2 = -a_3 * W_{lowering} + a_5 \qquad for \quad -12W_s < W_{lowering} \leq -6W_s \tag{3.56}$$

The unknowns are defined as parameters in the Simulink model. By using the parameter estimation method in Simulink®, the suitable parameters are detected with regarding the test data.

Stateflow module in Simulink® is the brain of the controller. It provides a graphical language that includes state transition diagrams, flow charts, state transition tables, and truth tables. Stateflow could be used to describe how MATLAB® algorithms and Simulink models react to input signals, events, and time-based conditions. It enables

to design and develop supervisory control, task scheduling, fault management, communication protocols, user interfaces, and hybrid systems.

With Stateflow, combinatorial and sequential decision logic might be modeled that can be simulated as a block within a Simulink® model or executed as an object in MATLAB®. Graphical animation enables to analyze and debug your logic while it is executing. Edit-time and run-time checks ensure design consistency and completeness before implementation [36].

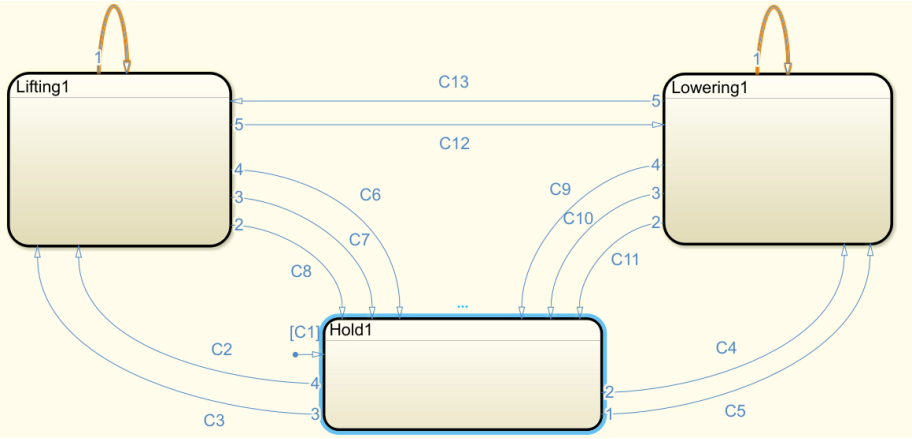

Figure 3.36. State flow conditions

Lifting, hold, and lowering are the three states of the Stateflow. There are 13 conditions and six phases in the Stateflow model. Signal initially enters to hold position from C1. Position control and draft control works simultaneously in the control logic.

In the first phase, from hold to lifting state, there are two conditions;

$$\theta_{delta} \geq 0.4^{\circ} \quad \text{(C2)}$$

$$W_{delta} > W_{sensing} \quad \text{(C3)}$$

Condition C2 related with the position control. If the angle difference is greater than 0.4°, then the signal is shifted to lifting state from the hold state. Condition C3 is related with draft control. If the load difference is greater than the sensitivity value,

then the same shifting movement occurs in the control algorithm. As a degree, 0.4^0 is the tolerance of the position control error.

In second phase, from hold to lowering state, there are two conditions;

$$\theta_{delta} \leq -0.4^{\circ} \tag{C4}$$

$$W_{delta} < -W_{sensing} \tag{C5}$$

Condition C4 is related to position control. If the angle difference is lower than minus 0.4°, then the signal is shifted to lowering from hold state. Condition C5 is related with draft control. If the load difference is greater than load sensitivity value, then the same shifting movement occurs with C4.

Third phase is the reverse of the first phase. In this phase, there are three conditions;

$$\theta_{delta} \leq -4^{\circ} \tag{C6}$$

$$-0.4^{\circ} < (\theta_{delta}) \,\&\, (\theta_{delta}) < 0.4^{\circ} \,\&\, W_{delta} \leq -W_{sensing} \tag{C7}$$

$$W_{delta} < W_{sensing} \,\&\, W_{delta} > -W_{sensing} \,\&\, \theta_{delta} < 0.4^{\circ} \tag{C8}$$

Condition C6 is directly related to the position of the system. This condition is made to prevent the system from nonsensical movements against instant reactions. It means that regardless of the loading conditions, the maximum difference between the user input and the actual mechanism position must not exceed the limit of $\pm 4^{\circ}$.

Conditions C7 is related both with position and draft control. It says that, while the elevation of the mechanism is under the specified band, if the load difference decreases to under the sensitivity limit, then the system should pass the holding position.

Condition C8 is again related to two main controllers. While the system is within the load sensitivity limit, if the angle difference decreases to below the specified value, again the system passes the holding position.

Like third phase, fourth phase also have three conditions;

$$\theta_{delta} > 4^{\circ} \quad \text{(C9)}$$

$$-0.4^{\circ} < (\theta_{delta}) \,\&\, (\theta_{delta}) < 0.4^{0} \;\&\; W_{delta} \geq W_{sensing} \quad \text{(C10)}$$

$$W_{delta} < W_{sensing} \,\&\, W_{delta} > -W_{sensing} \,\&\, \theta_{delta} > 0.4^{\circ} \quad \text{(C11)}$$

Condition C9, C10, and C11 are the mirror image of the previous three conditions.

There is only one condition in lifting to lowering state;

$$W_{delta} > W_{sensing} \,\&\, \theta_{delta} > -5^{\circ} \quad \text{(C12)}$$

Again, this condition controls both position and draft controller. Under the cultivating process, in order to respond to the momentary forces coming from the field sharply, the direct connection between the lifting and lowering states is established. Passing softer soil from harder soil is an example of the condition C12.

The sixth and final phase has one condition;

$$W_{delta} < -W_{sensing} \,\&\, \theta_{delta} > -5^{\circ} \quad \text{(C13)}$$

Like the previous phase, this phase also settles down to respond quickly to the momentary forces coming from the field. This situation comes true when instantaneous forces like stone coming to the equipment under the cultivating process.

In all states, the current is the output. The controller gives the current to the solenoids of the valve. The current could be supplied in the range of 0 to 4 Amperes.

In hold state, I_1 is a lifting current, and I_2 is a lowering current. They are the outputs of the controllers. Since there is no movement in the mechanism, any current is not supplied to the system in this state. Therefore, both values are equal to zero.

Since the proportional valve is used in the system, variable current is given to lowering and lifting states depending on the severity of load difference and angle difference.

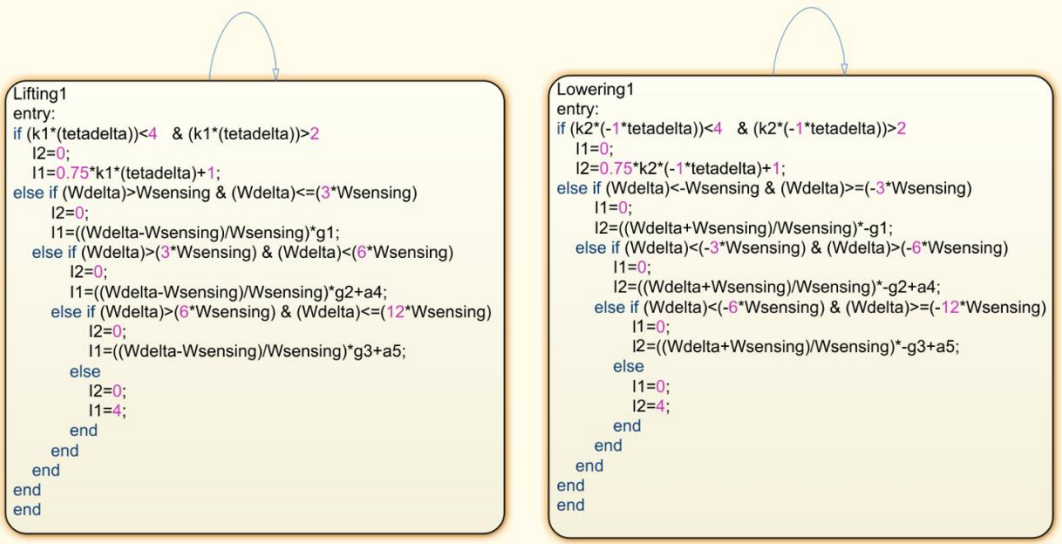

Figure 3.37. Lifting and lowering module state blocks

In the lifting state, there are five main conditions. The first one is related to the position of the 3PH mechanism. According to the lifting velocity (k1) and angle differences, the severity of the output lifting current (I_1) is changed. In order to implement this condition, angle difference must not below 2˚/k1 and must not exceed 4˚/k1.

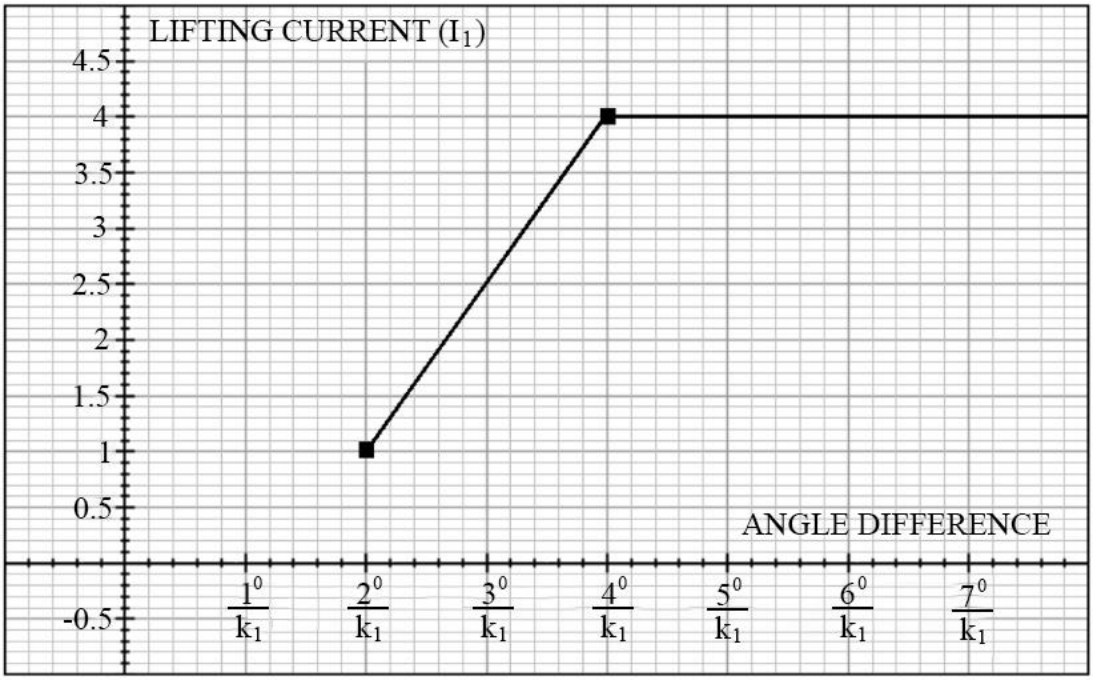

Figure 3.38. Position control characteristic of lifting module current wrt. angle difference

For draft load, there are three different characteristics shown in Figure 3.35. and equations (3.51), (3.52), and (3.53). In these equations lifting force represent as;

$$W_{lifting} = \frac{W_{delta} - W_{sensing}}{W_{sensing}} \tag{3.57}$$

In lowering state, there are five main conditions. The first one is related to the position of the 3PH mechanism.

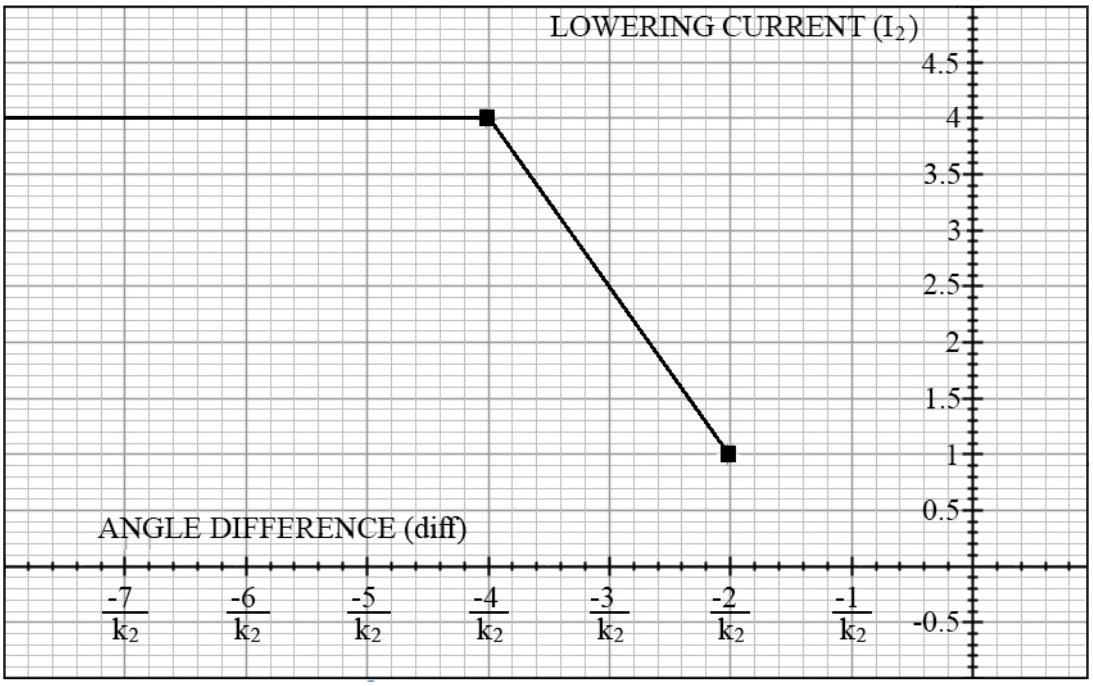

Figure 3.39. Position control characteristic of lowering module current wrt. angle difference

According to the lowering velocity (k2) and angle differences, the severity of the output lowering current (I_2) is changed. In order to implement this condition, angle difference must not below -2˚/k1 and must not exceed -4˚/k1.

For draft load, there are three different characteristics shown in Figure 3.35 and equations (3.54), (3.55) and (3.56). Lowering force represent as;

$$W_{lowering} = \frac{W_{delta} + W_{sensing}}{W_{sensing}} \tag{3.58}$$

Outside of the specified ranges for position and draft control, the maximum current is applied to the system. Besides, blue arrays in Figure 3.38 shows that in every new

step, all conditions will be reassessed. Additionally, in lifting state block, lowering current (I_2) is zero for all conditions, and vice versa is acceptable for lowering state block.

Note that, the characteristic of the position control for lifting and lowering module is determined by performing a small test. In test, position knob is turned gradually in CW direction for lifting case. The 3PL mechanism is activated when the knob is turned $2^{\circ}/k_1$ degree and reaches its maximum speed when the knob is turned $4^{\circ}/k_1$ degree. The transition phase is taken as linear. Then, the position knob is turned gradually in a CCW direction for lowering case. The 3PL mechanism is activated when the knob is turned $-2^{\circ}/k_1$ degree and reaches its maximum speed when the knob is turned $-4^{\circ}/k_1$ degree. The transition phase is taken as linear as the previous case. Figure 3.38 and Figure 3.39 takes form with test measurements.

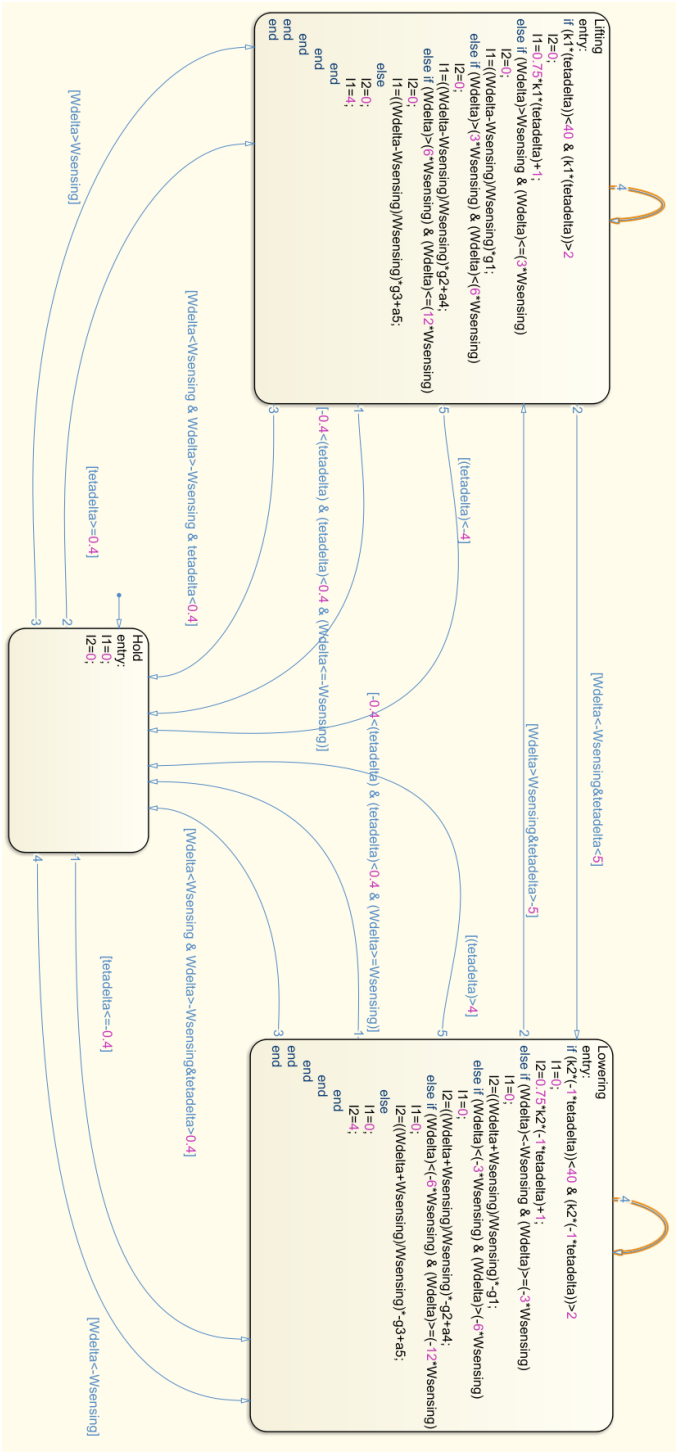

Figure 3.40. General view of Stateflow

CHAPTER 4

FIELD TESTS

4.1. Components of the System

As mentioned in the literature survey section, there are three different test methods to measure the acting forces to the 3PH mechanism from the soil based on the location of the force transducers. Tests are performed by using the third method. For some measurements, test tractor's sensors are used. Firstly, load cell sensors are needed for reading the force coming from the equipment. Secondly, in order to measure the location of the 3PH mechanism and also the elevation of the equipment, the angle sensor is appropriate. These sensors are well-calibrated and efficient. Next, to gauge the velocity of the vehicle, a radar sensor or GPS sensor is used. Finally, pressure sensors are essential to measuring the pressure of the top link and external lift cylinder. They are integrated into the system, and all measured values, including angle sensor and load cell force, are recorded to Arduino card.

Moreover, by considering literature, it is assumed that the system is planar. Two-dimensional approximation can be accepted for the studies of symmetric implements. Chisel plough, which is used in the test tractor, is an excellent example of the symmetric implements. Therefore, for simplicity, only longitudinal and vertical components are considered during the calculations.

The tractor is the main device of the test. Tractor has fix displacement open-loop pump system. Instead of mechanical control, it has an electro-hydraulic draft control system, EDC.

In EDC, there are load sensing pins which are integrated into the tractor. These pins are located at the left and right lower links. The pins react to draft shear forces only in the horizontal plane. Each load sensing pin consists of a hollow metal tube (1)

containing a circuit board (4) and load sensing core (2). Within the core material, three-wire coils (3) are found and supported by metal rods. The coils are energized and create a stable pattern of magnetic flux within the core. The outer casing of the pin is made from metal with unique electromagnetic properties. When the metal is subject to a shear force, which is centered on the wasted section (5) of the pin, the natural magnetism of the pin casing gets changed. This change distorts the magnetic flux pattern of the core and is transformed into an electrical output signal. This signal, which is proportional to the draft load acting on the implement, is then received by the electrical panel [8]. KMB series Rexroth load cells are used in the tractor.

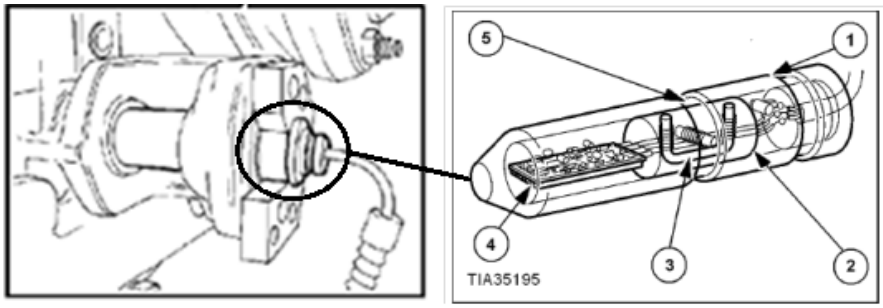

Figure 4.1. Load Sensing pin [8]

The characteristic of the load cell is shown in Figure 4.2.

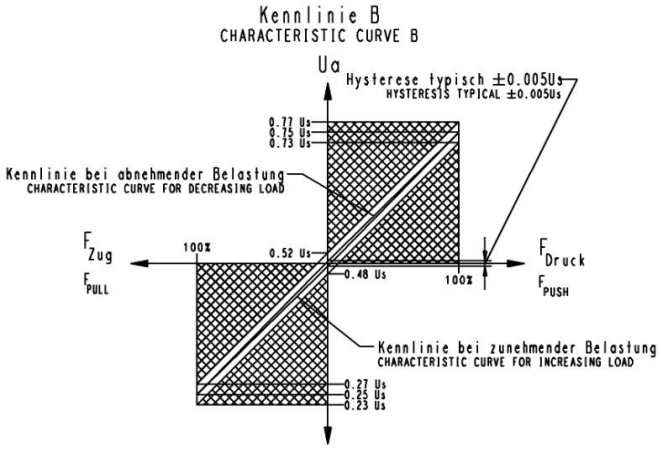

Figure 4.2. Characteristic of the load cell [38]

The imported data obtained from the load cells do not directly show the force values that are acting on the lower links. In order to obtain a meaningful number, appropriate conversions must be performed.

Firstly, Arduino transformation constant, A_r is calculated as;

$$A_r = \frac{V_{ard}}{1024} * \frac{11.28}{4.68} \tag{4.1}$$

where

V_{ard} : Arduino voltage (V)

The numbers in equation 4.1 are related to the resistance of the Arduino.

Since the Arduino voltage is 5V;

$$A_r = \frac{5}{1024} * \frac{11.28}{4.68} = 0.01176883 \tag{4.2}$$

Then, necessary conversion is as follows;

$$F_{real} = \frac{A_r * MV_{LC} - V_{LC} * 0.25}{(0.75 - 0.25) * V_{LC}} * 2F_{max} - F_{max} \tag{4.3}$$

where;

F_{max} : Maximum force that the sensor can be read (N)

MV_{LC} : Measured value from control panel for load cell force

V_{LC} : Maximum load cell voltage (V)

The selected load cell measures a maximum of 50 kN, and it supplies 8V utmost. Therefore;

$$F_{real} = \frac{0.01176883 * MV_{LC} - 2}{(0.75 - 0.25) * 8} * 2 * (50000) - 50000 \tag{4.4}$$

Or more simply terms;

$$F_{real} = 294.22 * MV_{LC} - 100000 \tag{4.5}$$

Next, in the tractor, there is also an angle sensor that is located in front of the HPL arm. The angle sensor potentiometer is directly connected with the HPL arm (DEF). It is a universal analog sensor used to measure absolute angular rotation of a mechanism.

A potentiometer is a three-terminal device that uses a moving contact from a variable resistor divider. The taper of a potentiometer describes the relationship between the position and the resistance. A linear taper is used in the system. The resistance varies proportionally to the rotation of the shaft of the potentiometer. For example, the shaft will measure 50% of the resistive value at the midpoint of the rotation. In linear potentiometers, the angle is deducted directly from the voltage.

In mechanism, the potentiometer set to zero at the lowermost position of the HPL arm. When HPL arms start to move, sensor potentiometer also moves and reads a certain amount of voltage. The severity of the voltage is proportional to the displacement of the potentiometer. The signal of the sensor is again read by the EDC control panel. Rockshaft sensor potentiometer specifications are written in Figure 4.3.

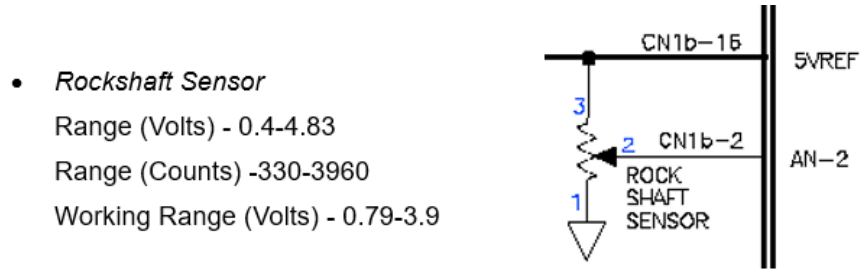

Figure 4.3. Rockshaft sensor potentiometer specifications [8]

The measured value from the EDC control panel does not directly show the angle of the 3PL system. Again, in order to obtain meaningful outputs, necessary conversions should be made.

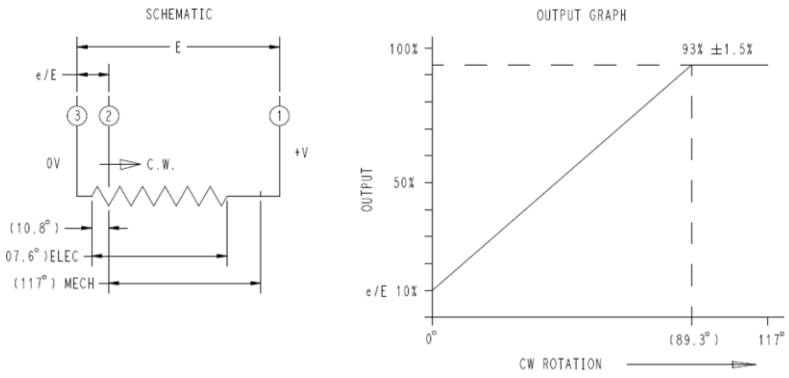

Figure 4.4. Characteristic of the angle sensor [8]

The necessary conversion formula according to the characteristic of the angle sensor is;

$$\alpha_{HPL} = \frac{A_T * MV_{AS} - V_{AS} * 0.1}{\left(\frac{93-10}{100}\right) * V_{AS}} * \alpha_{max} \tag{4.6}$$

where

α_{HPL} : HPL unit angle wrt. longitudinal axis (deg.)

V_{AS} : Maximum angle sensor voltage (V)

α_{max} : Maximum allowable measured angle (deg.)

MV_{AS} : Measured value from control panel for HPL angle

The selected angle sensor maximum allowable voltage is 5V, and from Figure 4.4, the maximum measured angle is 89.3^0.

With given numbers formula reduces to;

$$\alpha_{HPL} = \frac{0.01176883 * MV_{HA} - 0.5}{(0.83) * 5} * 89.3^0 \tag{4.7}$$

The aim of the thesis is that instead of control the 3PH system draft mechanism with load cells from the lower links, control it by using pressures from the external lift cylinders by predicting the loads coming from the equipment. In the current design,

since there is no need to read pressure in the system, any pressure sensor is not presented in the tractor hydraulic system In order to see the system pressure, one pressure sensor is integrated to top link and other pressure sensor is integrated to left external lift cylinder in the system. The sensors are precision pressure transducer Keller PA 21R. The capability of maximum measured pressure is 260 bar, and the corresponding voltage is 10V. The characteristic of the sensor is shown in Figure 4.5.

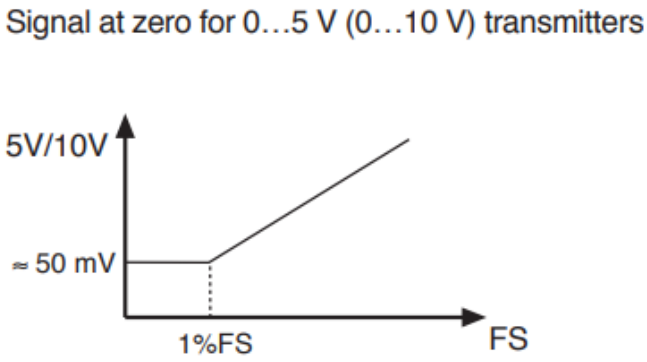

Figure 4.5. Characteristic of the pressure sensor [39]

The conversion formula for pressure sensor is;

$$P_{Ex} = \frac{A_T * MV_{PT} - 0.05}{(V_{PT} - 0.05)} * P_{max} * (\frac{100-1}{100}) \quad (4.8)$$

where

P_{Ex} : External lift pressure (bar)

V_{PT} : Pressure transducer maximum voltage (V)

P_{max} : Maximum allowable pressure (bar)

MV_{PT} : Measured value for pressure transducer

The voltage of the selected pressure transducer is 10V, and the maximum allowable pressure is 260 bar. Therefore:

$$P_{Ex} = \frac{0.01176883 * MV_{PT} - 0.05}{(9.95)} * 260 * (0.99) \quad (4.8)$$

4.2. Field Test Performance

The tractor is a construction vehicle. The main duty of the tractor is pulling something like a trailer or work the soil like plowing the field. For pulling issues, since any disturbance force does not affect the system, only position control is used. Whereas, during the plowing, apart from position control, force control or draft control is also used due to the presence of the variable disturbance force.

In the field test, Case IH FARMALL90A AD4 tractor is used. The engine power is 88 hp, and the EDC unit is given as standard. With the EDC unit, angle sensor and draft load cell sensors are also found in tractor as standard.

In addition to standard equipment, for the new design, pressure sensors are integrated into the tractor from the outside.

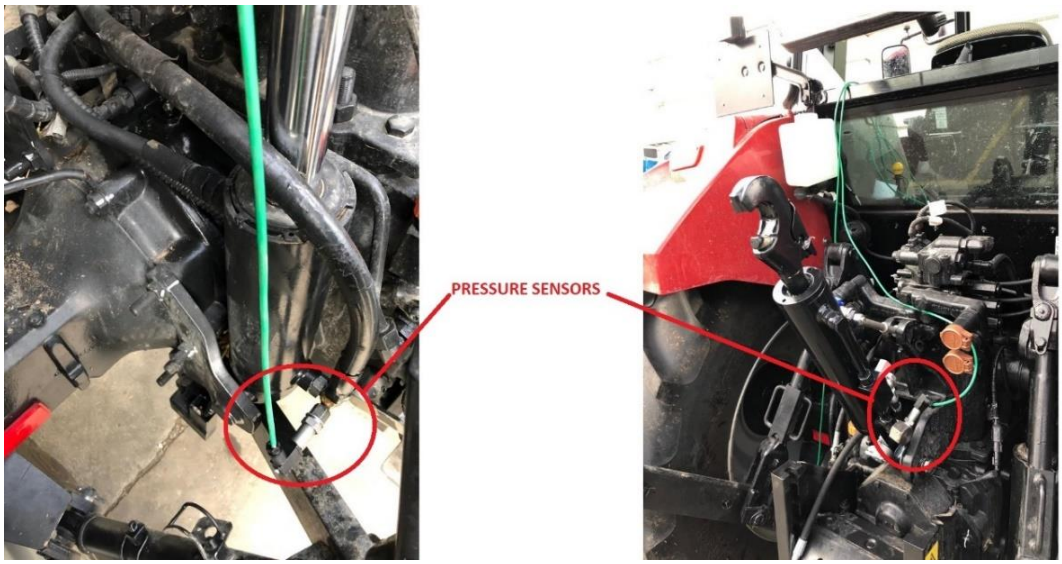

Figure 4.6. Locations of the pressure sensors in the tractor

The external lift piston is a single-acting cylinder. For that reason, there is only one connection port. The first sensor is mounted to the left external lift piston connection port to measure the pressure in the system. The sensor location is shown on the left-hand side of Figure 4.6.

The hydraulic top link is a double-acting cylinder. Therefore, it has two ports. One of them is bore side, which ensures the piston opens. Another one is the rod side, which ensures the piston close. During the cultivation process, in most of the case, equipment force acts the hydraulic top link as compression. For that reason, in order to measure the top link pressure, the second sensor is mounted to the hydraulic top link bore side. The sensor is shown on the right-hand side of Figure 4.6. Both sensors are mounted to the system with special connectors.

Additionally, the GPS kit is added to the system to see the location and the velocity of the tractor. Thanks to the GPS, the path characteristic of the tractor could be understood easily. The length of the field, user's driving style, soil type, and equipment constitute are count as the path characteristic.

Figure 4.7. Data acquisition and storage unit

Finally, in order to read and record the data that are obtained from the sensors, Data acquisition and storage unit with Arduino card is made and located inside of the cabin trim. Since load cell sensors and angle sensor are occurred in the tractor as a standard, these data are read from tractor ECU and recorded to the Arduino. Pressure values and GPS sensor data are read from external pressure sensors and external GPS sensor and enrolled to the Arduino. In the card, each data is taken and recorded in 0.1 second time interval in other words 10 Hz. Since the tractor speed is too low under the cultivating

process, and since the conformity of each recorded time data such as GPS, it is appropriate to use this time interval.

Figure 4.8. Test tractor with the test equipment

After installing the test setup, the equipment is mounted to the tractor. A chisel plow is used as equipment. The chisel plow is a common tool to get deep tillage with limited soil disruption. It is a symmetrical equipment. The main function of this plow is to loosen and aerate the soils while leaving crop residue at the top of the soil. This plow can be used to reduce the effects of compaction and to help break up the plow pan and hardpan.

Figure 4.9. Chisel Plough [40]

Unlike many other ploughs, the chisel will not invert or turn the soil. This characteristic has made it a useful addition to no-till and low-till farming practices that attempt to maximize the erosion-prevention benefits of keeping organic matter and farming residues present on the soil surface throughout the year. With these attributes, the use of a chisel plough is considered by some to be more sustainable than other types of plough, such as the traditional moldboard plough.

After mounting the test equipment, the user starts to plow the field. Certain scenarios are implemented during the cultivating process. With each scenario, a tractor plough one complete row. One row means a tractor cultivate a single line from beginning to end. In other words, for each scenario, the farmer starts to cultivating the process from the beginning of the field and proceed with the end of the land. When s/he reaches the end of the field, then s/he pushes LOM, turns the tractor, arranges the new scenario and starting the new scenario by pushing the LOM again.

Table 4.1. *Field Scenarios*

SCENARIOS	POSITION KNOB	DRAFT KNOB	SENSITIVITIY
1	3	6	middle (500N)
2	3	10	middle (500N)
3	0	6	middle (500N)
4	0	10	middle (500N)
5	2	4	middle (500N)
6	2	8	middle (500N)
7	2	10	middle (500N)
8	1	4	middle (500N)
9	1	8	middle (500N)
10	1	10	middle (500N)

In draft knob, the allowable force acting on the load cell increased with an increasing number. Number “10” represents the maximum allowable force. In position knob, minimum value points out the minimum position of the HPL arm. Number “0” represents the lowermost position in the 3PL system.

In each scenario, the sensitivity of the draft system keeps constant. For that reason, instead of taking as a variable, sensitivity assumed as a constant value. A small section of the test data is shown in Appendix F.

In the study, two rows are simulated. In the first row, the farmer arranges scenario 6 and starting the plough procedure by pushing the LOM. When s/he reaches the end of the field pushes the LOM again and turns the tractor. Then, farmer arranges the position and draft control like scenario 1 and starting the cultivating process by pushing the LOM button third time. The simulation is ended when the farmer reaches the end of the field and pushes the LOM feature for the last time. These two row lasts 363 seconds.

In the test, the sensor data is recorded. Angle data, $\theta_{1_{TEST}}$, are collected from the ECU of the tractor. Angle sensor has a critical role in understanding the correlation between the mathematical model and test data. By regarding the test scenario, the 3PL mechanism angle test data is shown in Figure 4.10.

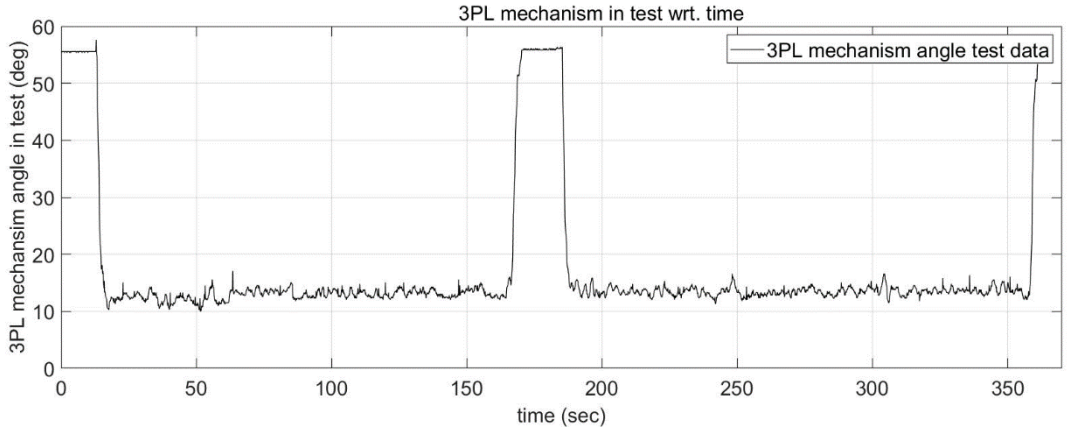

Figure 4.10. 3PL mechanism angle test data

The second sensor is the load cell sensor. It is integrated into the lower link point, and data are collected from the ECU of the tractor. According to the scenario, load cell force test data, $W_{A_{TEST}}$ is shown in Figure 4.11.

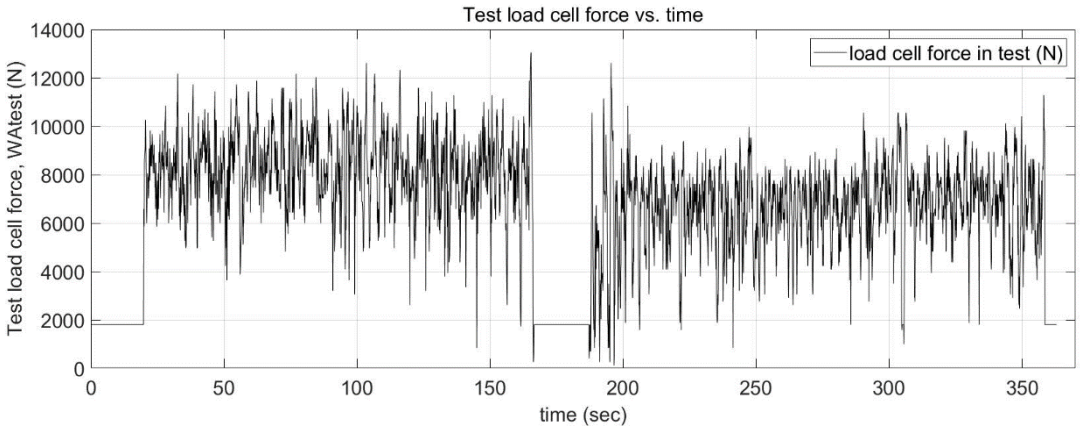

Figure 4.11. Load cell force test data

The last sensor is the pressure sensor. It is integrated into the left external lift cylinder of the tractor. Regarding the scenario, the external lift cylinder pressure, $P_{EX_{TEST}}$ is shown in Figure 4.12.

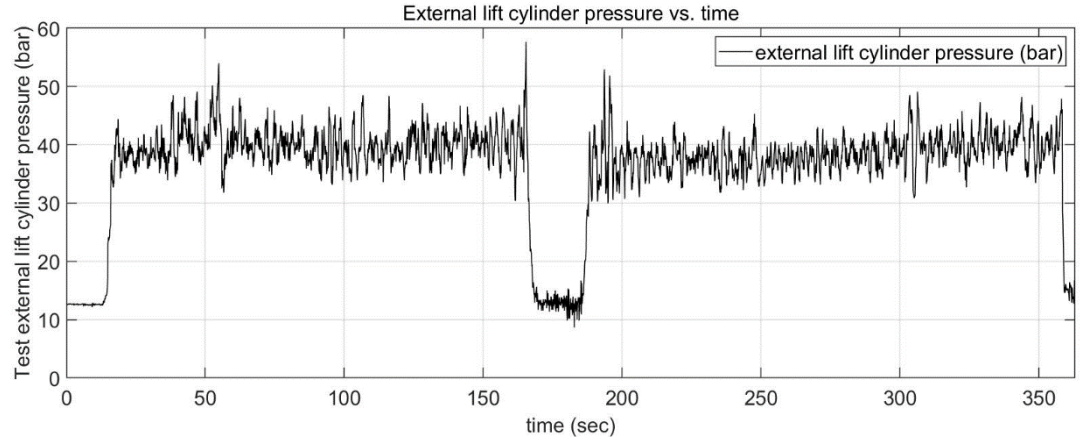

Figure 4.12. External lift cylinder pressure test data

Pressure sensor measures the pressure in the external lift cylinder bore side. The bore radius of the cylinder is 40 mm. Therefore;

$$A_{cyl} = \pi * (40)^2 = 5028.5 \quad (4.9)$$

Next, the unit of the measured data for pressure transducer is bar. Therefore, firstly we need to convert the bar to MPa and multiply it with the area of the cylinder in order to obtain the external lift force.

$$W_E = \frac{P_{EX}}{10} * A_{cyl} \quad (4.10)$$

where;

W_E : External lift cylinder force (N)

P_{EX} : External lift cylinder pressure (bar)

A_{cyl} : Bore area of the external lift cylinder (mm^2)

With regarding the scenario, the external lift cylinder force, $W_{E_{TEST}}$ is shown in Figure 4.13.

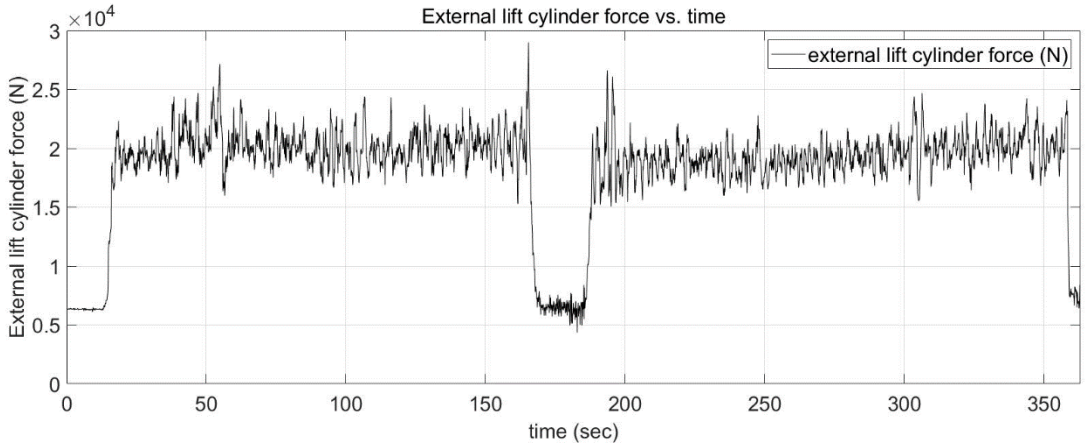

Figure 4.13. External lift cylinder force test data

CHAPTER 5

SIMULATIONS

5.1. Simulations with Current System

Up to this part, system sub-components are discussed in detail. In that part, the current model is handled entirely. The same inputs are given to model with test inputs, and the model results are compared with test results to verify the current model with respect to the angle of the HPL arm which represents the elevation of the 3PL mechanism.

5.1.1. Determination of Control Gains with Simplified Model

In the model, the characteristic of the controller has a significant role in managing the mechanism. The severity of the load difference, W_{delta}, affects the volume of the current that is acting to the solenoid of the valves. Unfortunately, there is no information about the applied current under a certain amount of load difference. For that reason, in order to determine the path of the applied current to valve with the chancing load difference, the Simulink parameter estimation method is used. For simplicity, instead of taking a non-linear equation, three different linear equations are taken. Gain scheduled P control is used as a controller

The aim of the parameter estimation is to make the system characteristic familiar with the test. With this method, the system runs approximately 100 times to get closer to the test data.

Normally, in the current system, the data taking from the sensor will be transformed into draught force and giving to the implement. Then the load cell force will be given to the controller. Unfortunately, this phase takes much time in the system. For that

reason, in a simplified model, the load cell force data directly granted to the controller. With this method, the process run time decreased fifty times. Note that, in order to include the moment of inertias and the effect of force measurements on the mechanism, the load sensor force data is added to the 3PL system as a disturbance. The block diagram of the simplified model for parameter estimation is shown in Figure 5.1.

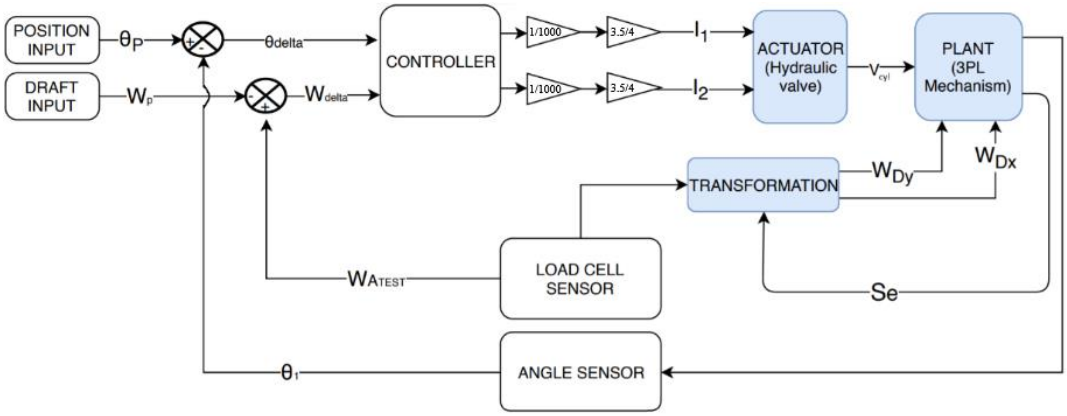

Figure 5.1. Block diagram of the simplified model for the parameter estimation

Position and draft control are the major features of the system. The remaining units, like LOM, are the auxiliary features. For simplicity, only the main features have been addressed in the thesis. In the light of this information, there are two inputs in the system which are position and draft input. These inputs numerical data' are taken from the field test.

In the field test, several alternatives are simulated. In each scenario, the tractor plough one complete row. In other words, for each scenario, the farmer starts to cultivating process from the beginning of the field and proceed with the end of the land. When s/he reaches the end of the field, then s/he pushes LOM, turns the tractor, arranges the new scenario and starting the new scenario by pushing the LOM again.

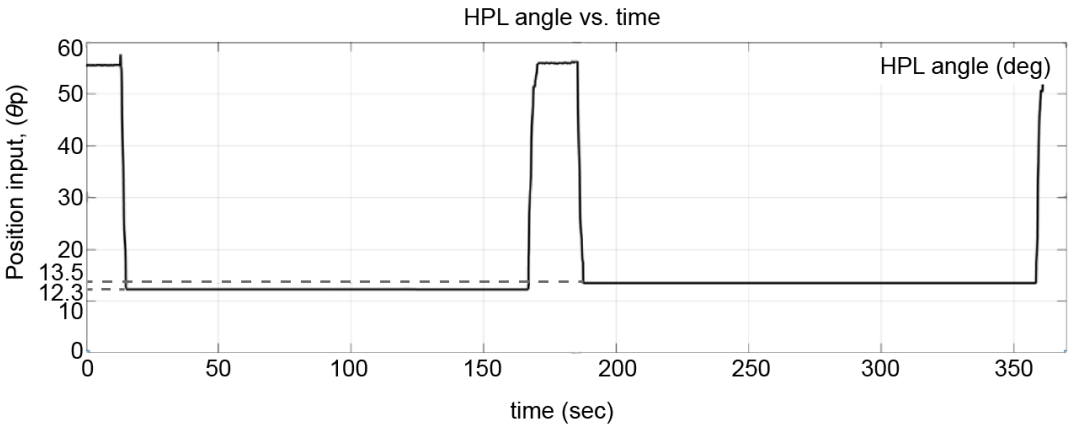

Figure 5.2. Position input

Draft input force corresponds to the desired load cell force or user input force. The mathematical model is patterned to automatically decreased the desired load cell force to 2000N when the LOM system is activated in order to avoid undesirable movements. Throughout the whole test, the sensitivity sets to ±500N. In Figure 5.3 black line represents the user draft force input, W_P, and the red-painted field represent the sensitivity interval of the system.

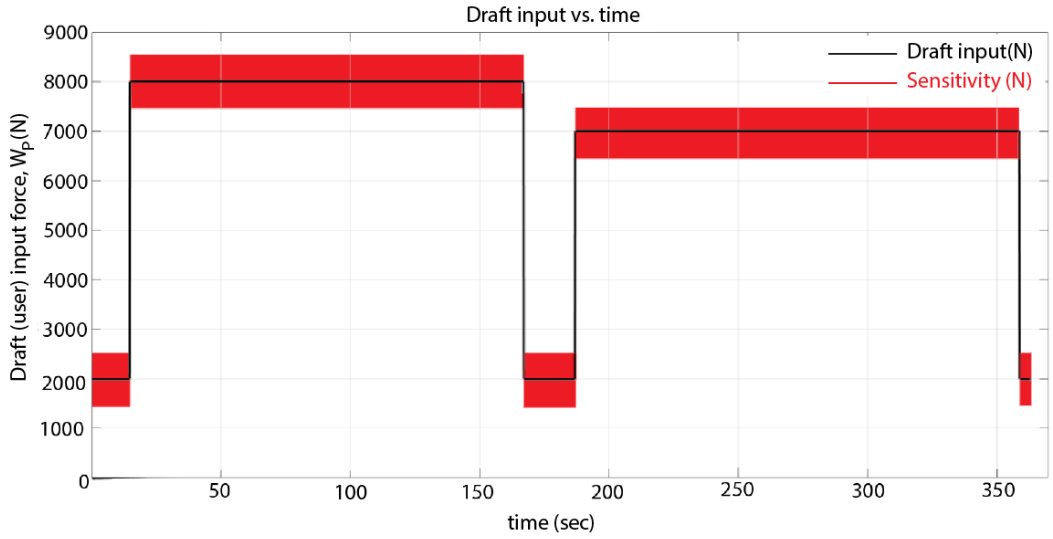

Figure 5.3. Draft input

Next, in the current system, load cells are the sensors of the load cell forces. They are located at the lower links body connection points.

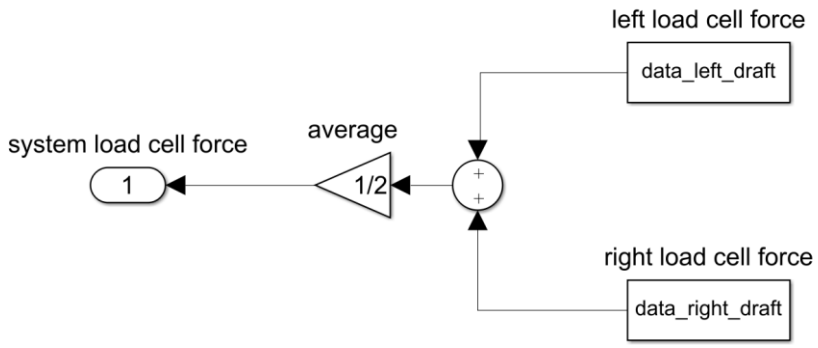

Figure 5.4. Detail of the load cell sensor (force sensor)

According to the Electro-Hydraulic Draft control system specifications [8], the average of the measured signals from left and right draft sensors should be taken. Then, the system load cell force, W_A, is obtained like Figure 5.4. Meanwhile, load cell force test data, $W_{A_{TEST}}$ is shown in the previous section, Figure 4.11.

The second type of sensor in the system is an angle sensor. In the angle sensor, instead of test data, mathematical model data is taken. At the end of this part, the result of the HPL angle θ_1 is compared with the 3PL mechanism test angle, $\theta_{1_{test}}$.

The error signals for draft and position values are obtained by using an error detector. Then, the angle difference (θ_{delta}), and load difference (W_{delta}) data enter the controller as an input. Data is converted to current in the controller in a certain ratio. Details about the controller occur in section 3.1.3.

Since the directional control valve has separate slices for lifting and lowering, there are two outputs in the controller. One of them is the lifting current (I_1) and the other one is the lowering current (I_2). The lifting current (I_1) directly goes to the lifting slice solenoid of the valve. With the same logic, lowering current (I_2) goes to the lowering slice solenoid of the valve.

There are two gains between the controller and the plant. The first one is related to unit conversion (meter to the millimeter). The next one is related to the current ratio between the controller and the hydraulic valve solenoid. The maximum allowable

Amperes value in the controller is taken as 4A whereas the valve solenoids have 3.5A as maximum allowable Amperes value. In order to adaptation the Ampere values, this conversion must be performed.

Hydraulic valve is an actuator of the system. The lifting and lowering current are the inputs of the hydraulic valve solenoids. The spool of each slice is opened with the proportion of the current. The spool gap is determined by the amount of oil pressurized into the cylinder. The details about the hydraulic valve are written in section 3.1.2.

The amount of oil pumping from the hydraulic valve determines the velocity of the external lift cylinder, V_{cyl}. This motion is transmitted to the 3PH model external lift cylinder, which is the plant of the system.

The 3PH system model is exported from PTC Creo 3.0®. Details about the procedure are written in section 3.1.1. Apart from the hydraulic cylinder velocity, the disturbance is another input of the plant.

The load cell measured forces are given to the 3PH model as a disturbance. Yet, since this location is the fixed point, any applied force to this location cannot be transferred to another side. For that reason, draft sensor force is relocated to the implement draught force point (W_D) by using the proper transformation equations. The transformation equations are obtained from section 3.1.1. The force diagram of the 3PH mechanism is shown in Figure 3.10. The outputs of the disturbance are longitudinal and horizontal components of the draught force.

Finally, the outputs of the plant are the mathematical model HPL angle (θ_1) and the piston stroke (S_e). Piston stroke is taken as an input in transformation equations. Since it affects almost all variables in the transformation equation, piston stoke has great importance for the accuracy of the transformed data.

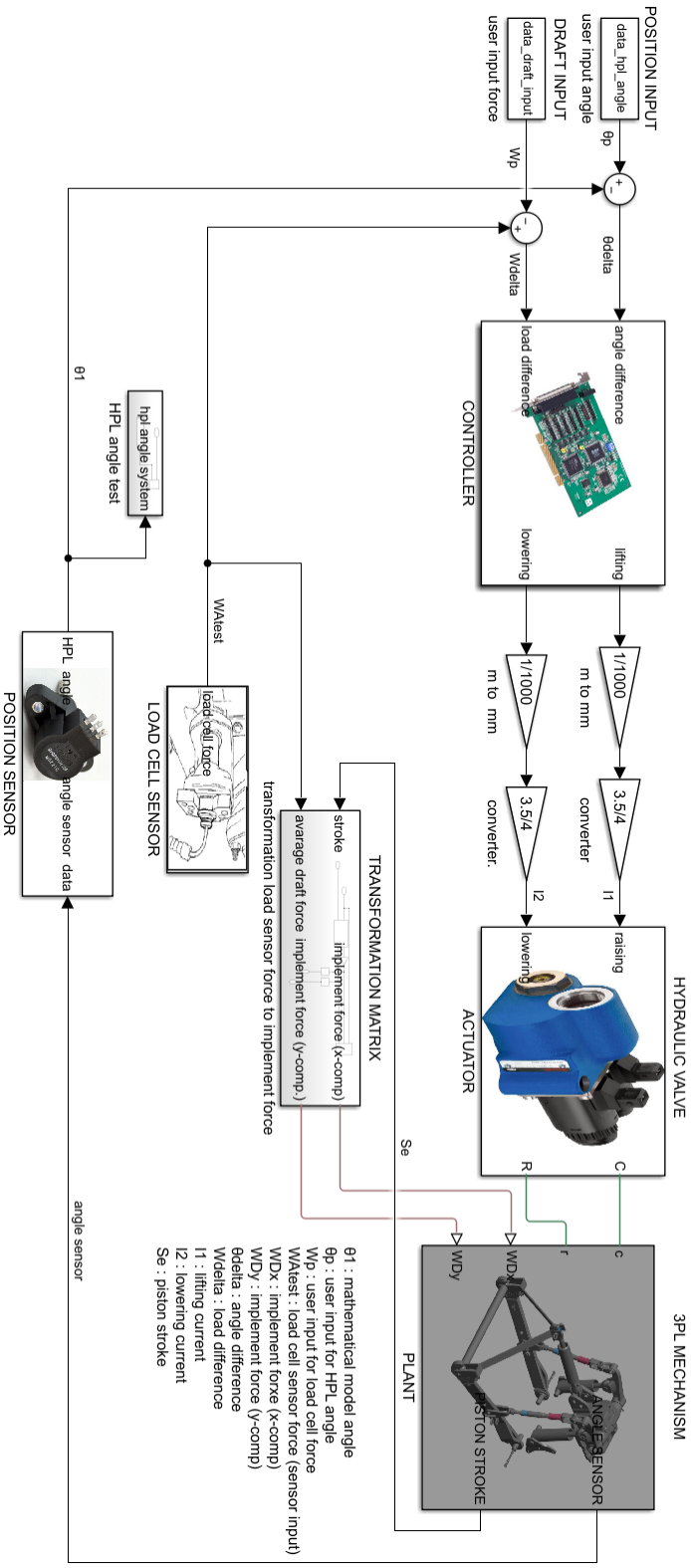

Figure 5.5. MATLAB Simulink model of the simplified model

The Simulink data of the simplified parameter estimation model is shown in Figure 5.5. Now, the simplified model for parameter estimation is established. There are five parameters to determine the characteristic of the controller. The equations of the parameters are shown in section 3.

Some initial conditions are given to the system in order to achieve the most relevant results in estimation cost. In every given initial condition, the system is encountered local minimum values. Hence, in order to approach global minimum points, a number of initial conditions are given to the system by considering the estimation cost of the parameter estimation. The most suitable initial conditions for parameters are found as follows;

$$a_1 = \frac{3}{4},\ a_2 = \frac{1}{3},\ a_3 = \frac{1}{2},\ a_4 = \frac{5}{6},\ a_5 = \frac{5}{4} \tag{5.1}$$

The aim of the parameter estimation is correlating the HPL arm angle for the test ($\theta_{1_{TEST}}$) and the HPL arm angle for the mathematical model (θ_1). For that reason, the 3PL mechanism angle test data ($\theta_{1_{TEST}}$) are chosen as an experiment in the parameter estimation method. Figure 4.10. shows the mechanism test angle along the period of test time.

Next, initial conditions are defined, and the estimation progress is started. Ninety iterations are done throughout the estimation. The results are shown below.

The parameter trajectory displays the parameter values as they change during estimation in Figure 5.6. Estimation cost displays the estimation cost as it changes during estimation in Figure 5.7.

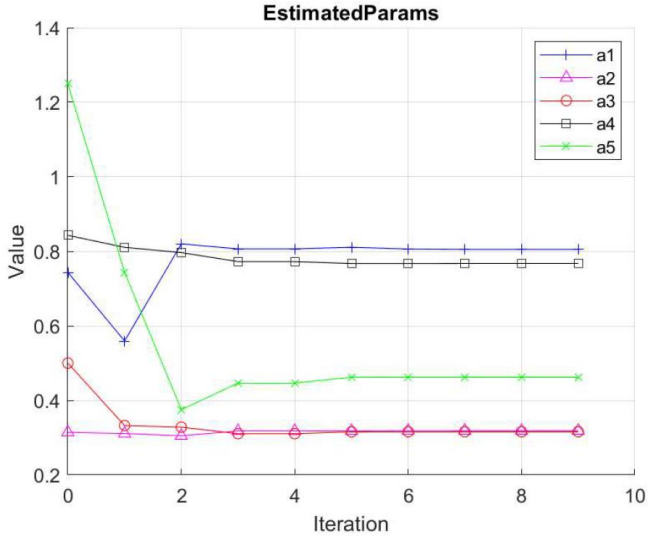

Figure 5.6. Parameter trajectory

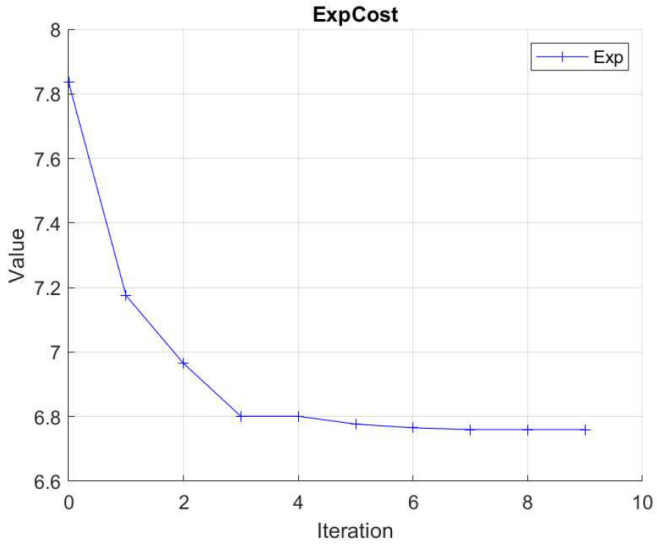

Figure 5.7. Estimation cost

At the end of the iterations the parameters are found as;

$$a_1 = 0.8256,\ a_2 = 0.3242,\ a_3 = 0.3191,\ a_4 = 0.7887,\ a_5 = 0.4624 \qquad (5.2)$$

From now on, these parameters will be used in the systems to obtain better results. In order to save time, the test data trimmed in the parameter estimation process. At the specified time period, the first 85 seconds is taken. With final estimation values, correlation result along the whole simulation process is shown in Figure 5.8.

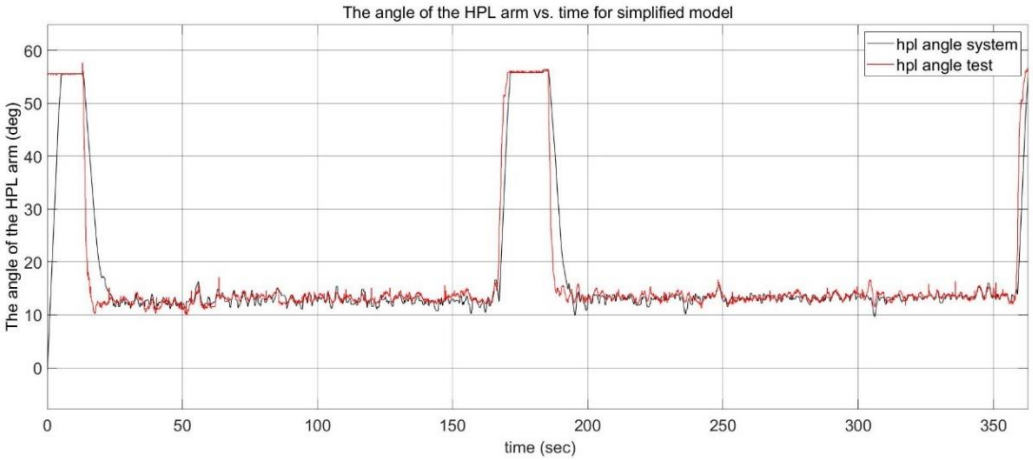

Figure 5.8. Correlation result for the parameter estimation model

5.1.2. 3PL Control System Simulation

In the simplified model, load cell force in the test is directly given to the controller. For that way, the plant could not be verified properly. Under normal working conditions, the load cell force in the test ($W_{A_{TEST}}$) should be transformed to the implement draught force. Then, it could be supplied to the mechanism as a disturbance. Next, the load cell force is measured from the 3PL mathematical model, which is exported from PTC Creo 3.0®. With that way, the plant is added to the mathematical model, and it is verified. Except for this procedure, the remaining components of the 3PL control system simulation are the same as the previous simulation model.

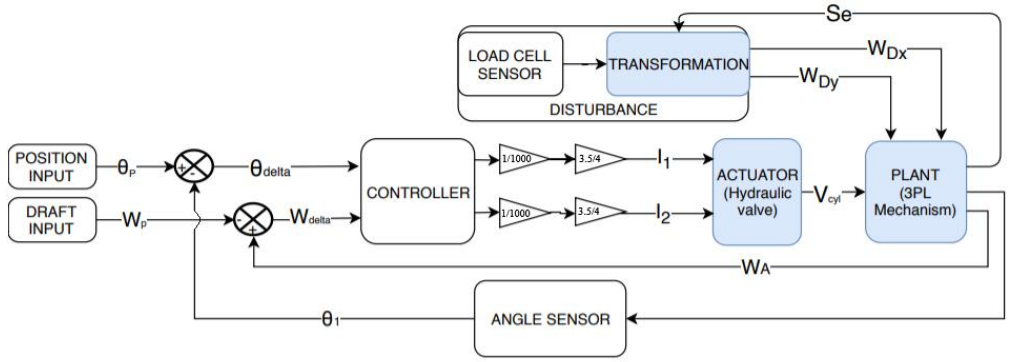

Figure 5.9. Current model block diagram

Since, instead of test data, mathematical model load cell force results are got in contact with the controller, there are three outputs in the plant. Load cell force is the additional output of the plant.

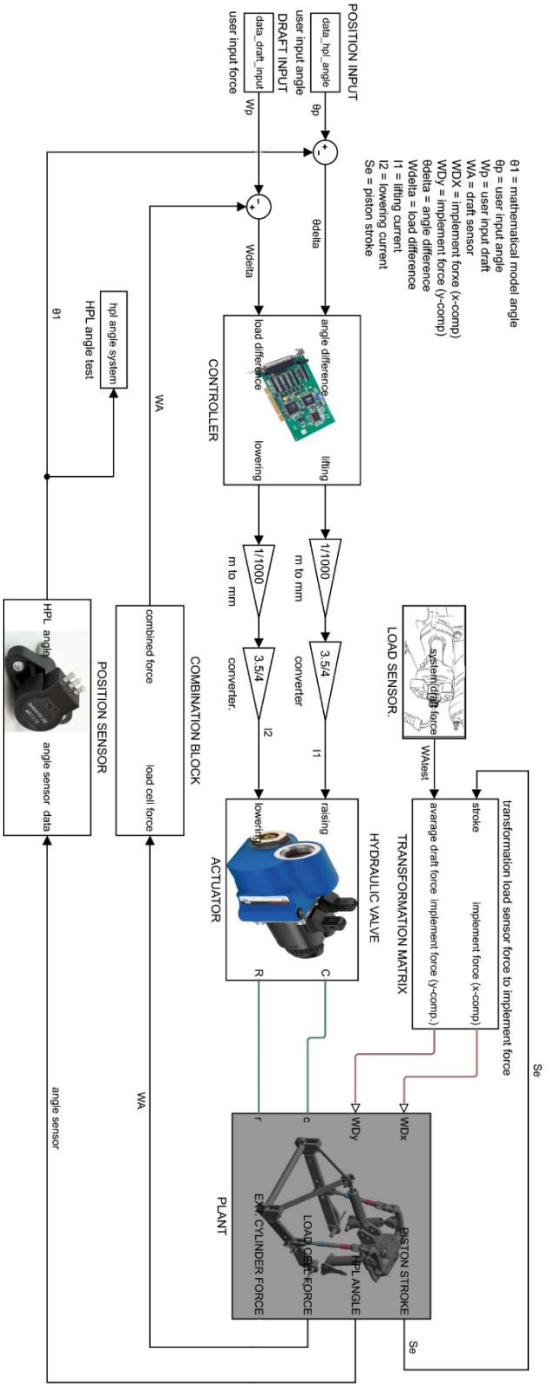

Figure 5.10. MATLAB Simulink model of the current model

In the MATLAB Simulink model, mathematical load cell output has three axes. Formerly, it was assumed that the effect of the lateral axis is neglected. For that reason, only the longitudinal and vertical axes are combined. Then combined load cell force is given to the system as feedback.

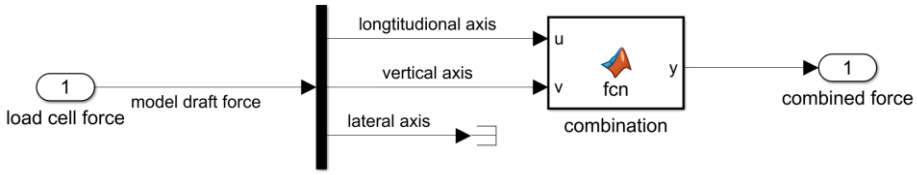

Figure 5.11. Detail of the combination block in MATLAB Simulink model

In this part, the mathematical model of the whole system is simulated. The angle of the HPL arm is the main output of the mathematical model. In Figure 5.12, HPL arm angle test data and the angle of the HPL arm for the mathematical models are compared. By looking at the figure, it can be observed that the mathematical model is correlated with the test data.

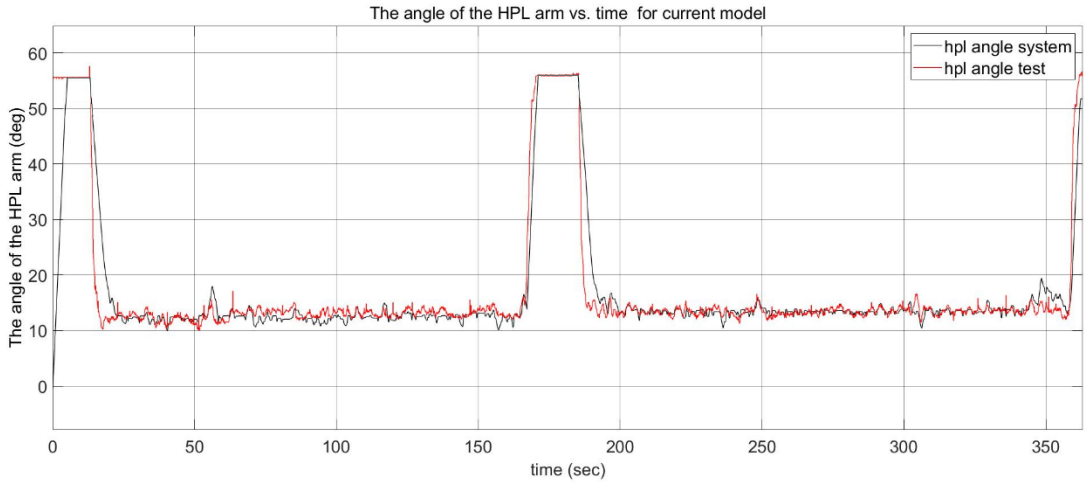

Figure 5.12. HPL arm angle comparison for test and current mathematical model

5.2. Proposed 3PL Mechanism Control System Simulation

The main goal of the thesis is obtaining a novel draft control mechanism by eliminating the load cells and integrating pressure sensors to the external lift cylinders.

In order to understand the usability of the new sensor, it is necessary to see the external lift cylinder forces at the current system. For that purpose, the previous section model plant section is modified. External lift cylinder force is added to the system as an output like in Figure 5.13.

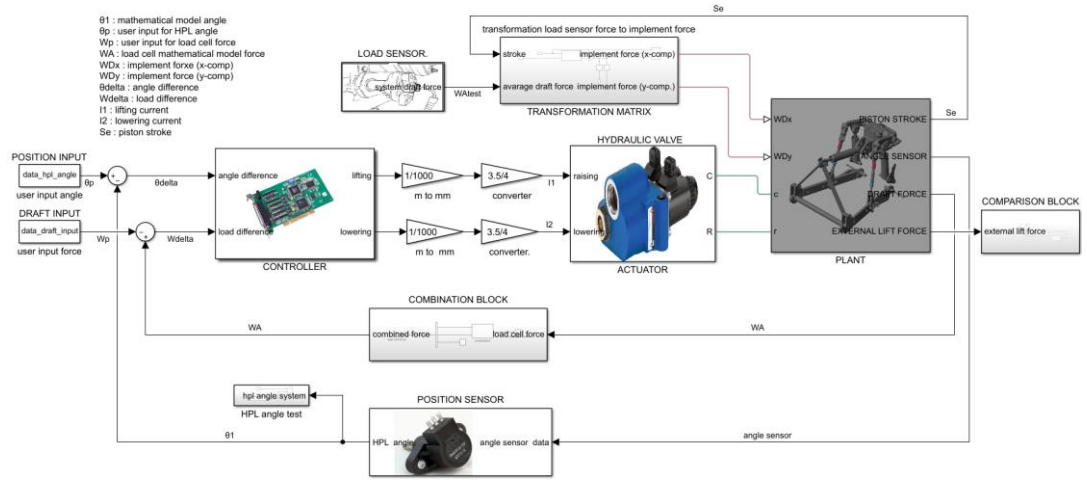

Figure 5.13. Modified current model

In Figure there is a comparison block. The detail of the comparison block is shown in Figure 5.14. The mathematical model, external lift cylinder data enters the comparison block. Then, the longitudinal and vertical axes are combined. The mathematical model and pressure transducer test data are compared in that block.

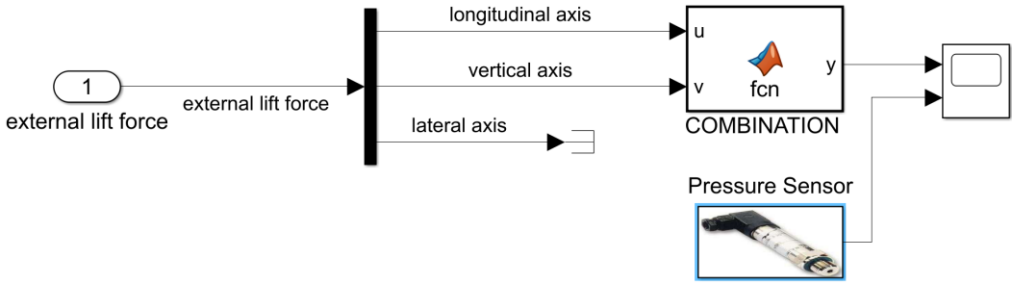

Figure 5.14. Detail of the comparison block

The mathematical model and test results are compared in Figure 5.15. Red line represents the mathematical model result for the external lift cylinder, and black line represents pressure sensor test data for the external lift cylinder.

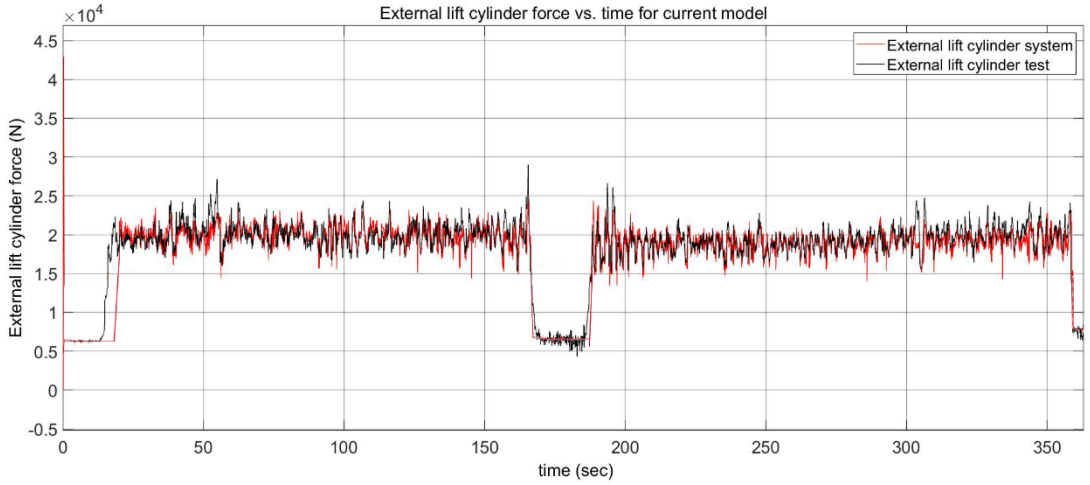

Figure 5.15. Comparison of the external lift cylinder force for test data and mathematical model

It can be seen that the external lift cylinder force mathematical model and the test data are correlated. Therefore, the pressure sensor might be used to control the draft mechanism.

The new proposed mechanism block diagram is shown in Figure 5.16.

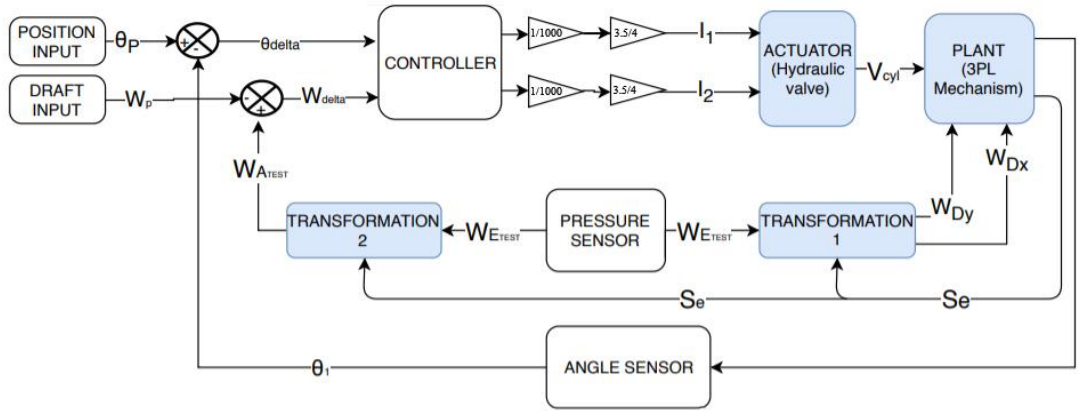

Figure 5.16. Block diagram of the proposed model

The only difference between the current design and the new design is sensors. In the new design, a pressure sensor is used. In the controller, load cell force is evaluated, so pressure sensor value must be transformed, which is the first method. Another method is instead of transforming, chancing the controller logic, but, this method is more complicated with respect to the first case. For that reason, transformation 2 is used to

transform the pressure sensor force to load cell force. In the meantime, the pressure sensor data is transformed to implement draught force by using transformation 1.

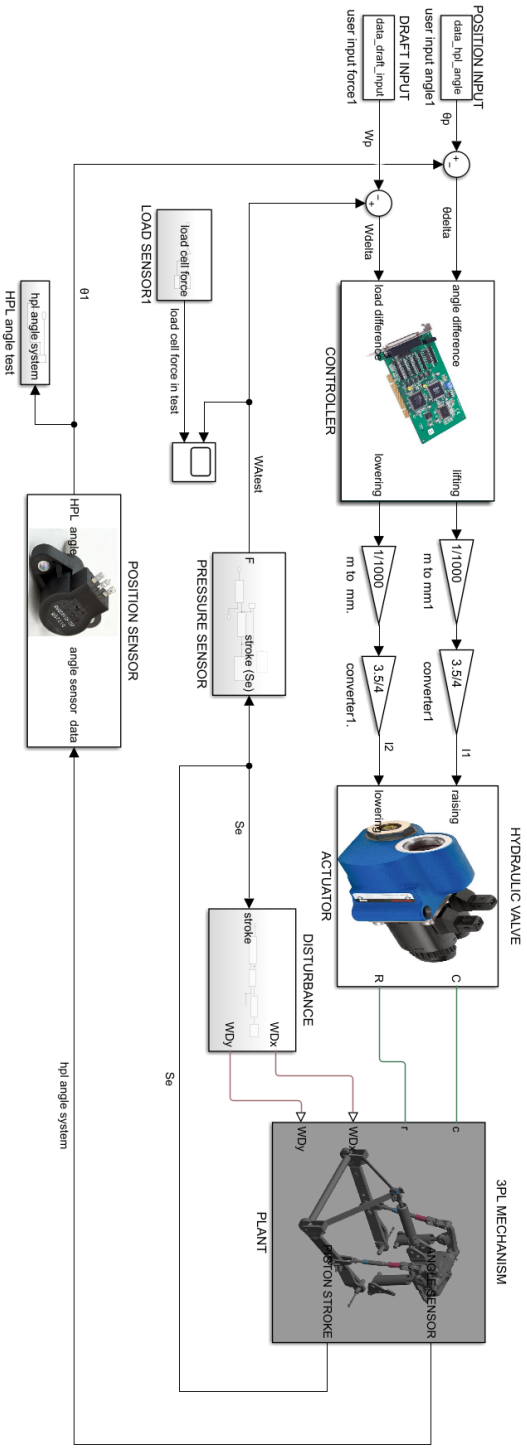

Figure 5.17. MATLAB Simulink model of the new proposed design

In the MATLAB Simulink model, pressure sensor and new disturbance are added to the system. The controller, plant, position sensor, and the inputs are exactly same as the current model. Pressure sensor and the disturbance input are the main differences with respect to the current model.

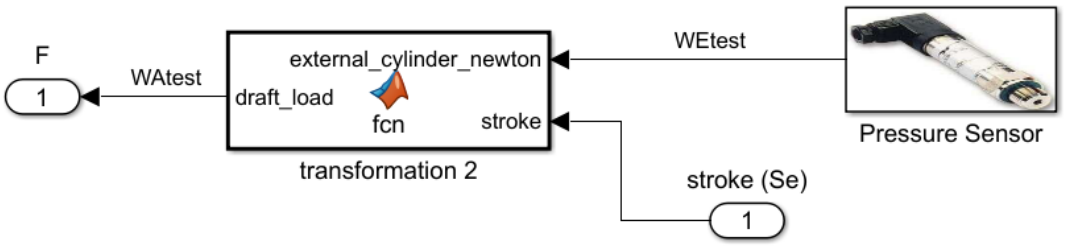

Figure 5.18. MATLAB Simulink model of the pressure sensor in new model

Pressure sensor measures the pressure in the external lift cylinder bore side. The bore radius of the cylinder is 40 mm. Therefore;

$$A_{cyl} = \pi * (40)^2 = 5028.5 \tag{5.3}$$

Next, the unit of the measured data in the pressure transducer is bar. Therefore, firstly we need to convert the bar to MPa and multiply it with the area of the cylinder in order to obtain the external lift force.

$$F_{ext} = \frac{P_{cyl}}{10} * A_{cyl} \tag{5.4}$$

where;

W_E : External lift cylinder force (N)

P_{cyl} : External lift cylinder pressure (bar)

A_{cyl} : Bore area of the external lift cylinder (mm^2)

Next, with transformation 2 equations, external lift cylinder force, W_E, converted to load cell force W_A in order to give the controller appropriate data input.

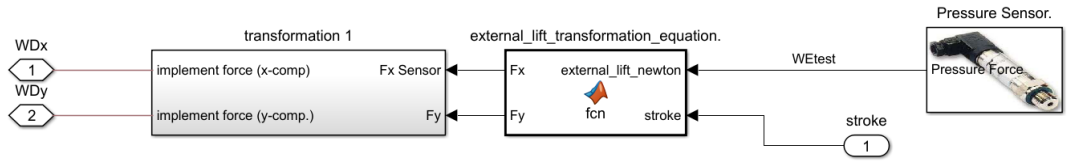

Figure 5.19. MATLAB Simulink model of the disturbance in new model

In the current model, since the applied location of the load cell is fixed, it is not possible to read any reaction forces on other joints. For that reason, the load cell force is transformed to implement draught force, W_D. In the new model, usually, the applied force acting on the external lift cylinder is a revolute joint (point G). Yet, in order to provide the same environment with the current model, force is transformed into the implement draught force by using the transformation 1 equation.

Note that, all transformation equations need piston stroke because almost all angle in the kinematic equations is altered along with chancing stroke.

In the light of this information, the new mathematical model HPL angle is obtained. The comparison between the test data HPL angle and the mathematical model HPL angle is tabulated in Figure 5.21.

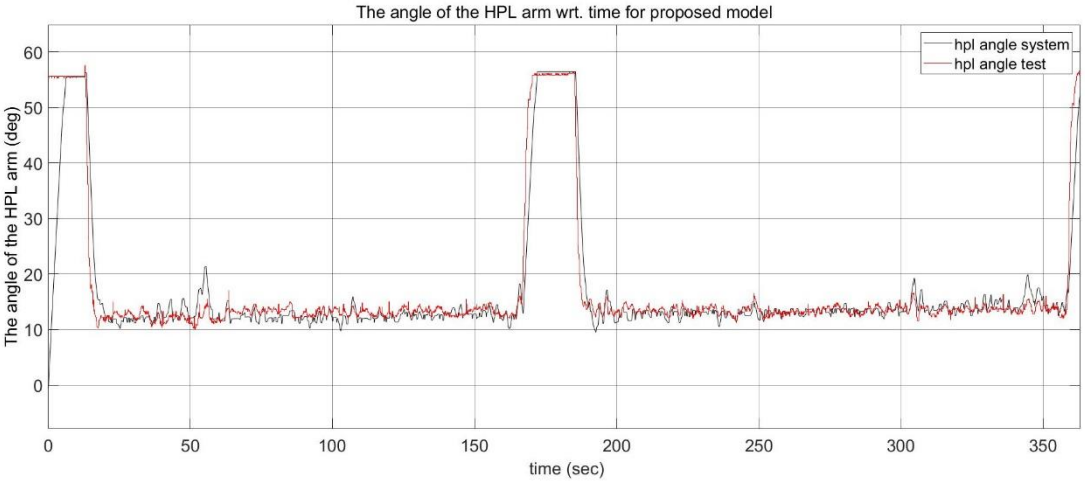

Figure 5.20. Angle comparison for the test and the new proposed model

CHAPTER 6

DISCUSSION, CONCLUSIONS AND RECOMMENDATIONS

6.1. Outline of the Study

The tasks carried out within the scope of this thesis study include;

- Defining tractor and tractor related sub-components to understand the thesis study content better
- Surveying the literature to identify data sources that other researchers have used and to develop alternative research projects to better understand the system and its requirements
- Performing kinematic analysis and force analysis of the 3PL mechanism and validating them with ADAMS® simulation software
- Exporting the solid model to MATLAB® Simscape Multibody® version and defining the joints to make a dynamic analysis.
- Modeling of a solenoid actuated three slices directional control valve in MATLAB® software Simulink tool.
- Modelling a gain scheduled proportional controller in MATLAB® Simulink Stateflow module
- Defining the test materials and conducting the field tests by considering the different editing scenarios
- Estimating the controller draft load characteristic by using the MATLAB® parameter estimation method
- Establishing the system control model and simulate the field test
- Constituting the new proposed model by eliminating the load cell sensors from the system and by adding the pressure sensors to the system

6.2. Discussion and Conclusions

The agricultural tractor is used for various duties, and there is a large variety of implements to satisfy for this purpose. In order to mount numerous types of equipment, there are specific standards. The test tractor has 4 cylinders 88 hp Diesel engine. In this study, the category of the tractor of interest is cat2. All dimensions of the 3PL mechanism are designed by considering the chosen category.

At the beginning of the study, the definition of the tractor and tractor-related components are given. Hydraulic power lift, three-point hitch mechanism, and hydraulic lift system control units are scrutinized. Position control and draft control are the main controllers of the system. On the other hand, lift-o-matic control and slip control are auxiliary control mechanisms. In order to simplify the system in the mathematical model, auxiliary controller mechanisms are neglected. Only the main controllers are taken into account.

In order to transform the forces acting upon the mechanism, kinematic analysis and force analysis have crucial roles. With these analyses, the force at any point and angle of the mechanism can be estimated and recorded.

During the calculations, there are two main assumptions. Firstly, the tractor is not a rapid device. The moment of inertia of the components and masses does not affect the dynamic analysis excessively. For that reason, masses and moment of inertias of the components are neglected during the calculation of the force analysis. Note that, under normal working conditions, PTC Creo 3.0® solid model is exported to the system and the moment of inertia and masses are taken into account. They are neglected only for transformation equations for simplicity and reduce the possible calculation errors.

Secondly, according to Bentaher [26] study, since the magnitudes of the lateral direction forces are quite low, especially for symmetric equipment, they rarely affect the 3PL mechanism. For simplicity, the lateral forces are neglected. Besides, the system dimension is decreased two instead of three by neglecting the lateral axis. In order to verify this assumption, the ADAMS® model is used. The lateral axis is added

to the ADAMS® model. The kinematic model and ADAMS model run with the same scenario. According to the scenario, both systems are exposed to 18 kN draught force, and they are lifted at the same speed. The results show that the simplifying assumption of the two-dimensional system affects the system at most by 2.6 percent. However, when the assumption is not made, the solution time will be very long. Further, the risk of calculation errors increases.

For simulation, the solid model is created from PTC Creo 3.0® and exported to MATLAB® Simulink. During this process, some connection ports such as revolute joints or cylindrical joints lost their definitions. They had to be re-defined in the Simulink® tool. According to the signal coming from the controller, the movements of the mechanism can be seen in the system in concrete form. Besides, note that, since the fixed points are not reacted by the applied forces, they must be transformed. For example, load cell forces are located at fixed points. Therefore, these forces are transformed into the equipment draught load applied point. Then, the draught force is applied to the solid model.

BOSCH EHR5 hydraulic valve is used as an actuator. There are three slices in the valve, which are compensator, lowering module, and lifting module. The compensator compensates the pressure just for the lifting side. Lifting and lowering modules are controlled with the help of the solenoids. Since the valve is not standard, every module is modeled in Simulink by using variable orifices, hydraulic cylinder, and 2/2 DCV.

Hydraulic pump speed, the gap of the lifting module spool, equipment weight, and disturbance force or acting force are the variables that affect the flow rate of the lifting valve. The flow rate shows the lifting velocity of the external lift cylinders, which corresponds to the velocity of the 3PL mechanism. Since fixed displacement hydraulic pump is used in the system, the rotational speed of the motor is the only variable that specifies the hydraulic pump speed. In field conditions, generally, tractor engine runs at 1500 rpm. For that reason, in the model, it is assumed that the tractor engine runs at this constant speed. Next, the Ampere value of the solenoid is directly proportional to

the gap of the spool. In the test, chisel plow with a weight of 200 kg is used as equipment. These variables also affect the lowering valve.

There are two controllers and three different stages in the system. Draft control and position control are the two controllers in the system. Moreover, lifting, lowering, and hold positions are the three operational stages. In order to manage these two-controllers and the three different stages, MATLAB Stateflow® module is used.

In order to select the controller type, the simulations using the mathematical model and the test results are analyzed. The speed of the tractor and the speed of the 3PH mechanism are too slow, especially when compared to the robotic systems. Moreover, as a construction machine, the tractor does not need a short response time as in the case of robotic systems. On the contrary, with short response times, the controller might have an impact on the system frequently. This situation might cause a non-smooth surface on the soil during the cultivating process, which is an annoying issue for farmers. Typically, derivative control tries to reduce the overshoot and rise time error. In our system, no matter how much is the proportional constant, the system does not overshoot. Since the study system is slow, there is no need to use derivative control.

As a requirement, there is an offset error in the system. The mechanism works in a manner that does not react within a specified range. This specified range is called sensitivity. In control theory, integral control tries to minimize the offset error. In the study, offset error, and the corresponding particular band is desirable. In the meantime, integral control might be creating wind up problems. For those reasons, integral control is not used in the mechanism. In the light of this information, only the P-control is used in the controller.

The parameters of the position control for lifting and lowering valve module are determined by performing tests. The details of the tests can be found in the controller design part. During the test, it is observed that the character of the lifting or lowering valve module current is changed non-linearly while changing the magnitude of the

load difference. Since the system is non-linear, the use of a single constant proportional gain is not sufficient. For that reason, gain scheduled P control is used to determine the characteristics of the draft control. The nonlinear characteristics are represented by, for simplicity, three different linear equations instead of a non-linear equation.

The test tractor has force sensors and 3PL mechanism angle sensor. In order to measure the pressure in the system, a pressure sensor is integrated into the system with the help of the special connector. Besides, in order to understand the driving characteristic of the tractor, a GPS module is also integrated into the system. The recording process has a crucial role in the study. However, there is no recording facility in the test tractor. Therefore, an Arduino card is designed to collect and record all data, including the sensor data, time, GPS location, the velocity of the tractor, and the height of the sensor location. In order to understand the characteristic of the cultivation process, ten different scenarios are performed in the test.

Up to now, controller, actuator, plant, and sensors are handled. Moreover, the test is performed to give inputs to the established mechanism. The only remaining unknown is the controller characteristic for which no information is available. Therefore, test data is the only acceptable choice to determine the gain scheduled P control constants. For that reason, the parameter estimation method is used to determine the constants, and a specified section of the test is the experiment for the parameter estimation method.

3PL mechanism control system simulation is performed after finding all of the variables. Load cell force is first transformed into the draught force, and it is given to the plant as a disturbance. Then, the mechanism angle and lower link point force are read by considering the disturbance. The error covariance for position angle and load cell forces are calculated and these values enter the controller. The controller evaluates the results and sends the electrical current signal to the actuator. Finally, the actuator arranges the flow rate or the velocity of the 3PL mechanism by regarding the currents

with the help of the external lift cylinder of the system. At the final stage, the measured HPL arm angle and the HPL arm angle from the mathematical model are compared. It can be seen that both results are well correlated, both qualitatively and quantitatively.

Finally, in the proposed model, the main idea is that instead of controlling the 3PH system draft mechanism with load cells in the lower links, it can be controlled by using pressures from the external lift cylinders by predicting the loads coming from the equipment. Under these circumstances, firstly, mathematical model external lift cylinder force data and external lift cylinder force test data are compared. According to the comparison in Figure 5.15, it can be seen that results are very similar, which is an indication that the pressure sensor might be used to control the draft mechanism.

Next, instead of the load cell sensor, a pressure sensor is integrated into the system. In the controller, under normal working conditions, the load cell force is evaluated. There are two methods to adapt the new sensor to the current system. Firstly, pressure sensor value could be transformed to load cell force value. Another method is to change the controller logic instead of transforming. However, this method is more complicated by considering the first case. For that reason, the first method is chosen. Figure 5.20, shows that the proposed model works well.

There are several possible reasons why companies might use the proposed model in the tractor draft control mechanism. Firstly, at the load cells, force only in one direction could be measured. Whereas, in addition to the longitudinal axis, vertical axis forces could also be measured with the use of the pressure sensors. Although according to the studies, the effect of the vertical forces is small with respect to the longitudinal forces, even the smallest force may have a vital role in proper draft control.

Secondly, in the current mechanism, load cell sensors measure the amount of deformation in the load sensing pins. Then, load cell sensors stimulate the ECU electrically. Therefore, the draft control mechanism is controlled electrically and

mechanically in the current system. In the proposed system, pressure sensors measure the pressure in the external lift cylinder and stimulate the ECU electrically. Therefore, the draft control system is controlled electrically and hydraulically in the new proposed design. Mechanical control response time is slower than the hydraulic system. Due to the shorter response time, it is better to use a pressure sensor instead of the load cell sensor.

Thirdly, nowadays, during the design process, it is essential to keep production and operation costs low. The cost of pressure sensors is lower than the cost of the load cell sensor, in general. Additionally, the housing of the pressure sensor is straightforward with respect to the load cell sensor because the housing of the load cell sensor must be rigid. It is expected that costs will be reduced in the proposed system with respect to the current system in use.

To sum up, in the light of the foregoing findings, the usage of the pressure sensor in the draft control system of the tractor may be a better solution with respect to the use of load cell sensor for accuracy of the measurement, response time, and cost.

6.3. Recommendations and Future Work

In the thesis study, all simulations are performed by considering the test data. Therefore, the established model is an off-line system. According to the test data, all calculations and systems are validated. On the other side, it is vital to see and validate the system under all environmental conditions. However, it is not possible to perform tractor tests under different conditions due to the high costs. For that purpose, it is planned to establish a test setup. With this test setup, various test conditions may be performed under different loading conditions and different loading angles. It is planned to use one pneumatic double acting cylinder in the test setup. It will be connected to the tractor 3PL mechanism, and the force will be applied to the system gradually from the pneumatic double acting cylinder at any desired angle.

After establishing the test setup, certain types of simulation could be performed. By regarding different simulations, the soil model will be constituted in Simulink®. During the creation of the soil model, MATLAB® parameter identification method would be the right choice. With proper soil model, every working conditions of the tractor will be simulated, and in this way, the online system would be obtained.

During the tests, apart from the external lift cylinder, top link pressure was also measured. The pressure sensor was mounted to the hydraulic top link bore side. However, it was observed during the cultivation process, that the direction of the hydraulic top link acting force is changed during the up and down motion of the 3PL mechanism. When the force acts as tension, the vacuum occurs in the bore side of the hydraulic top link, and the pressure sensor does not read the vacuum data. For that reason, it is not possible to obtain correct data by mounting a single sensor to the top link. In the future, it is planned to mount two pressure sensors to the top link and perform a new test. With the new data, the top link force will be integrated into the proposed model.

REFERENCES

[1] Carroll E. Goering and Alan C. Hansen, *Engine and Tractor Power, 4th Edition*. St. Joseph, MI: American Society of Agricultural and Biological Engineers, 2004.

[2] U. Usinin, S. Gladyshev, M. Grigoryev, A. Shishkov, A. Bychkov, and E. Belousov, "Electric Drive of an Industrial Tractor," *SAE Tech. Pap. Ser.*, vol. 1, 2013.

[3] K. C. C. G.G. Liversidge J.F. Bishop, D.A. Czekai, "United States Patent (19) 54," vol. 96, no. 19, pp. 62–66, 1980.

[4] Karl Th. Renius Prof., "Continuously Variable Tractor Transmissions", ASAE– the Society for engineering in agricultural, food, and biological systems 2950.

[5] Y. M. Masatsugu Tone, "Tractor Power Take-off System," 140,222.

[6] G. Keçecioglu and E. Gülsoylu, "Traktör ve Tarım Makinanaları Hidroliği," pp. 57–66, 2003.

[7] B. Bhondave, T. Ganesan, N. Varma, R. Renu, and N. Sabarinath, "Design and Development of Electro Hydraulics Hitch Control for Agricultural Tractor," *SAE Int. J. Commer. Veh.*, vol. 10, no. 1, pp. 405–410, 2017.

[8] "Electronic Draft Control (EDC) EE System Specifications," Italy, 2014.

[9] "56 Serisi Hidrolik Kaldırma Ünitesi," Turkey, Ankara, 5, 1990.

[10] "Three-Point Hitch," *2000-2019 - TractorData™. Notice*. [Online]. Available: http://www.tractordata.com/articles/technical/threepoint.html.

[11] T. F. Attachment, H. Implements, and A. W. Tractors, "ASAE S217.12 DEC01 (ISO+730-1:1994) Three-Point Free-Link Attachment for Hitching Implements to Agricultural Wheel Tractors," *Power*, vol. 01, 1994.

[12] I. O. for Standardization, *ISO 730 Agricultural wheeled tractors— Rear-mounted three-point linkage — Categories 1N, 1, 2, 3N, 3, 4N and 4*. 2007, p. 16.

[13] Prod. Dr. Ahmet SARAL, *Tarım Traktörleri*, 2nd editio. Ankara: Ankara Üniversitesi Ziraat Fakültesi Yayınları No:1471, 1997.

[14] S. R. Bello, *Farm Tractor Systems: Operations and Maintenance*. 2012.

[15] R. H. Macmillan, *The Mechanics of Tractor - Implement Performance: Theory and Worked Examples*, 1st editio. Melbourne: Senior Academic Associate, Agricultural Engineering International Development Technologies Centre University of Melbourne.

[16] 302223 International Tractors Limited Jalandhar Rd. Hoshiarpur- (Pb). 146 001 Phones: +91-1882- 302220, 302221, "OPERATOR MANUAL SOLIS 75," 1999.

[17] T. Purposes, "Agricultural Tractors," *Eng. Agrícola*, vol. 24, no. 3, pp. 727–735, 2004.

[18] all of I. Richard Wayne Hook Des Moines; William Wayne Jackson, Altoona; Lamar William, Cedar Falls; Kenneth Earl Murphy, both of Cedar Falls, "Hydraulic Power Lift System for Tractor and Trailing implement."

[19] Wilhelm von Allwijrden, Erbach, "THREE POINT LINKAGE," 1977.

[20] J. Otto Mueller, "ELECTRONIC TRACTOR CONTROL," 1987.

[21] *Hydraulic Power Lift Controls and Power Utilization for Larger Tractors*. SAE Transactions Vol. 80, SECTION 4: Papers 710619–710867 (1971), pp. 2378-2385 (8 pages).

[22] L. Cordesses, J. P. Poirier, and C. Véron, "Performance analysis of a three point hitch controller," *IEEE Int. Conf. Intell. Robot. Syst.*, vol. 3, no. October, pp. 2233–2238, 2002.

[23] G. Gebresenbet, “Measurement and prediction of forces on plough components. I. Measurement of forces and soil dynamic parameters.,” *Utredning/Rapport - Nord. Jordbrugsforskeres Foren. 1990 No.56 pp.88-95 ref.18.*

[24] A. Formato, S. Faugno, and G. Paolillo, “Numerical simulation of soil-plough mouldboard interaction,” *Biosyst. Eng.*, vol. 92, no. 3, pp. 309–316, 2005.

[25] H. F. Al-Jalil, A. Khdair, and W. Mukahal, “Design and performance of an adjustable three-point hitch dynamometer,” *Soil Tillage Res.*, vol. 62, no. 3–4, pp. 153–156, 2001.

[26] H. Bentaher, E. Hamza, G. Kantchev, A. Maalej, and W. Arnold, “Three-point hitch-mechanism instrumentation for tillage power optimization,” *Biosyst. Eng.*, vol. 100, no. 1, pp. 24–30, 2008.

[27] A. Al-Janobi, “A data-acquisition system to monitor performance of fully mounted implements,” *J. Agric. Eng. Res.*, vol. 75, no. 2, pp. 167–175, 2000.

[28] L. Naderloo, R. Alimadani, A. Akram, P. Javadikia, and H. Zeinali Khanghah, “Tillage depth and forward speed effects on draft of three primary tillage implements in clay loam soil,” *J. Food, Agric. Environ.*, vol. 7, no. 3–4, pp. 382–385, 2009.

[29] R. K. Sahu and H. Raheman, *A decision support system on matching and field performance prediction of tractor-implement system*, vol. 60. 2008.

[30] ASAE, “S T A N D A R D ASAE D497.4 MAR99 Agricultural Machinery Management Data,” 2000.

[31] R. Morselli, R. Zanasi, and P. Ferracin, “Dynamic model of an electro-hydraulic three point hitch,” no. 1, p. 6 pp., 2006.

[32] “Dimensional Synthesis of a Three Point Hitch Linkage System of Trractor – An Approach Based on Maximizing Mechanical Advantage,” pp. 548–553, 2013.

[33] J. Laceklis-Bertmanis and E. Kronbergs, “Model of hydropneumatic three point hitch,” *Eng. Rural Dev.*, pp. 49–54, 2013.

[34] “Configure Simscape Multibody Link.” [Online]. Available: https://www.mathworks.com/help/physmod/smlink/ref/configure-simmechanics-link.html.

[35] Bosch Rexroth AG, *Hitch control valves EHR5-OC, EHR5-LS, EHR23-EM2 RE*. Schwieberdingen, Germany, 2013.

[36] “Stateflow,” *1994-2019 The MathWorks, Inc.*, 2019. [Online]. Available: https://www.mathworks.com/products/stateflow.html.

[37] J. S. Shamma and M. Athans, “Analysis of Gain Scheduled Control for Nonlinear Plants,” *IEEE Trans. Automat. Contr.*, vol. 35, no. 8, pp. 898–907, 1990.

[38] Bosch Rexroth AG, “Draft sensor KMB,” 2018. [Online]. Available: https://www.boschrexroth.com/en/xc/products/product-groups/mobile-hydraulics/mobile-electronics/bodas-sensors/kmb.

[39] KELLER AG für Druckmesstechnik, “Piezoresistive Pressure Transmitters” 2017. [Online]. Available:https://www.endress.com/en/field-instruments overview/pressure/Absolute-gauge-pressure-measurement.

[40] Agrimir, “Soil Tillage / Chisel.” [Online]. Available: http://www.agrimir.com/en-415182035-p415075846-502509276/Ploughs-Chisel-Plough.

[41] A. C- and A. P. I. Gl-, “Fulltrac Fluid X 10W-30 High Protection for Transmissions of Tractor And Agricultural Machines,” pp. 1–2, 2018.

APPENDICES

A. 3PL DESIGN CONSTRAINTS

		CATEGORY			
UNIT	**DEFINITION**	**1**	**2**	**3**	**4**
13	Mast Height	460±1.5	610±1.5	685±1.5	685±1.5
14	Lower Hitch Point Height	200 max.	200 max.	230 max.	230 max.
15	Movement Range	610 min.	650 max.	735 min.	760 min..
16	Transport Height	820 min.	950 min.	1065 min.	1200 min.
17	Lower Hitch Point Clearance	100 min.	100 min.	100 min.	100 min.
18	Horizontal Convergence Distance	1700 mm to 2400 mm	1800 mm to 2400 mm	1900 mm to 2700 mm	1900 mm to 2800 mm
19	Vertical Convergence Distance	>0.9 times the tractor wheelbase	>0.9 times the tractor wheelbase	>0.9 times the tractor wheelbase	>0.9 times the tractor wheelbase
L	Distance between PTO shaft and Lower Hitch Point	500 to 575	550 to 625	575 to 675	575 to 675
l_1	Distance between the Lower Links	359	435	505	610 or 612
l_2	Rocker (left-right motion) Distance of the Links	100 min.	125 min.	125 min.	130 min.

=

B. DRAFT PARAMETERS AND AN EXPECTED RANGE IN DRAFTS ESTIMATED BY THE MODEL PARAMETERS FOR TILLAGE AND SEEDING IMPLEMENTS [30]

Table 1 – Draft parameters and an expected range in drafts estimated by the model parameters for tillage and seeding implements

	SI Units				English Units							
		Machine Parameters				Machine Parameters			Soil Parameters			
Implement	Width units	*A*	*B*	*C*	Width units	*A*	*B*	*C*	F_1	F_2	F_3	Range ±%
MAJOR TILLAGE TOOLS												
Subsoiler/Manure Injector												
narrow point	tools	226	0.0	1.8	tools	129	0.0	2.7	1.0	0.70	0.45	50
30 cm winged point	tools	294	0.0	2.4	tools	167	0.0	3.5	1.0	0.70	0.45	50
Moldboard Plow	m	652	0.0	5.1	ft	113	0.0	2.3	1.0	0.70	0.45	40
Chisel Plow												
5 cm straight point	tools	91	5.4	0.0	tools	52	4.9	0.0	1.0	0.85	0.65	50
7.5 cm shovel/35 cm sweep	tools	107	6.3	0.0	tools	61	5.8	0.0	1.0	0.85	0.65	50
10 cm twisted shovel	tools	123	7.3	0.0	tools	70	6.7	0.0	1.0	0.85	0.65	50
Sweep Plow												
primary tillage	m	390	19.0	0.0	ft	68	5.2	0.0	1.0	0.85	0.65	45
secondary tillage	m	273	13.3	0.0	ft	48	3.7	0.0	1.0	0.85	0.65	35
Disk Harrow, Tandem												
primary tillage	m	309	16.0	0.0	ft	53	4.6	0.0	1.0	0.88	0.78	50
secondary tillage	m	216	11.2	0.0	ft	37	3.2	0.0	1.0	0.88	0.78	30
Disk Harrow, Offset												
primary tillage	m	364	18.8	0.0	ft	62	5.4	0.0	1.0	0.88	0.78	50
secondary tillage	m	254	13.2	0.0	ft	44	3.8	0.0	1.0	0.88	0.78	30
Disk Gang, Single												
primary tillage	m	124	6.4	0.0	ft	21	1.8	0.0	1.0	0.88	0.78	25
secondary tillage	m	86	4.5	0.0	ft	15	1.3	0.0	1.0	0.88	0.78	20
Coulters												
smooth or ripple	tools	55	2.7	0.0	tools	31	2.5	0.0	1.0	0.88	0.78	25
bubble or flute	tools	66	3.3	0.0	tools	37	3.0	0.0	1.0	0.88	0.78	25
Field Cultivator												
primary tillage	tools	46	2.8	0.0	tools	26	2.5	0.0	1.0	0.85	0.65	30
secondary tillage	tools	32	1.9	0.0	tools	19	1.8	0.0	1.0	0.85	0.65	25
Row Crop Cultivator												
S-tine	rows	140	7.0	0.0	rows	80	6.4	0.0	1.0	0.85	0.65	15
C-shank	rows	260	13.0	0.0	rows	148	11.9	0.0	1.0	0.85	0.65	15
No-till	rows	435	21.8	0.0	rows	248	19.9	0.0	1.0	0.85	0.65	20
Rod Weeder	m	210	10.7	0.0	ft	37	3.0	0.0	1.0	0.85	0.65	25
Disk-Bedder	rows	185	9.5	0.0	rows	106	8.7	0.0	1.0	0.88	0.78	40
MINOR TILLAGE TOOLS												
Rotary Hoe	m	600	0.0	0.0	ft	41	0.0	0.0	1.0	1.0	1.0	30
Coil Tine Harrow	m	250	0.0	0.0	ft	17	0.0	0.0	1.0	1.0	1.0	20
Spike Tooth Harrow	m	600	0.0	0.0	ft	40	0.0	0.0	1.0	1.0	1.0	30
Spring Tooth Harrow	m	2,000	0.0	0.0	ft	135	0.0	0.0	1.0	1.0	1.0	35
Roller Packer	m	600	0.0	0.0	ft	40	0.0	0.0	1.0	1.0	1.0	50
Roller Harrow	m	2,600	0.0	0.0	ft	180	0.0	0.0	1.0	1.0	1.0	50
Land Plane	m	8,000	0.0	0.0	ft	550	0.0	0.0	1.0	1.0	1.0	45
SEEDING IMPLEMENTS												
Row Crop Planter, prepared seedbed												
mounted												
seeding only	rows	500	0.0	0.0	rows	110	0.0	0.0	1.0	1.0	1.0	25
drawn												
seeding only	rows	900	0.0	0.0	rows	200	0.0	0.0	1.0	1.0	1.0	25
seed, fertilizer, herbicides	rows	1,550	0.0	0.0	rows	350	0.0	0.0	1.0	1.0	1.0	25
Row Crop Planter, no-till												
seed, fertilizer, herbicides												
1 fluted coulter/row	rows	1,820	0.0	0.0	rows	410	0.0	0.0	1.0	0.96	0.92	25
Row Crop Planter, zone-till												
seed, fertilizer, herbicides												
3 fluted coulters/row	rows	3,400	0.0	0.0	rows	765	0.0	0.0	1.0	0.94	0.82	35
Grain Drill w/press wheels												
< 2.4 m drill width	rows	400	0.0	0.0	rows	90	0.0	0.0	1.0	1.0	1.0	25
2.4 to 3.7 m drill width	rows	300	0.0	0.0	rows	67	0.0	0.0	1.0	1.0	1.0	25
> 3.7 m drill width	rows	200	0.0	0.0	rows	25	0.0	1.0	1.0	1.0	1.0	25
Grain Drill, no-till												
1 fluted coulter/row	rows	720	0.0	0.0	rows	160	0.0	0.0	1.0	0.92	0.79	35
Hoe Drill												
primary tillage	m	6,100	0.0	0.0	ft	420	0.0	0.0	1.0	1.0	1.0	50
secondary tillage	m	2,900	0.0	0.0	ft	200	0.0	0.0	1.0	1.0	1.0	50
Pneumatic Drill	m	3,700	0.0	0.0	ft	250	0.0	0.0	1.0	1.0	1.0	50

C. KINEMATIC MODEL MATLAB CODE OF 3PL MECHANISM

```
clc
clear all
close all

%read field data to the matlab
dataset=xlsread('adams.xlsx');
external_lift_adams=dataset(:,2);
draft_load_adams=dataset(:,4);
top_link_force_adams=dataset(:,6);
stroke_adams=dataset(:,7);
draft_load_adams_x=dataset(:,8);

WD=input('Draught force(N) =');

teta=15*pi/180;   %the angle of the draft load
WDx=WD*cos(teta);
WDy=WD*sin(teta);

%---define constraints
Ey=350;   %mm-distance btw equipment and point C in y-dir.
Eyx=300;
Ex=650;  %mm-distance btw equipment and point C in x-dir.
Ecx=500; %mm-distance btw center of gravity of the equipment and point C in x-dir.
mi=500;   %kg-mass of the equipment
g=9.81;   %N/mm^2
i=1;
j=1;
o=1;
m=5;
%calculation of four bar mechanism
min=375;
max=550;
stroke=min:5:max;
for s1=min:m:max %stroke=175mm
    k=(max-min)/m+1;
P1(k,1)=zeros;
P2(k,1)=zeros;
%define numbers
DF=310; AB=473.6;
DE=158.5; l2=DE;
DG=456.1; l1=DG;
teta7=285.3*pi/180;

%------equations for three bar mechanism DEG---------
alfa1=acos((l1^2+l2^2-s1^2)/(2*l1*l2));
teta1=teta7+alfa1;
teta8=acos((l1*cos(teta7)-l2*cos(teta1))/s1);

%--------------3 bar mechanism DEG---------------
plot([130 130+l2*cos(teta1)], [410 410+l2*sin(teta1)], 'ro-');
hold on
grid on
plot([130 250.1], [410 -30], 'ro-');
hold on
plot([130+l2*cos(teta1) 250.1], [410+l2*sin(teta1) -30], 'ro-');
hold on;

%--------CONSTRAİNTS for DFAB-----------------
alfa2=23.8*pi/180;
DF=310;AB=473.6;
AD=622.7;FB=717.9;
alfa5=2.8*pi/180;
AG=sqrt((250.1-160.1)^2+(212-30)^2);
alfa7=acos(((DG^2)+(AD^2)-(AG^2))/(2*DG*AD));

%------equations for four bar mechanism DFBA---------
AF=sqrt((DF^2)+(AD^2)-2*DF*AD*cos(alfa1+alfa2+alfa7));
alfa3=acos(((AD^2)+(AF^2)-(DF^2))/(2*AD*AF));
alfa4=acos(((AF^2)+(FB^2)-(AB^2))/(2*AF*FB));
alfa6=alfa4-alfa3+alfa5;
teta3=((3*pi)/2)+alfa6;
```

```
alfa8=acos(((AF^2)+(AB^2)-(FB^2))/(2*AF*AB));
teta4=pi/2-alfa8-alfa3+alfa5;

%------------4 bar mechanism DFBA--------------
plot([130 130+DF*cos(teta1+alfa2)], [410 410+DF*sin(teta1+alfa2)], 'ro-');
hold on;
plot([130+DF*cos(teta1+alfa2)                    130+DF*cos(teta1+alfa2)+FB*cos(teta3)],
[410+DF*sin(teta1+alfa2) 410+DF*sin(teta1+alfa2)+FB*sin(teta3)], 'ro-');
hold on;
plot([130 160.1], [410 -212], 'ro-');
hold on;
plot([160.1                 130+DF*cos(teta1+alfa2)+FB*cos(teta3)],                 [-212
410+DF*sin(teta1+alfa2)+FB*sin(teta3)], 'ro-');
hold on;

%-------------constraints for ACHI----------------
alfa17=28.5*pi/180;
teta10=241.5*pi/180;
HI=730;  IC=610;
HA=565.6;  AC=980;

%------equations for four bar mechanism ACHI---------
alfa12=pi/2-alfa17-teta4;
HC=sqrt((HA^2)+(AC^2)-2*HA*AC*cos(alfa12));
alfa9=acos(((HA^2)+(HC^2)-(AC^2))/(2*HC*HA));
alfa10=acos(((IC^2)+(HC^2)-(HI^2))/(2*HC*IC));
alfa11=alfa9-alfa17-alfa10;
teta6=3*pi/2+alfa11;
alfa13=acos(((HI^2)+(HC^2)-(IC^2))/(2*HC*HI));
teta5=alfa9-alfa17+alfa13-pi/2;

%-------for bar machanism ACHI--------
plot([430.1 430.1+HI*cos(teta5)],[285 285+HI*sin(teta5)], 'ro-');
hold on;
plot([430.1+HI*cos(teta5)      430.1+HI*cos(teta5)+IC*cos(teta6)],      [285+HI*sin(teta5)
285+HI*sin(teta5)+IC*sin(teta6)], 'ro-');
hold on;
plot([430.1 160.1], [285 -212], 'ro-');
hold on;
plot([160.1   430.1+HI*cos(teta5)+IC*cos(teta6)],[-212   285+HI*sin(teta5)+IC*sin(teta6)],
'ro-');
hold off;

axis([-1000 1600 -500 1000]);
pause(1);

%---------define cylinder piston areas--------
A1=5026.5;    %mm^2 - external lift cylinder area (40^2*pi)
A2=3117.2;    %mm^2 - hydraulic top link cylinder area (31.5^2*pi)

%define implement angles and measurements
alfa11i=-0.0174533;   %alfa 11 initial value
gama=alfa11-alfa11i;
Exx=Ex*cos(gama);
Exy=Ex*sin(gama);
Eyy=Ey*cos(gama);
Eyx=Ey*sin(gama);
Exp=Exx+Eyx;
Eyp=Eyy-Exy;
Ecxx=Ecx*cos(gama);
Ecxy=Ecx*sin(gama);

%Forces acting on the 3PH mechanism coming from equipment
%define WI (forces acting on the upper link)
WI=(WD*sin(teta)*Exp+mi*g*Ecxx-WD*cos(teta)*Eyp)/(IC*(cos(-teta5)*cos(alfa11)
-sin( teta5)*sin(alfa11)));
WIx=WI*cos(-teta5);
WIy=WI*sin(-teta5);
WCx=(WD*cos(teta)-WI*cos(-teta5))/2;
WCy=(WD*sin(teta)+mi*g-WI*sin(-teta5))/2;

%define WB
WB=(WCy*AC*cos(teta4)+WCx*AC*sin(teta4))/(AB*cos(alfa6)*cos(teta4)+sin(alfa6)*AB*sin(teta
4));
WBx=WB*sin(alfa6);
```

```
WBy=WB*cos(alfa6);

%define load cell forces (forces acting on the lower links)
WAx=WB*sin(alfa6)-WCx;
WAy=WCy-WB*cos(alfa6);
draft_load1=sqrt(WAx^2+WAy^2);
%draft load
draft_load(o,1)=draft_load1;
draft_load_x(o,1)=WAx;
o=o+1;

%define main cylinder forces, point E
alfa14=15.27*pi/180;
alfa15=acos(((DG^2)+(s1^2)-(DE^2))/(2*DG*s1));
alfa16=alfa15-alfa14;

WE=(WB*cos(alfa6)*DF*cos(teta1+alfa2)+WB*sin(alfa6)*DF*sin(teta1+alfa2))/(sin(alfa16)*DE*
sin(teta1)+cos(alfa16)*DE*cos(teta1));

%P1 is the main cylinder, connected to the lower link, pressure
P11=10*WE/A1;  %bar
P1(i,1)=P11;
external_cylinder(i,1)=P11*A1/10;
i=i+1;

%P2 is the lift arm pressure
P22=10*WI/A2;  %bar
P2(j,1)=P22;
top_link=P2/10*A2;
j=j+1;
AD
end

Figure
plot(stroke,draft_load,'-b','Linewidth',2)
grid
hold on
plot(stroke_adams,draft_load_adams,':r','Linewidth',3)  %red
legend('draft load matlab','draft load adams')

Figure
plot(stroke,draft_load_x,'-b','Linewidth',2)
grid
hold on
plot(stroke_adams,draft_load_adams_x,':r','Linewidth',3)  %red
legend('draft load matlab x component','draft load adams x component')

Figure
plot(stroke,external_cylinder,':r','Linewidth',2)
grid
hold on
plot(stroke_adams,external_lift_adams,'-b','Linewidth',3)
legend('external cylinder matlab','external cylinder adams')


Figure
plot(stroke,top_link,'--k','Linewidth',2)
grid
hold on
plot(stroke_adams,top_link_force_adams,'-b','Linewidth',3)
legend('top link matlab','top link adams')
```

D. OPET FULLTRAC FLUID-X 10W-30 HYDRAULIC OIL SPEC. [41]

opet technical data sheet

Fulltrac Fluid X 10W-30

High Protection for Transmissions of Tractor And Agricultural Machines

PRODUCT DESCRIPTION

Fulltrac Fluid X 10W-30, is a multi purpose transmission oil for automatic or manuel transmissions, hydraulic, axle, wet brake systems, final drives and PTO (Power Take Off) of tractor and agricultural machines. Quality base oils and anti-friction additives in its formulation provides high performance while power transmission of moving equipments.

CHARACTERISTICS

- It provides effective protection against high velocity/low torque and low velocity/high torque wear.
- Its excellent viscosity-temperature characteristic offers reliable performance at very low temperatures.
- Its anti-friction additives allow wet brake system to operate efficiently and silently.
- Its specially developed formula provides long service life by controllig rust, corrosion and foam formation.
- Its high thermal and oxidation stability prevents sludge formation and increases efficiency.

APPLICATIONS

- It is suitable to use in manuel transmissions, hydraulic, axle, wet brake systems, final drives and PTO of tractor and agricultural machines.

PERFORMANCES

- ALLISON C-4
- API GL-4
- CASE MS 1210
- CNH MAT3525/3509
- FORD ESN-M2C86-B/C/ESN-M2C134-D
- JOHN DEERE JDM J20D/C
- KUBOTA UDT FLUID
- MASSEY FERGUSON CMS M 1145/1143/1141/1135
- ZF TE-ML 17E/06K/05F/03E

OPET.TDS.0804/Rev.09/24.05.2018

1/2

technical data sheet

TYPICAL PROPERTIES

Density@15°C, g/ml	ASTM D 4052	0,877
Viscosity@ 40°C, mm²/s	ASTM D 445	58,7
Viscosity@100°C, mm²/s	ASTM D 445	9,7
Viscosity Index	ASTM D 2270	151
Flash Point, °C	ASTM D 92	224
Pour Point, °C	ASTM D 97	-36

HEALTH AND SAFETY RECOMMENDATIONS

Waste oils must not be discharged into underground or surface water sources, sewage systems or garbage cans. Prolonged or repeated contact with used oils may cause skin diseases. Therefore sterilized gloves should always be used. If part of the skin comes into contact with waste oil, that part should be immediately washed with plenty of soap and water. In case of skin irritation or redness caused by contact, seek advice of your doctor immediately. For more information contact Material Safety Data Sheet (MSDS).

The vehicle and equipment manufacturers spesifications and relevant international standards were taken into consideration while preparing the content of this Technical Data Sheet. The expressions in the content of this Technical Data Sheet can not be considered as guarantee commitment or similar way in terms of product characteristics and product use in any applications.

The correct use of this product, compliance with applicable laws and regulations is responsibility of the user. Opet Fuchs Madeni Yağ. San. ve Tic. A.Ş. can not be held responsible for any loss or damage arising from the abnormal use and misuse or any hazards of product content and its results.

This Technical Data Sheet is valid from the date of publication. The information in the content of this Technical Data Sheet are subject to change without notice. Please contact with Opet Fuchs Technical Services Department for more information.

Koç

OPET FUCHS MADENİ YAĞ SANAYİ VE TİCARET A.Ş.
Ord. Prof. Dr. Fahrettin Kerim Gökay Cad. Eşref Çakmak Plaza
No: 32 Giriş Kat: TR 34662 Altunizade/Üsküdar/İSTANBUL

Phone: +90 216 522 69 00
Fax : +90 216 522 69 90
teknikservisler@opetfuchs.com.tr

E. TECHNICAL SPECIFICATIONS OF BOSCH EHR-5 VALVE [35]

Technical data

general				EHR5	EHR23
Design				Flange design	Sandwich plate design
Weight	EHR5-OC		kg	3.1	
	EHR5-OC Subplate		kg	1.5	
	EHR5-LS		kg	3.1	
	EHR23		kg		6.5
Installation position				Axis Z–Z, max. 30 ° variation from the horizontal	
Line connections				Screw-in threads see page 21	
Ambient temperature range		θ	°C	–30 to +80	

hydraulic				EHR5	EHR23
Maximum operating pressure at the port	P	p_{max}	bar	220	250
	A	p_{max}	bar	220	
	Y	p_{max}	bar		250
	R	p_{max}	bar		30
	R1	p_{max}	bar	5, but smaller than load pressure	
	R2	p_{max}	bar	10	
Flow rate		q	l/min	See table page 6 and 10	See table page 14 to 19
Maximum load drop off at port A			cm³/min	4 (with 125 bar, viscosity 35mm²/s)	
Hydraulic fluid				Mineral oil (HL, HLP) according to DIN 51524 Additional hydraulic fluids, e.g. environmentally friendly fluids, upon request.	
Hydraulic fluid temperature range	Admissible range	θ	°C	+20 to +90; +100 for a short time	
	Admissible range for start	θ	°C	–30	
Viscosity range	Admissible range	ν	mm²/s	10 to 800	
	Recommended range	ν	mm²/s	20 to 100	
	Admissible range for start	ν	mm²/s	Up to 2000	
Max. admissible degree of contamination of the hydraulic fluid	Cleanliness class according to ISO 4406 (c)			Class 19/16	For this we recommend using a filter with a minimum retention rate of $\beta_{25} = 75$
	Cleanliness class according to NAS 1638			Class 10	
electric					
Direct shutter actuation by means of proportional solenoids		U	V	12	
		I_{max}	A	3.35	
Electrical connections				Plug-in connection, 2-pole	
Protection class				IP64A	

F. SECTION OF TEST DATA

left load cell sensor data	left draft load (N)	right load cell sensor data	right draft load (N)	average load cell data	external lift pressure data	external lift pressure (bar)	external lift force (N)	angle sensor data	angle of HPL (deg)	top link pressure data	top link pressure (bar)	top link force (N)	velocity
315	7320,46	320	5849,36	6584,911875	249	74,5150667	37470,43354	89	11,77	45	12,40687014	3869,082	5
317	6732,02	323	4966,69775	5849,36	237	70,86164337	35633,28352	88	11,52	41	11,18906236	3489,309	5
317	6732,05	322	5260,9185	5996,470375	244	72,99280698	36704,95437	88	11,52	40	10,88461042	3394,36	5
312	8203,12	309	9085,78825	8644,457125	262	78,47294197	39460,67939	87	11,27	41	11,18906236	3489,309	5
311	8497,34	310	8791,5675	8644,457125	265	79,3862978	39919,96689	91	12,28	38	10,27570653	3204,479	5
308	9380,00	311	8497,34675	8938,677875	262	78,47294197	39460,67939	89	11,77	32	8,448994869	2634,81	5
312	8203,12	306	9968,4505	9085,78825	265	79,3862978	39919,96689	90	12,03	49	13,62467792	4248,855	5
300	11733,77	310	8791,5675	10262,67125	266	79,69074975	40073,06273	90	12,03	47	13,01577403	4058,96	5
310	8791,56	305	10262,67125	9527,119375	275	82,43081724	41450,92524	90	12,03	31	8,144542925	2539,875	5
315	7320,46	308	9380,009	8350,236375	255	76,34177836	38389,00855	92	12,53	48	13,32022597	4153,912	5
320	5849,36	309	9085,78825	7467,574125	248	74,21061476	37317,33771	92	12,54	45	12,40687014	3869,082	5
320	5849,36	319	6143,58075	5996,470375	250	74,81951864	37623,52937	91	12,28	21	5,100023486	1590,442	5
320	5849,36	317	6732,02225	6290,691125	246	73,60171087	37011,14604	92	12,53	50	13,92912986	4343,799	5
317	6732,02	316	7026,243	6879,132625	260	77,86403808	39154,48772	92	12,53	42	11,49351431	3584,252	5
318	6437,80	312	8203,126	7320,46375	247	73,90616281	37164,24187	90	12,03	50	13,92912986	4343,799	5
314	7614,68	311	8497,34675	8056,015625	253	75,73287447	38082,81688	91	12,28	42	11,49351431	3584,252	5
314	7614,68	312	8203,126	7908,90525	254	76,03732642	38235,91271	92	12,53	35	9,362350701	2919,649	5
315	7320,46	311	8497,34675	7908,90525	248	74,21061476	37317,33771	90	12,03	45	12,40687014	3869,082	5
316	7026,24	316	7026,243	7026,243	241	72,07945115	36245,66686	90	12,03	41	11,18906236	3489,30	5
319	6143,58	311	8497,34675	7320,46375	246	73,60171087	37011,14604	90	12,03	43	11,79796625	3679,195	5
312	8203,12	312	8203,126	8203,126	250	74,81951864	37623,52937	89	11,77	45	12,40687014	3869,082	5
312	8203,12	306	9968,4505	9085,78825	259	77,55958614	39001,39189	89	11,77	42	11,49351431	3584,252	5
311	8497,34	308	9380,009	8938,677875	261	78,16849003	39307,58356	91	12,28	34	9,057898757	2824,705	5
313	7908,90	314	7614,6845	7761,794875	249	74,5150667	37470,43354	90	12,03	46	12,71132208	3964,025	5
312	8203,12	315	7320,46375	7761,794875	251	75,12397059	37776,62521	90	12,03	45	12,40687014	3869,082	5
310	8791,56	303	10851,11275	9821,340125	266	79,69074975	40073,06273	90	12,03	38	10,27570653	3204,479	6
306	9968,45	312	8203,126	9085,78825	259	77,55958614	39001,39189	90	12,03	52	14,53803375	4533,685	6
305	10262,67	318	6437,8015	8350,236375	254	76,03732642	38235,91271	92	12,53	48	13,32022597	4153,912	6
304	10556,82	314	7614,6845	9085,78825	266	79,69074975	40073,06273	90	12,03	26	6,622283205	2065,159	6
306	9968,45	311	8497,34675	9232,898625	265	79,3862978	39919,96689	91	12,28	37	9,971254588	3109,535	6
311	8497,34	312	8203,126	8350,236375	271	81,21300947	40838,5419	91	12,28	42	11,49351431	3584,252	6
308	9380,00	312	8203,126	8791,5675	256	76,64623031	38542,10438	102	15,07	55	15,45138958	4818,51584	6
309	9085,78	305	10262,67125	9674,22975	264	79,08184586	39766,87106	94	13,04	35	9,362350701	2919,649	6
308	9380,009	308	9380,009	9380,009	267	79,99520169	40226,15856	93	12,79	46	12,71132208	3964,025	6
313	7908,90	304	10556,892	9232,898625	258	77,25513419	38848,29605	94	13,04	49	13,62467792	4248,855	6
311	8497,34	310	8791,5675	8644,457125	264	79,08184586	39766,87106	94	13,04	36	9,666802644	3014,592	6
318	6437,80	307	9674,22975	8056,015625	257	76,95068225	38695,20022	95	13,29	43	11,79796625	3679,195	6
313	7908,90	307	9674,22975	8791,5675	264	79,08184586	39766,87106	94	13,04	47	13,01577403	4058,96	6
314	7614,68	307	9674,22975	8644,457125	259	77,55958614	39001,39189	94	13,04	42	11,49351431	3584,252	6